NASA CR-72365
LMSC K-07-68-2

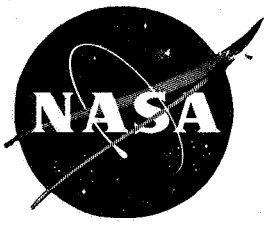

LIQUID PROPELLANT THERMAL CONDITIONING SYSTEM

FINAL REPORT

by

W. H. Sterbentz

prepared for

NATIONAL AERONAUTICS AND SPACE ADMINISTRATION

CONTRACT NAS 3-7942

LOCKHEED MISSILES & SPACE COMPANY
A GROUP DIVISION OF LOCKHEED AIRCRAFT CORPORATION

NOTICE

This report was prepared as an account of Government sponsored work. Neither the United States, nor the National Aeronautics and Space Administration (NASA), nor any person acting on behalf of the NASA:

A) Makes any warranty or representation, expressed or implied, with respect to the accuracy, completeness, or usefulness of the information contained in this report, or that the use of any information, apparatus, method, or process disclosed in this report may not infringe privately owned rights; or

B) Assumes any liaibilities with respect to the use of, or for damages resulting from the use of any information, apparatus, method or process disclosed in this report.

As used above, "person acting on behalf of NASA" includes any employee or contractor of NASA, or employee of such contractor, to the extent that such employee or contractor of NASA, or employee of such contractor prepares, disseminates, or provides access to, any information pursuant to his employment or contract with NASA, or his employment with such contractor.

Requests for copies of this report should be referred to

National Aeronautics and Space Administration
Office of Scientific and Technical Information
Attention: AFSS-A
Washington, D.C. 20546

NASA CR-72365
LMSC-K-07-68-2

FINAL REPORT

LIQUID PROPELLANT THERMAL CONDITIONING SYSTEM

by

W. H. Sterbentz

prepared for

NATIONAL AERONAUTICS AND SPACE ADMINISTRATION

15 August 1968

CONTRACT NAS 3-7942

Technical Management
NASA Lewis Research Center
Cleveland, Ohio
Liquid Rocket Technology Branch
Gordon T. Smith

LOCKHEED MISSILES & SPACE COMPANY
P. O. Box 504
Sunnyvale, California

FOREWORD

The Lockheed Missiles & Space Company (LMSC), as prime contractor, and AiResearch Manufacturing Company, as subcontractor, are submitting this final report, in partial completion of the requirements of Contract NAS 3-7942, Liquid Propellant Thermal Conditioning System, dated 26 January 1966. The total scope of work, data, results, and conclusions covering this program, to date, are presented in two volumes: "Interim Report, Liquid Propellant Thermal Conditioning System," NASA CR-72113, dated 20 April 1967, and this final report. This work is being conducted for the National Aeronautics and Space Administration through the NASA Lewis Research Center, Cleveland, Ohio.

The success of this program is in large measure attributable to the efforts of Mr. G. T. Smith, NASA LeRC Project Manager, and Mr. D. L. Nored, Branch Chief, NASA LeRC. Their timely and stimulating consultations, technical seminars, and guidance were extremely valuable to the conduct of the program.

Appreciation is also expressed to Mr. K. L. Abdalla and his associates for providing experimental and motion-picture data on the NASA-LeRC drop-tower tests and on the Aerobee rocket flight experiments. These data provided considerable insight into the behavior of fluids, including boiling hydrogen, in a zero-gravity environment.

On the AiResearch team, the efforts of Messrs. J. G. Kimball, J. M. Ruder, and T. C. Coull were invaluable in making available to this program the full scope of technical, engineering, production, and administrative capabilities of the AiResearch Manufacturing Company.

Much of the associated cryogenic space propulsion vehicle systems hardware and unique large space vehicle flight simulator facilities needed on this program were developed by Lockheed prior to or concurrent with this program. This hardware

included a full-scale Mars orbit-injection stage propellant tank capable of nonvented storage of liquid hydrogen for the 220-day space flight mission of prime interest on this program. On the Lockheed team, acknowledgment is given the efforts of Mr. B. R. Bullard for his technical and managerial contributions as assistant program manager and of Messrs. D. R. Stevenson and J. H. Young for their expertise in large-scale liquid hydrogen vehicle system testing.

Lockheed is pleased to have conducted this program for the NASA Lewis Research Center. A complete description of the liquid propellant thermal conditioning system, its function, operation, and performance is presented in this report.

William H. Sterbentz
Program Manager

CONTENTS

ILLUSTRATIONS

TABLES

INTRODUCTION AND SUMMARY

The storability of liquid hydrogen for long-duration space missions has been demonstrated in a full-scale Mars orbit-injection space vehicle tankage system by Lockheed in its large space flight simulator. So effective was the thermal protection system that nonvented storage of liquid hydrogen is now a practical consideration for Earth-orbital and planetary injection missions. Even so, in all propellant tankage systems a pressure-relief system is mandatory from safety and system operational considerations.

Tank venting may be desired for reduction of tank pressure after an engine firing so that repeated pressurization may be accomplished for successive engine firings without excessively increasing tank pressure. In this way lower tank operating pressures and tank weights may be obtained and still provide the required net positive suction pressure to the engine.

Normally, a gas-vent relief valve might be considered for venting the hydrogen tank. In space flight, however, long periods of near-zero-gravity coast of the spacecraft occur. Space flight experience has shown that in zero gravity the location and movement of the liquid propellant in the tank are uncertain. Thus, under such conditions, pressure relief of the tank through an ordinary gas vent relief valve is unreliable and at best very inefficient because of the likely ingestion of large amounts of liquid hydrogen that would be vented directly overboard. Prolonged venting of propellant in such a manner could cause mission failure because of dissipation of propellant and consumption of attitude-control propellants to correct for large variations and unbalances in vehicle motions induced by the vent system.

Provision on the vehicle of propellant settling rockets to allow for positive location of the ullage bubble at the ordinary gas vent valve to eliminate liquid propellant venting

is a possible solution. However, such a system can be very heavy and limited in its utility. For a spacecraft such as the Earth-Mars Kickstage Mission (2) vehicle shown in Fig. 1 and Table 1, a minimum of 55 separate vent cycles would be required to maintain the hydrogen tank at 17 psia ± 1/2 psi for the 220 days duration of the flight. Firing of appropriate propellant settling rockets for each of the 55 vent cycles would require a settling rocket system weighing about 560 lb. Obviously, such a system weight is exorbitant.

A light-weight pressure-relief vent system concept has been defined that will avoid these difficulties. This concept, referred to as a liquid propellant thermal conditioning system, maintains tank pressure control through extraction of either liquid or gaseous hydrogen and through utilization of the heat-transport properties of this extracted fluid. By passing this extracted fluid through a high-pressure-drop valve, the resulting refrigerated vapor, when passed through a heat exchanger, can be used to efficiently absorb heat from the bulk propellant and ullage in the propellant tank. This chilling of the tank fluid contents causes condensation of some of the ullage gases with a concomitant drop in tank pressure. Upon passing through the heat exchanger the refrigerated vapor is converted into a saturated or superheated gas and is vented from the propellant tank.

The full scope of this program to date to successfully develop and demonstrate such a pressure-relief system is presented in two reports. The first report (Ref. 1), published 20 April 1967, is entitled " Interim Report, Liquid Propellant Thermal Conditioning System, " NASA CR-72113. This second report presents the results of the program developed since the interim report.

Three missions and vehicles were chosen as being representative of a realistic application of cryogenic propellants to a space mission. Figure 1 shows the three spacecraft chosen. They are a cryogenic propulsion module as a service module of a Saturn V Apollo vehicle, an Earth-Mars kickstage spacecraft, and a manned Mars vehicle utilizing nuclear propulsion. Table 1 presents pertinent data for each mission and spacecraft.

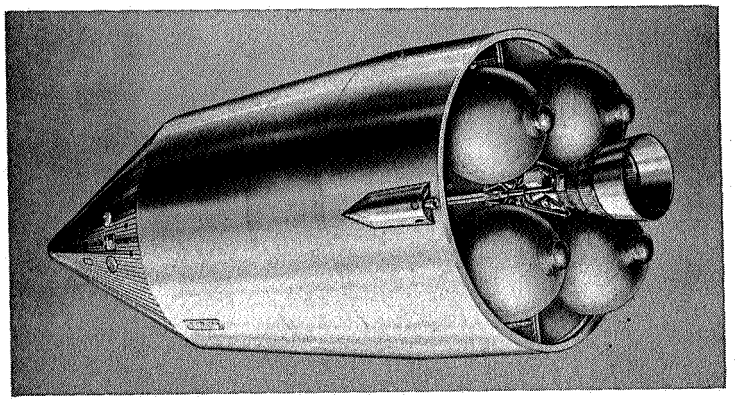

Mission (1) – Earth-Lunar Logistics Mission

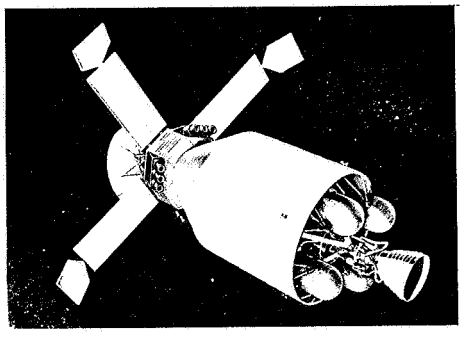

Mission (2) – Earth-Mars Kickstage Mission

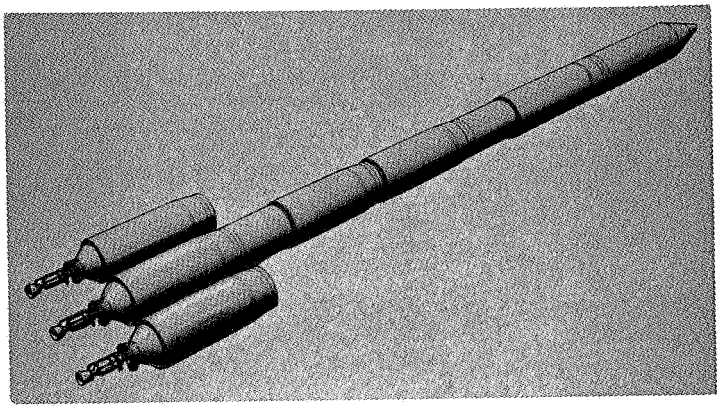

Mission (3) – Earth-Mars Manned Mission

Fig. 1 Reference Mission Vehicles

Table 1

REPRESENTATIVE APPLICATION OF CRYOGENIC PROPELLANTS TO A SPACE MISSION – MISSION AND SPACECRAFT DATA

Mission 1: Earth/Lunar Logistics Mission

LH_2 Tank

Dimensions: Diam. = 167 in. (spherical)

Pressurant: Helium for pressurization, hydrogen gas for expulsion

Pressure: 28 psia

Nominal Working Bulk Liquid Temperature for Engine Use: 37.7° R (corresponding to 17 psia)

Expulsion Profile:

Firing Number	Weight (lb)	Firing Time (sec)	Time (hr after launch)
1	274	47	13.5
2	64	11	19.5
3	3,284	565	76.5
4	156	27	82.5
5	1,039	179	124.5
6	56	10	133.5

Heat Leak: Maximum = 188 Btu/hr, Minimum = 97 Btu/hr, Average = 160 Btu/hr

Mission 2: Earth/Mars Kickstage Mission

LH_2 Tank

Dimensions: (Oblate-Spheroid) Semi-Major Axis: 52 in.
Semi-Minor Axis: 42.9 in.

Pressurant: Helium for pressurization, hydrogen gas for expulsion

Duration: 220 days

Nominal Working Pressure: 28 psia

Bulk Liquid Temperature for Engine Use: 37.7° R (corresponding to 17 psia)

Expulsion Profile:

Firing Number	Weight (lb)	Firing Time (sec)	Time (days after launch)
1	80	80	10
2	40	40	180
3	Remainder	$\frac{\text{Remainder}}{33.8\ \text{lb/sec}}$	220

Heat Leak: Maximum = 17.2 Btu/hr, Minimum = 5.8 Btu/hr, Average = 11.5 Btu/hr

Mission 3: Earth/Mars Manned Mission

LH_2 Tank

Dimensions: (Cylindrical-Hemipsherical Heads) Diam. = 30 ft, total length = 60 ft

Pressurant: Helium for pressurization, hydrogen gas for expulsion

Duration: 220 days

Nominal Working Pressure: 28 psia

Bulk Liquid Temperature for Engine Use: 37.7° R (corresponding to 17 psia)

Expulsion Profile:

Firing Number	Percent Total Propellant Used	Date After Launch
1	5	10 days
2	5	180 days
3	Remainder	220 days

Heat Leak: Maximum = 40 Btu/hr, Minimum = 12 Btu/hr, Average = 22 Btu/hr

This development program, initiated in January 1966, was divided into five individual tasks:

Task I – System Design Concepts and Analysis
Task II – Optimization of System Designs
Task III – Mixing Requirements Evaluation and Test of the Mixer Unit
Task IV – Design, Fabrication, and Test of the Thermal Conditioning Unit
Task V – Evaluation of System Fabrication and Test Data

The results of Tasks I, II, and III were fully presented in Ref. 1. Reported herein are all the results and data generated in Tasks IV and V. Furthermore, this report relates and interprets the the experimental data obtained in all the Tasks with the analytical and theoretical data as developed and presented in Ref. 1.

The broad objective of the program was to provide an evaluation of both the theoretical and experimental effectiveness of liquid propellant thermal conditioning systems for tank pressure control in terms of the main system variables:

(1) Propellant pressure level in the tank during venting
(2) Expansion process outlet pressure
(3) Bulk propellant heating rates

Specific objectives of the program which served to accomplish the foregoing broad objective were as follows:

1. Identify and arrive at conceptual liquid propellant thermal conditioning system designs.
2. Perform a detailed analysis of the physical processes occurring within each component of each conceptual design.
3. Develop experimental and theoretical criteria for propellant circulation requirements in zero, low, and high gravity environments.
4. Develop a system and component design method utilizing the foregoing criteria.

5. Utilize this design method to provide a definition of the optimum thermal conditioning system for each of the reference missions (Fig. 1 and Table 1).
6. Design and fabricate the optimum system in full scale for the Mission (2) vehicle.
7. Test this optimum system under simulated space flight conditions and demonstrate automatic operation of the system.
8. Evaluate the test data and correlate the one-g to zero-g conditions.
9. Identify and specify any desirable changes in the design of the system and its performance.

In Task I the specific objectives of (1) arriving at conceptual designs for a liquid propellant thermal conditioning system, and (2) performing an analysis of the processes occurring within each component of each conceptual design was accomplished.

Many different conceptual designs were screened and the system finally selected is shown schematically in Fig. 2. This system, as designed in Task II for the selected Mission (2), is depicted in Fig. 3. It is shown mounted in the preferred position on the inside surface of the tank access-hole cover.

The selected system consisted of the following basic components (as shown in Figs. 2 and 3):

(1) Fluid-removal unit (fluid filter)
(2) Expansion unit (pressure-drop valve)
(3) Heat-exchanger unit (compact counter-flow heat exchanger)
(4) Flow-control unit (solenoid shutoff valve)
(5) Mixer unit (electric motor-driven axial fan)
(6) Pressure switch

Proper control of the tank pressure by means of the thermal conditioning unit requires that the propellant cooled within the unit be circulated to all zones within the tank. This requirement arises because of the low thermal conductivity of liquid hydrogen.

Thus, maintenance of bulk liquid pressure and temperature conditions requires more than only local heat removal within the heat exchanger. In addition, proper circulation of liquid hydrogen within the tank must be induced and maintained under zero-gravity conditions. This circulation must be sufficient to ameleorate conditions to either prevent formation of, or to readily remove and collapse vapor bubbles or pockets at local areas of high heat input.

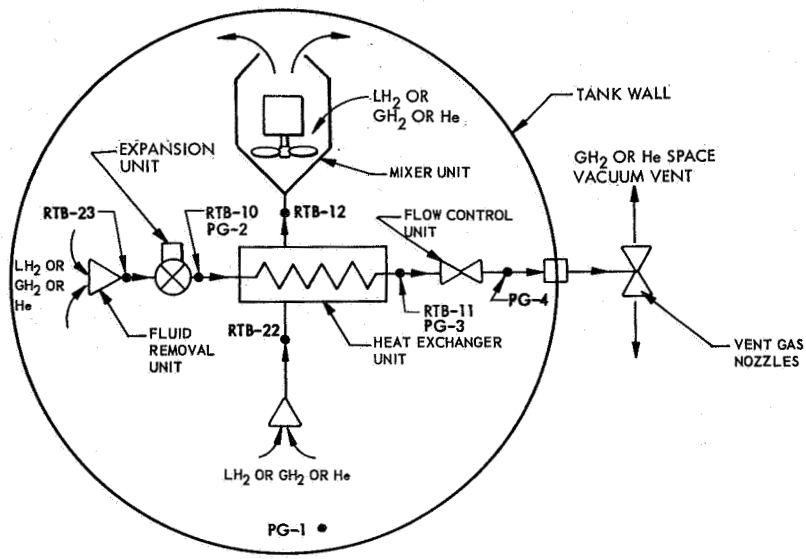

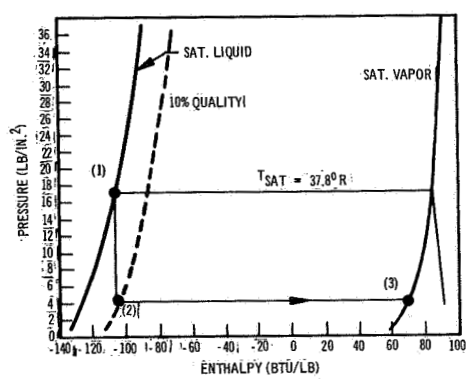

(a) Fluid Removal Unit Immersed in Liquid Hydrogen

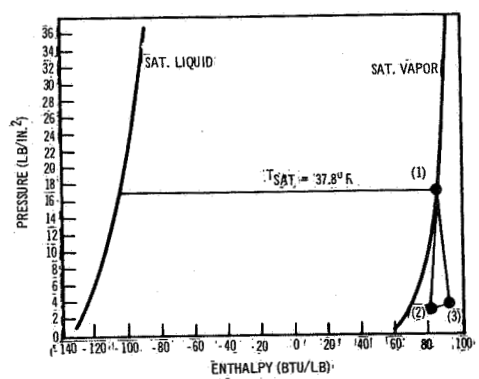

(b) Fluid Removal Unit Immersed in Gaseous Hydrogen

Fig. 2 Selected Liquid Propellant Thermal Conditioning System Schematic

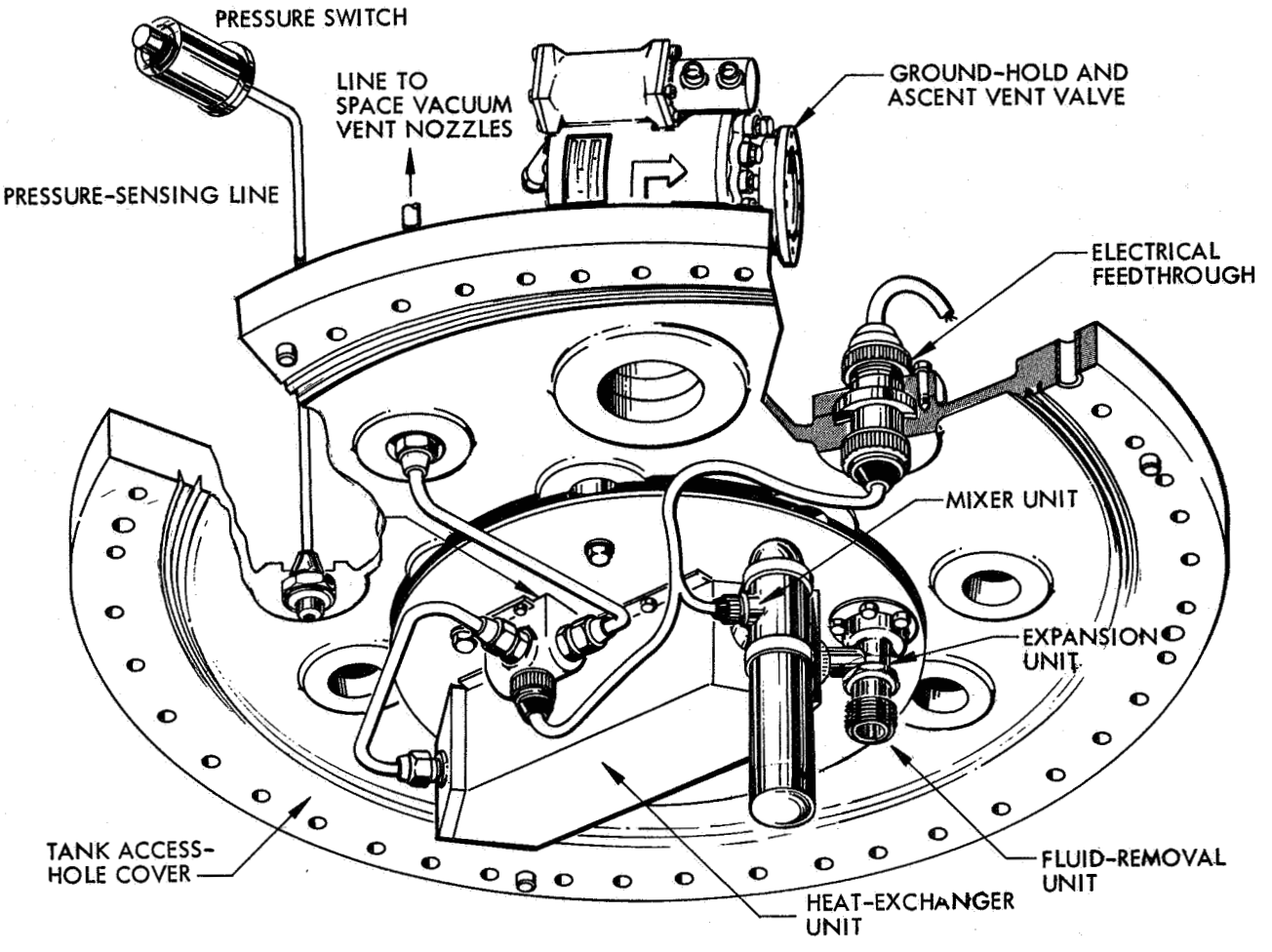

Fig. 3 Selected Thermal Conditioning System

New criteria, both theoretical and experimental, were established to provide the needed design data. Three significant new theoretical developments were formulated to provide the necessary theoretical relationships, scaling laws, and non-dimensional parameters for this program. These theories defined the physical relationships for determining the local mixer induced liquid velocities required to remove vapor bubbles attached to the tank walls in zero gravity; for determining the mixer jet velocities needed to totally penetrate intervening liquid or gas pockets in zero gravity; and for determining the local forced convection conditions needed to condense or collapse vapor pockets in zero gravity.

No experiments to check the validity relating to vapor bubble detachment or to vapor bubble condensation have been conducted. Experiments were conducted, however, at both Lockheed and the NASA-LeRC verifying the jet penetration theory in zero-gravity. At Lockheed an extensive series of simulated zero-gravity mixer tests with water-air and with alcohol-air mixtures were conducted in a test apparatus consisting of two plates of plexiglass 1/8-in. apart (Fig. 4). The flow patterns with these fluids in cross sections (1/8-in. thick slices) of two circular tanks 1 ft and 2 ft in diameter were investigated. When the apparatus is mounted perfectly horizontal (Fig. 4), the gravity effects on the simulated mixer jet fluid motions are almost negligible. Only inertial, surface tension, and viscous forces are dominant. Figure 5 shows a series of these simulated zero-gravity mixer flow photographs that provided experimental verification of the new theoretical zero-gravity mixer flow design criteria. Additional experimental verification of the theory was obtained at NASA-LeRC in mixer jet experiments in 10, and 20-centimeter diameter tanks conducted in a large drop tower facility. Some selected photographs illustrating the flow patterns obtained in actual zero-gravity are shown in Fig. 6. Both wall jets and axial or central jet tests were conducted with the apparatus shown in Fig. 7.

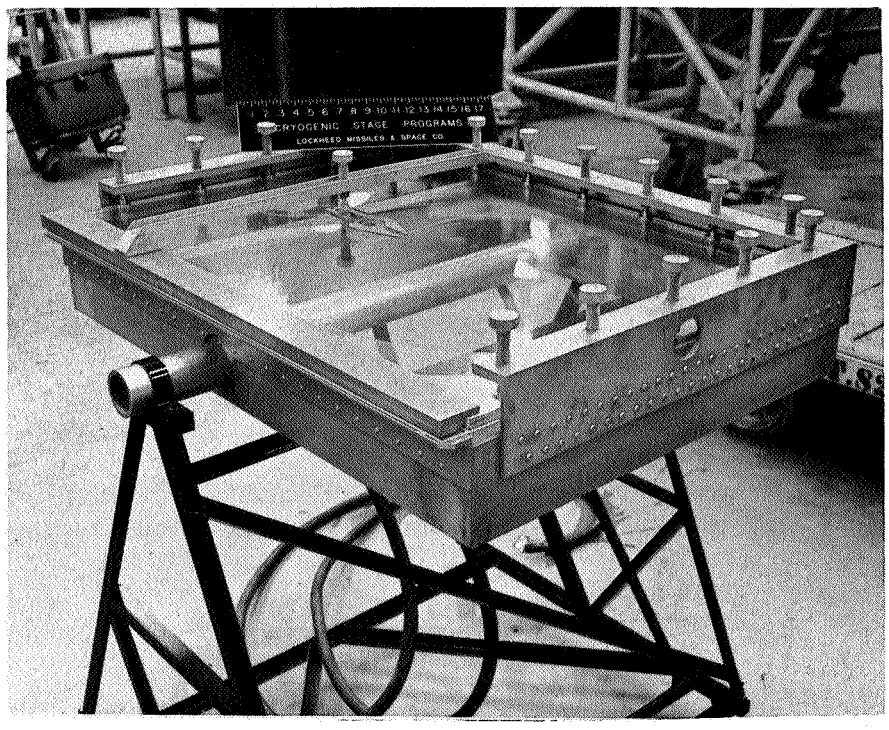

Fig. 4 Two-Dimensional Flow Test Apparatus

Below Critical Circulation – Central jet will not penetrate intervening fluids and gas bubbles or pockets to the opposite tank wall (large stagnant regions in the tank).

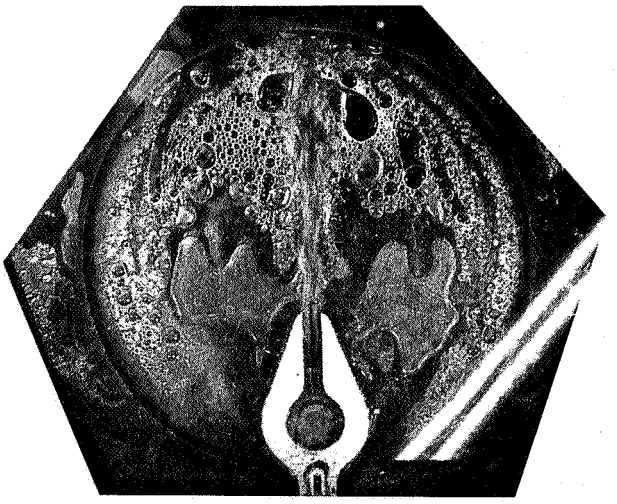

Critical Circulation – Central jet will just penetrate all intervening fluid and bubbles to the opposite tank wall (some circulation throughout the tank).

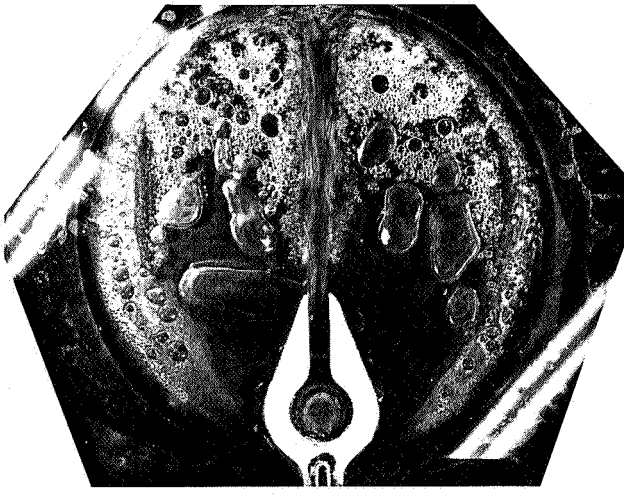

Above Critical Circulation – Central jet readily penetrates all intervening fluids and bubbles to the opposite tank wall (vigorous mixing in all regions of the tank).

Fig. 5 Experimental Liquid-Ullage Patterns With an Axial Jet in a Propellant Tank in 2-D Simulated Zero Gravity

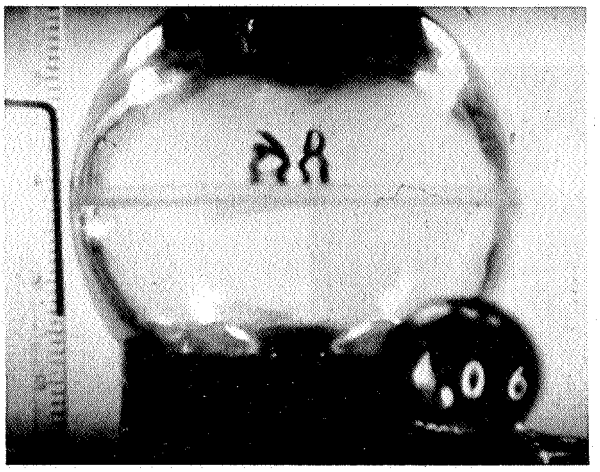

Below Critical Circulation with a Wall-Bound Jet – Wall jet will not penetrate intervening fluids and gas pockets attached to the tank wall (large stagnant regions in the tank).

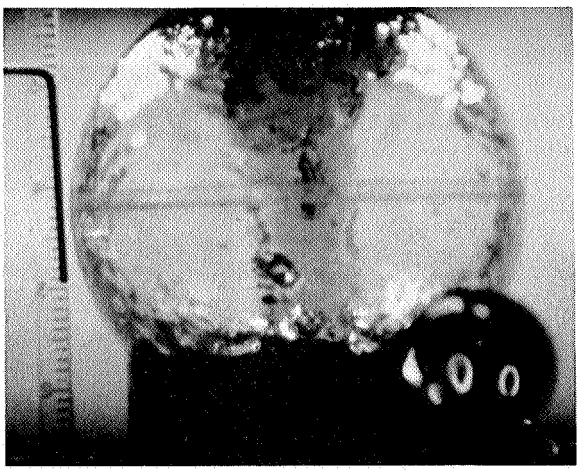

Above Critical Circulation with a Wall-Bound Jet – Wall jet readily penetrates all intervening bubbles and fluids attached to the tank walls (vigorous mixing throughout the tank).

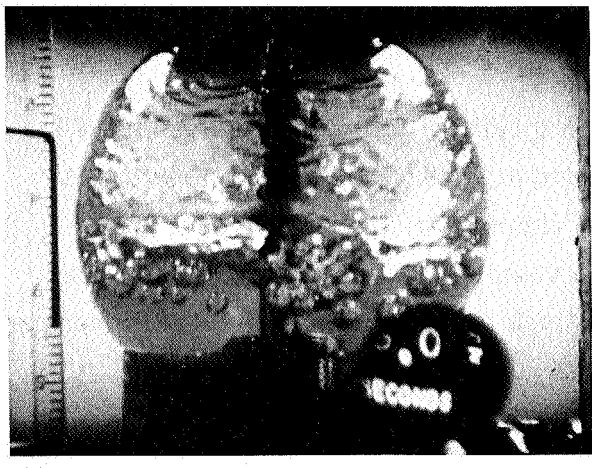

Above Critical Circulation with a Central Jet and Standpipes – Central jet readily penetrates all intervening fluids and bubbles along the central standpipe to the opposite tank wall (vigorous mixing throughout the tank).

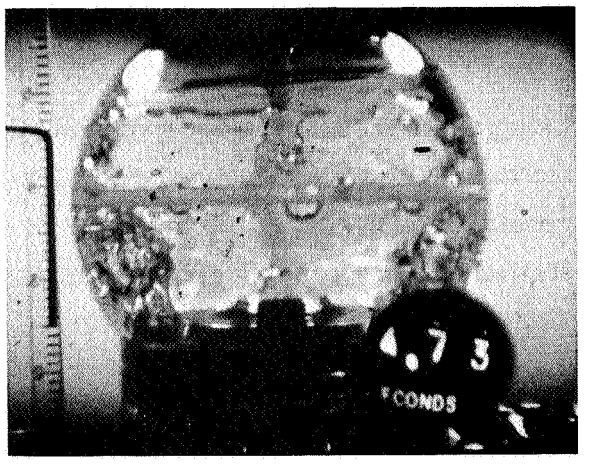

Above Critical Circulation with a Central Jet – Central jet readily penetrates all intervening fluids and bubbles to the opposite tank wall (vigorous mixing throughout the tank).

Fig. 6 Circulation Patterns in Zero Gravity as Determined From Drop-Tower Tests With Ethanol (Tank Diameter = 10 cm)

Fig. 7 10-Centimeter-Diameter Experiment Tank

Using these theoretical and experimental data a central jet mixer was designed for the thermal conditioning system which provided a jet size and velocity ten times greater than needed in zero gravity to obtain vigorous mixing and total jet penetration to the opposite wall of the Mission (2) vehicle tank. This mixer also provided the required forced convection flow through the warm side of the heat exchanger unit.

Following approval of this selected thermal conditioning system the unit was fabricated. Figure 8 shows this unit as mounted to the inside surface of the access-hole cover of Lockheed's 110-in. diameter liquid hydrogen tank (Fig. 9). This tankage system was a full-scale version of a flight-type system as would be employed on the selected Mars orbiter Mission (2). This thermal conditioning system was tested in the 110-in. diameter tank within the cryogenic space vehicle flight simulator facility (Fig. 10). This facility is 16 ft in diameter by 23 ft high; it has the capability of

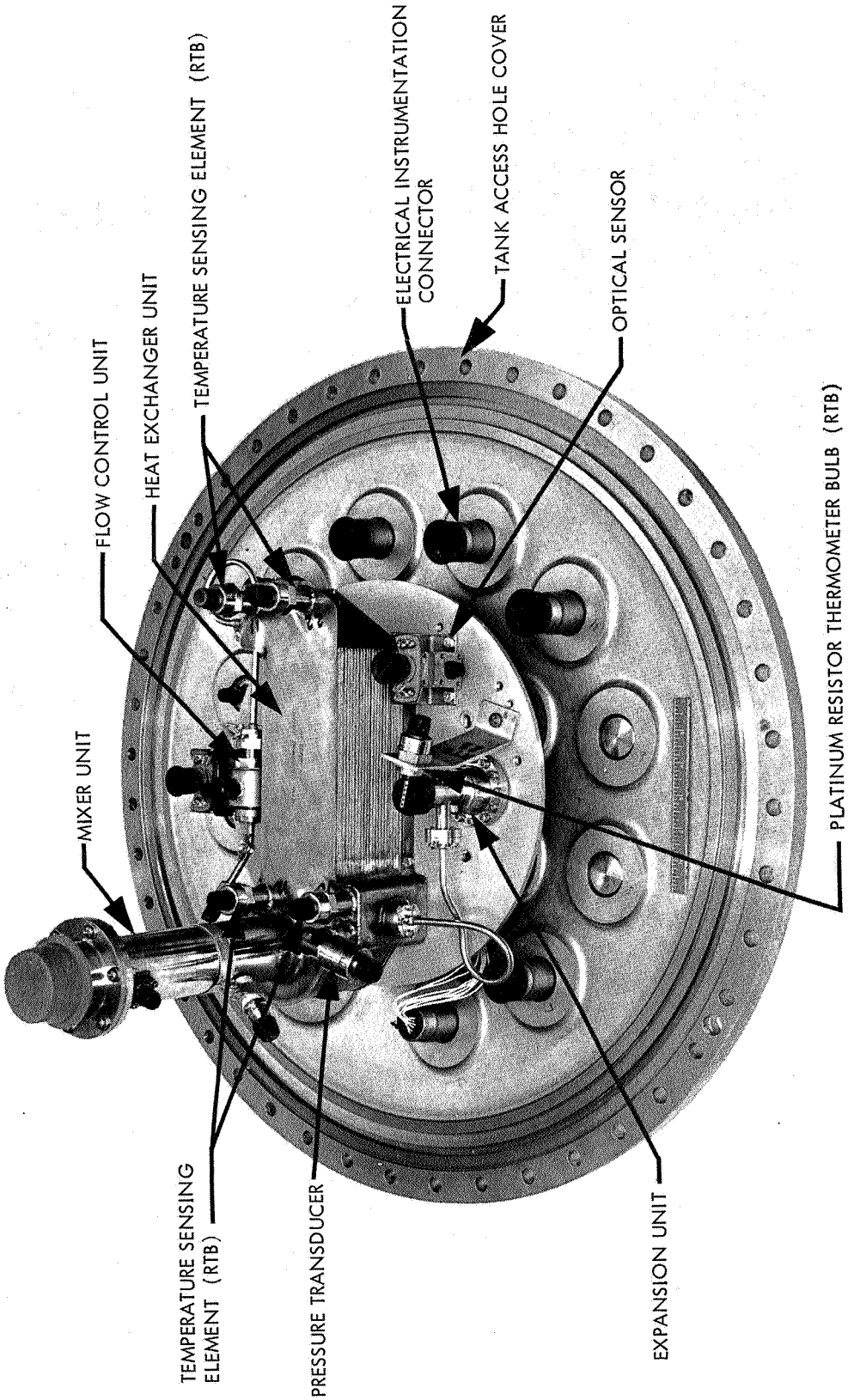

Fig. 8 Thermal Conditioning System Mounted on Inside Surface of Access-Hole Cover

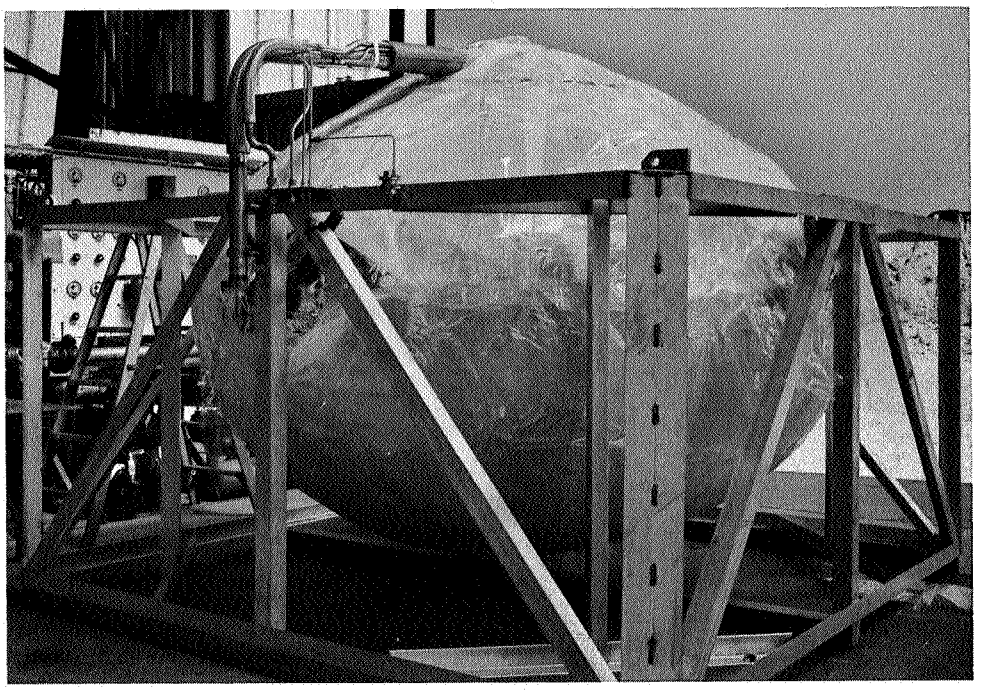

Fig. 9 110-in.-Diameter Liquid Hydrogen Tank

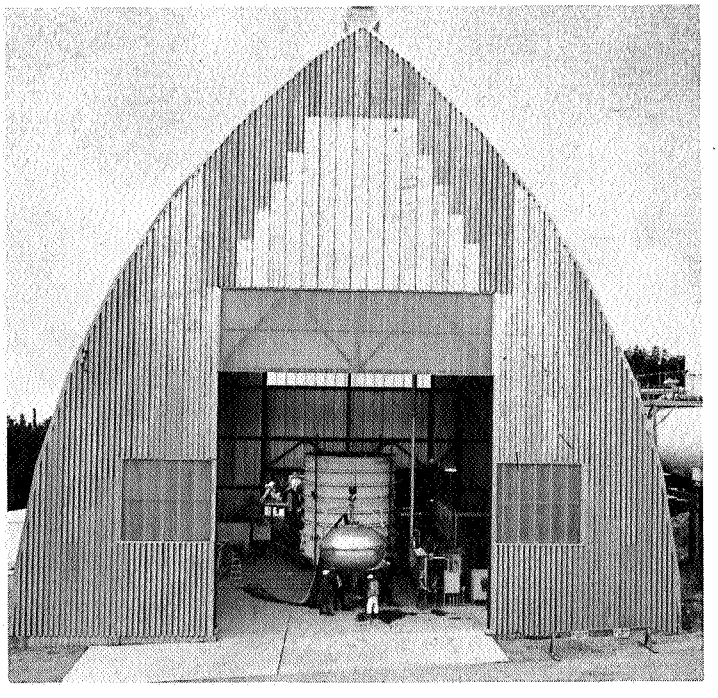

Fig. 10 Cryogenic Flight Simulator Facility

duplicating a launch-vehicle ascent pressure-drop rate down to 0.5 psia and of achieving 10^{-4} Torr vacuum within 1-1/2 hr and 10^{-6} Torr steady-state vacuum within 6 hr. Ascent and space thermal heat flux is programmable by means of liquid nitrogen cold walls and heat lamps to simulate vehicle orientation effects. The thermal conditioning unit was tested both at the top or side of the tank to determine orientation effects relative to the one-g gravitational forces. Figure 11 shows the unit mounted on the side of the 110-in.-diameter tank. This complete series of extensive testing of the unit and the liquid hydrogen tankage system covered more than 120 hr, with one series covering 90 hr of continuous operation of alternate venting and nonventing.

This thermal conditioning system development program demonstrated that a lightweight unit (15 lb) automatically and efficiently controls the pressure of a full-scale, flight-type, liquid hydrogen tank—whether the unit is submerged entirely in the liquid hydrogen, only partially submerged, or entirely exposed to only the ullage gases. Little or no significant differences in system operations were noted for the unit in either the tank top- or side-mounted locations.

In summary, consistent, highly effective operation of the unit was obtained regardless of its orientation, location, or degree of submergence within the liquid hydrogen tank. Furthermore the unit was designed for such operation in zero-gravity flight based upon the latest zero-gravity technology. It is expected, therefore, that this system will perform equally successfully in zero-gravity space flight. However, positive confirmation of such a conclusion can only come from an actual space flight demonstration of the unit in a liquid hydrogen tankage system.

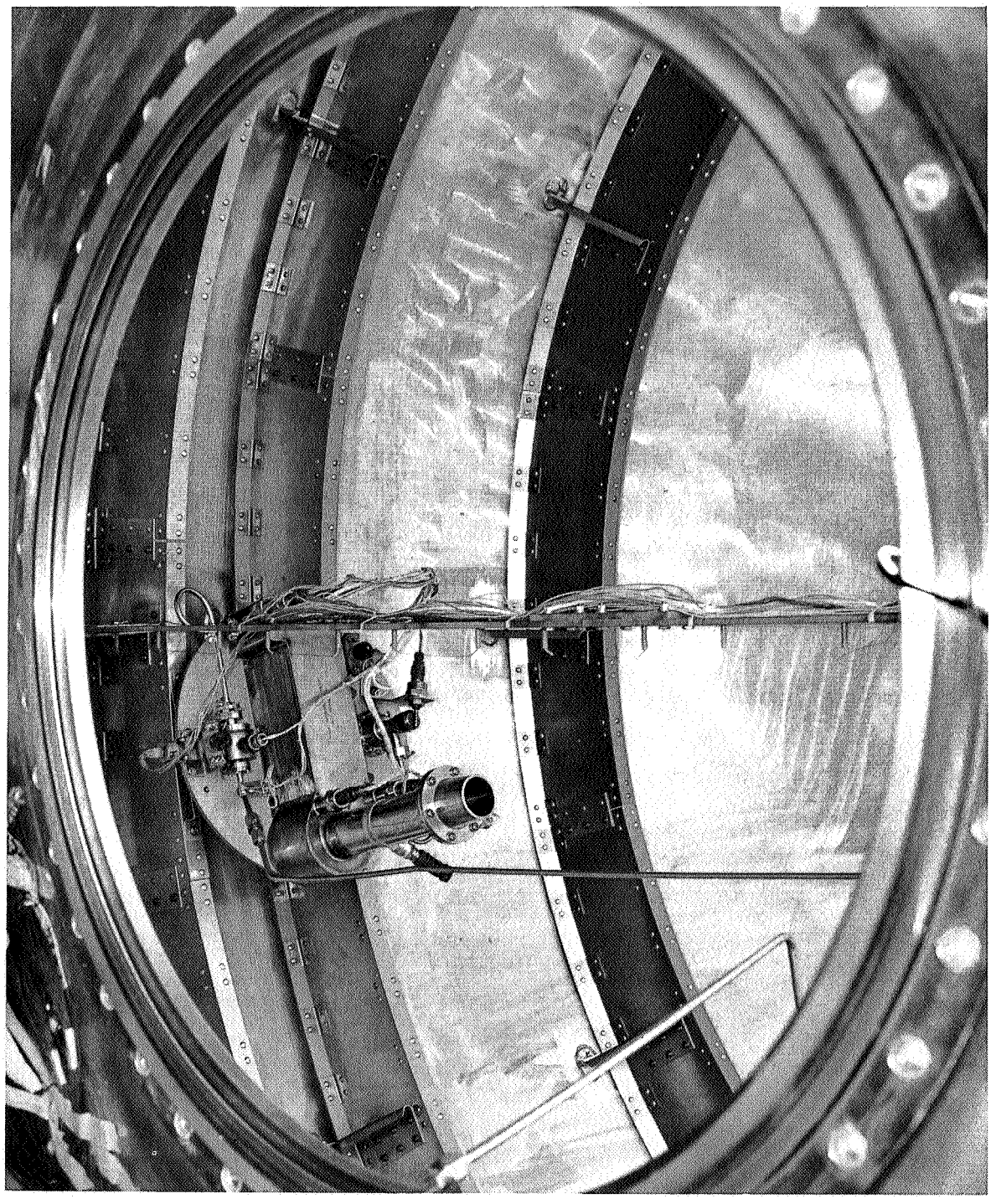

Fig. 11 Thermal Conditioning System Mounted on Side of 110-in.-Diameter Tank

SYSTEM DESIGN AND PERFORMANCE REQUIREMENTS

SYSTEM DEFINITION AND PERFORMANCE

The basic function of the liquid propellant thermal conditioning system is to maintain pressure control of the liquid hydrogen tank during zero- and low-gravity coast periods in space flight when location of the gas ullage region is somewhat uncertain. Control of the tank pressure is accomplished through the combined use of the six basic units listed below and shown in Fig. 2. Figure 2 also shows the basic thermodynamic process as applied to the vent fluid.

- Fluid-removal unit
- Expansion unit
- Heat-exchanger unit
- Mixer unit
- Flow-control unit
- Pressure switch

The fluid-removal unit provides gaseous or liquid hydrogen [State (1), on Fig. 2] to the expansion unit and heat exchanger so that the total enthalpy change is adequate to remove heat deposited in the propellant from heat leaks through insulation, plumbing, and tank support structure. This unit is simply a fluid filter intake.

The expansion unit lowers the pressure and temperature of the incoming fluid [State (2), Fig. 2] . When flowing liquid hydrogen, this temperature drop provides the necessary thermal driving potential for operation of the heat exchanger. When flowing gaseous hydrogen and/or helium pressurant gas, tank pressure control is accomplished by direct venting of hydrogen boiloff and pressurant gas. This unit is basically a high pressure-drop pressure regulator.

The heat exchanger is the unit where heat is transferred from the propellant in the tank to the refrigerated vent vapor coming from the expansion unit. In the process, the propellant in the tank is cooled and the refrigerated vent vapor is converted to a saturated or superheated vapor, which is then discharged from the propellant tank [State (3), Fig. 2]. A compact, counterflow heat exchanger was selected for this unit.

The mixer unit serves two functions that are particularly important in a zero-gravity environment. It induces flow of the tank propellant through the warm side of the heat exchanger; thus providing cooling of this fluid by forced convection rather than by pure conduction. This results in a relatively compact, lightweight heat exchanger and also provides more uniform energy extraction and faster pressure response.

However, a reduction in tank pressure is not achieved by cooling the bulk liquid unless the subcooled liquid can be used to induce vapor condensation. An analysis is presented in Ref. 1, which shows that the condensation rate is related to the circulation velocity of the subcooled liquid at the liquid-vapor interface. The mixer unit creates velocity gradients throughout the propellant tank which provide the mechanism for the vapor condensation and the associated positive pressure control. On the basis of the analysis conducted in Tasks I, II, and III, and reported in Ref. 1, a dc electric brushless motor-driven axial fan was recommended for flight application.

The flow-control unit provides the system vent-flow shutoff function, as well as a fixed-orifice flow area. Because only gaseous hydrogen and/or helium will be present downstream on the heat exchanger cold side, a relatively constant vent flow rate will be attained during periods of tank venting. This unit is a carefully sized solenoid-operated valve.

The pressure switch mounted outside the tank senses tank pressure. The aneroid within the pressure switch contracts as the tank pressure increases; an actuator then moves, causing the electrical switch element to close; and the solenoid of the flow control unit and the electric motor of the mixer units are activated at a preset pressure level. In a similar manner, these units are deactivated at a preset lower pressure level reached after tank venting.

The performance and weight of each of the components is effected in different ways by the design flow rate, and it is imperative that they be properly matched to give the lightest total system weight consistent with positive pressure control. The minimum possible vent rates correspond to continuous venting with constant tank pressure. These minimum rates are determined by the external heating rates and the vent pressure. Increasing the vent rates decreases the vent frequency and requires higher fan powers. However, it also provides higher warm-side heat transfer coefficients through the heat exchanger, and results in smaller heat exchangers. In addition, the operating time decreases and the fan-unit efficiencies increase, thus indicating the possibility that an optimum vent flow rate exists for any given vehicle and mission.

The total effective system weight includes the hardware weights, the propellant boiloff resulting from the energy supplied to the mixer unit, and the increased weight of the power supply needed to furnish power to the mixer. Figure 12 shows the effect of vent rate on the contributing weight elements as well as the total system weight for Mission (2) 220-day duration. Also shown are the optimum design points for the Missions (1) and (3) vehicles, which occur for a design vent rate of 1.4 lb/hr. It can be seen that the optimum vent rate for Mission (2) is actually 1.1 lb/hr, but the selected design point of 1.4 lb/hr makes the same thermal conditioning system applicable to all three missions with an insignificant increase in weight of the Mission (2) vehicle.

The minimum vent rate considered for Mission (2) is 0.13 lb/hr for which the electrical heat input weights are much larger than the fixed hardware weights because of very low fan and motor efficiences for a mixer and heat exchanger matched at the flow rate.

As the design vent rate is increased, the flow and motor efficiences also increase, and the net result is a decrease in the total heat input penalty. This heat input penalty decreases faster than the hardware weight increases until the optimum design point is reached. For flow rates higher than the optimum, the hardware weight increase is greater than the electrical heat input penalty decrease.

It should be noted that Fig. 12 is a loci of design points for matched components for which the energy transfer rates in the heat exchanger and at the liquid/vapor interface

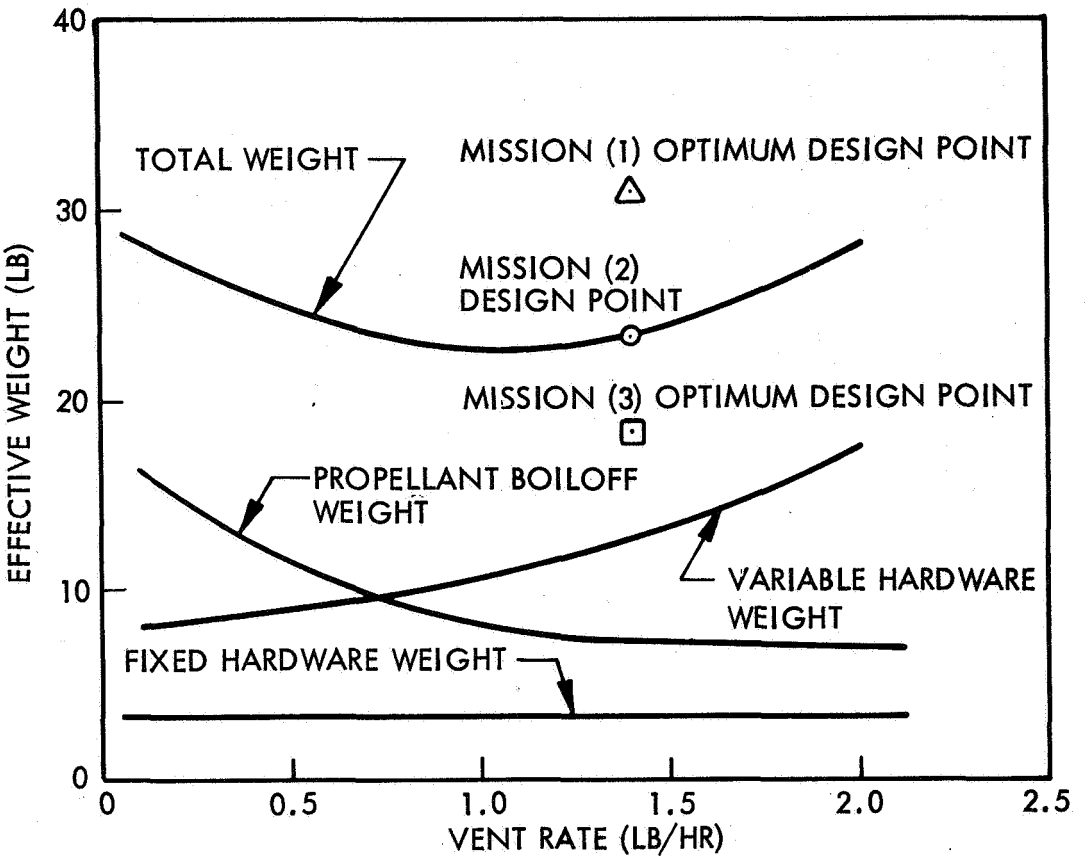

Fig. 12 Optimum Thermal Conditioning System Vent Flow Rate for Mission (2) (Fuel Cell Power Supply)

are equal (i.e., no subcooling). Therefore, increasing the size of the heat exchanger without increasing the size of the mixer, or vice-versa, would not necessarily increase the pressure response. However, for the flow-matched systems, the higher the vent rate, the faster will be the pressure response, although this faster response is achieved at the expense of increased weight.

Figure 8 shows the assemblage of these components into the thermal conditioning unit shown conceptually in Fig. 3. Each of the basic components is identified for easy recognition. The thermal conditioning system is shown mounted to the inside surface of the tank access-hole cover. When the cover is installed, the mixer discharge is pointed downward into the tank. This mounting position is the recommended location,

primarily from considerations of ease of installation, accessibility, and checkout. Other locations within the tank, such as tank bottom or tank side, are equally effective with the top-mounted position from considerations of tank pressure control. This will be subsequently shown in comparison of the top- and side-mounted data in the test program section of this report.

The thermal conditioning unit was fabricated for extensive testing in liquid hydrogen. Figures 8, 13, and 14 show the fabricated unit. The caps shown in Figs. 13 and 14 are removed when the system is installed for operation in the liquid hydrogen tank. Such caps covering instrumentation ports, fluid removal unit intake, mixer unit discharge, and the like are used to protect the system from accidental entry of dirt or contamination by foreign substances. All of these assembled components, except the pressure switch, are mounted to an aluminum plate. The pressure switch is mounted external to the tank and, therefore, operates at temperatures of $400 \pm 200°R$. The principal material of construction of all components, except the base plate, is stainless steel.

Table 2 shows the system design operating conditions. This thermal conditioning system is designed to function properly and to control tank pressure under each of the environments that could be expected in the liquid hydrogen tank of the selection Mission (2) vehicle (Fig. 1) for which it was designed.

Each of the components of the thermal conditioning system were tested individually prior to assembly into the complete system. These included leakage and liquid nitrogen thermal shock tests on each component; flow tests on the heat exchanger, mixer, and flow control units; and pressure regulation tests on the pressure switch and expansion unit. Hydrogen was not employed in any of these component tests; such testing was conducted only on the assembled system. Each component, its design specifications and test results, are discussed in the following paragraphs.

Fluid Removal and Expansion Units

Design of the selected expansion unit incorporates features necessary to produce a minimum-weight unit of high reliability. A sectional view of the valve is shown in

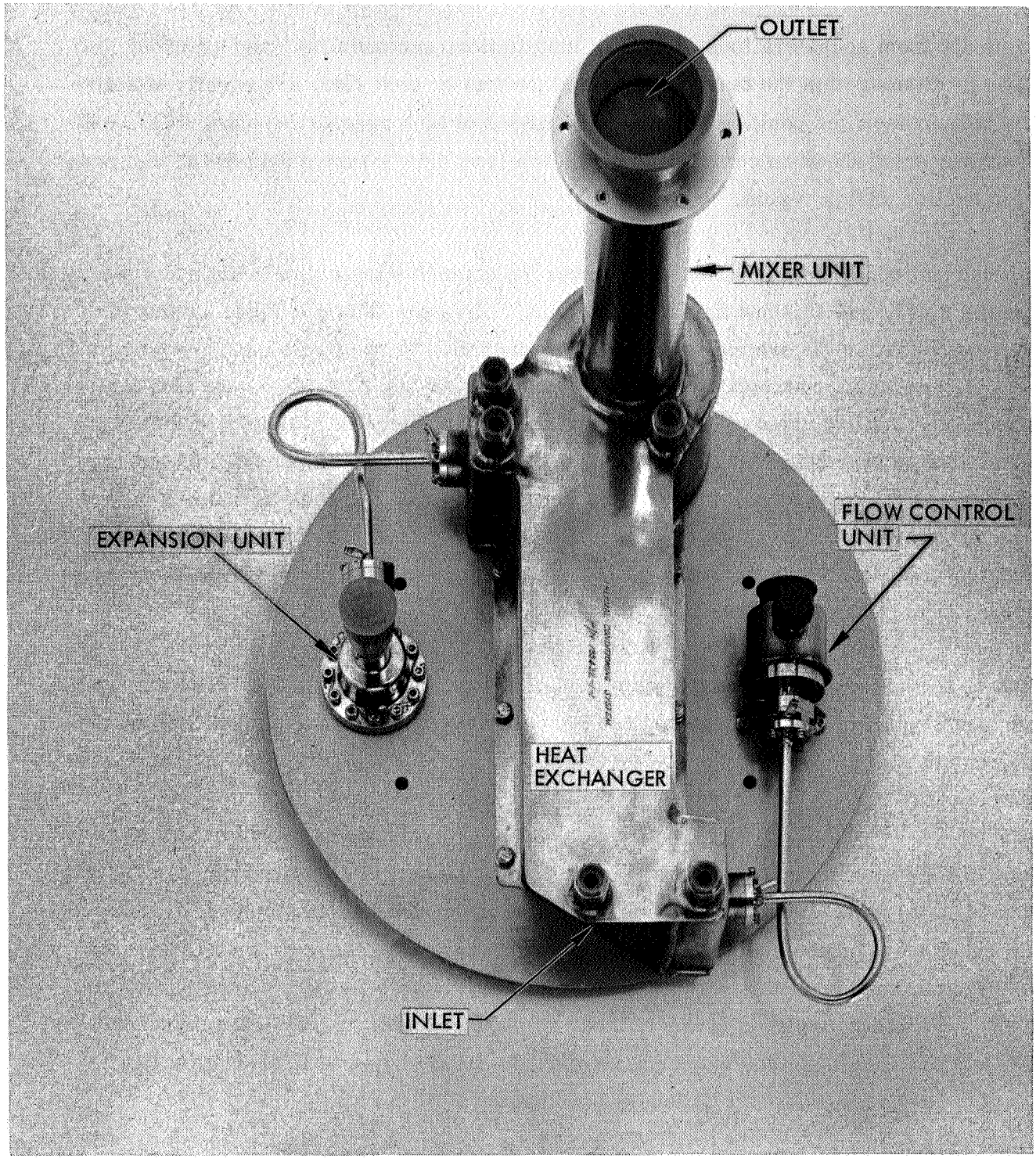

Fig. 13 Assembled Liquid Propellant Thermal Conditioning System Components

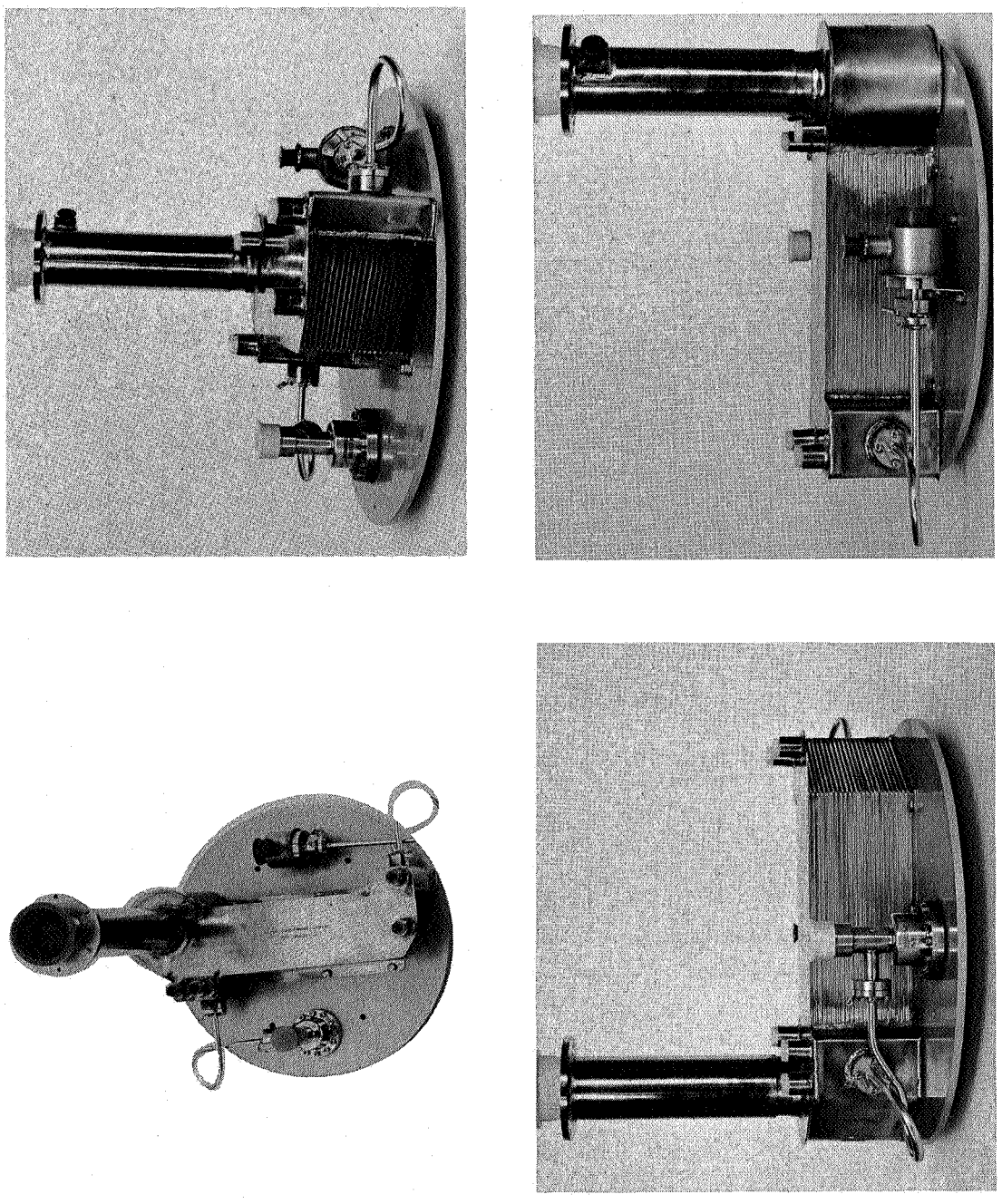

Fig. 14 Assembled Liquid Propellant Thermal Conditioning System

Table 2

SYSTEM DESIGN OPERATING CONDITIONS

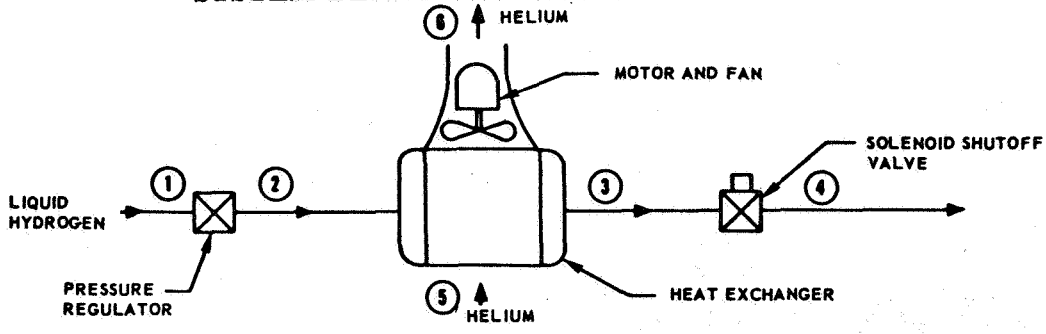

Conditions									
Station	Temperature (°R)	Pressure (psia)	Velocity (ft/sec)	Flow Rate (lb/hr)	Quality (lb vapor/lb fluid)	LH_2	Two-Phase Hydrogen	GH_2	GHe
Cold-Side Fluid — LH_2, Warm-Side Fluid — LH_2									
1	37.4	17	0	1.4	0	X			
2	29.6	4	0.037	1.4	0.08		X		
3	29.6	4	0.5	1.4	1.00			X	
4	29.6	< 2	88.0	1.4	1.0			X	
5	37.4	17	2.7	1320	0	X			
6	37.4	17	5.0	1320	0	X			
Cold-Side Fluid — LH_2, Warm-Side Fluid — GHe									
1	37.4	17	0	1.4	0	X			
2	29.6	4	0.037	1.4	0.08		X		
3	29.6	4	0.50	1.4	1.0			X	
4	29.6	< 2	88.0	1.4	1.0			X	
5	37.4	17	2.7	57.4	1.0				X
6	34.1	17	5.0	57.4	1.0				X
Cold-Side Fluid — GH_2, Warm-Side Fluid — GH_2									
1	37.4	17	0	1.3	1.0			X	
2	37.0	4	0.56	1.3	1.0			X	
3	37.0	4	0.56	1.3	1.0			X	
4	37.0	< 2	105.0	1.3	1.0			X	
5	37.4	17	2.7	28.5	1.0			X	
6	37.4	17	5.0	28.5	1.0			X	
Cold-Side Fluid — LH_2, Warm-Side Fluid — GH_2									
1	37.4	17	0	1.4	0	X			
2	29.6	4	0.037	1.4	0.08		X		
3	29.6	4	0.5	1.4	1.0			X	
4	29.6	< 2	88	1.4	1.0			X	
5	37.4	17	2.7	28.5	1.0			X	
6	37.4	17	5.0	28.5	0.95		X		
Cold-Side Fluid — GH_2, Warm-Side Fluid — GHe									
1	37.4	17	0	1.3	1.0			X	
2	37.0	4	0.56	1.3	1.0			X	
3	37.0	4	0.56	1.3	1.0			X	
4	37.0	< 2	105.0	1.3	1.0			X	
5	37.4	17	2.7	57.4	1.0				X
6	37.4	17	5.0	57.4	1.0				X

Fig. 15. The unit is a normally closed, downstream absolute pressure regulating valve. Liquid hydrogen, under tank pressure, enters the valve body and acts against an evacuated bellows sensing element. The internally evacuated bellows is externally exposed to the regulated downstream pressure. This element is initially positioned by the calibration spring to be in a slightly contracted position when downstream pressure is above 4 psia; thus, the spring force and the pressure force acting on the bellows keeps the poppet seated. As the regulated pressure drops below 4 psia, the bellows expands, causing the metering valve to modulate open and maintain the desired pressure at the heat-exchanger inlet. The unit is sized to operate with inlet pressures from 17 to 28 psia with an outlet pressure of 4.0 to $\pm$0.4 psia. The required sensitivity and minimum hysteresis are obtained in this configuration by designing for the least possible number of friction points and by maintaining high actuation-to-friction-force ratios. Also, the valve seat can be machined as an integral part of the outlet body, thus eliminating an insert arrangement requiring static sealing.

The design shown in Fig. 15 is based on all stainless steel construction for the following considerations:

- An aluminum housing would result in a potential leak path introduced by the necessity of incorporating a hard-seat insert.
- The reliability of stainless steel bellows capsules is substantially greater than aluminum capsules because of the greater uniformity of the material and the more advanced manufacturing techniques associated with welding stainless steel bellows elements.
- The use of more than one material could introduce potential problems associated with differential thermal expansion and galvanic corrosion.

An expansion valve discharge pressure of 4 psia was selected for the following reasons: It is sufficiently above the hydrogen triple point (1 psia) to prevent solid hydrogen from forming in the heat exchanger core or within the valve itself, which could result in jamming. It also provides sufficient pressure for actuation of the expansion valve by the bellows and allows a choked orifice for the flow control unit to be placed downstream from the heat exchanger.

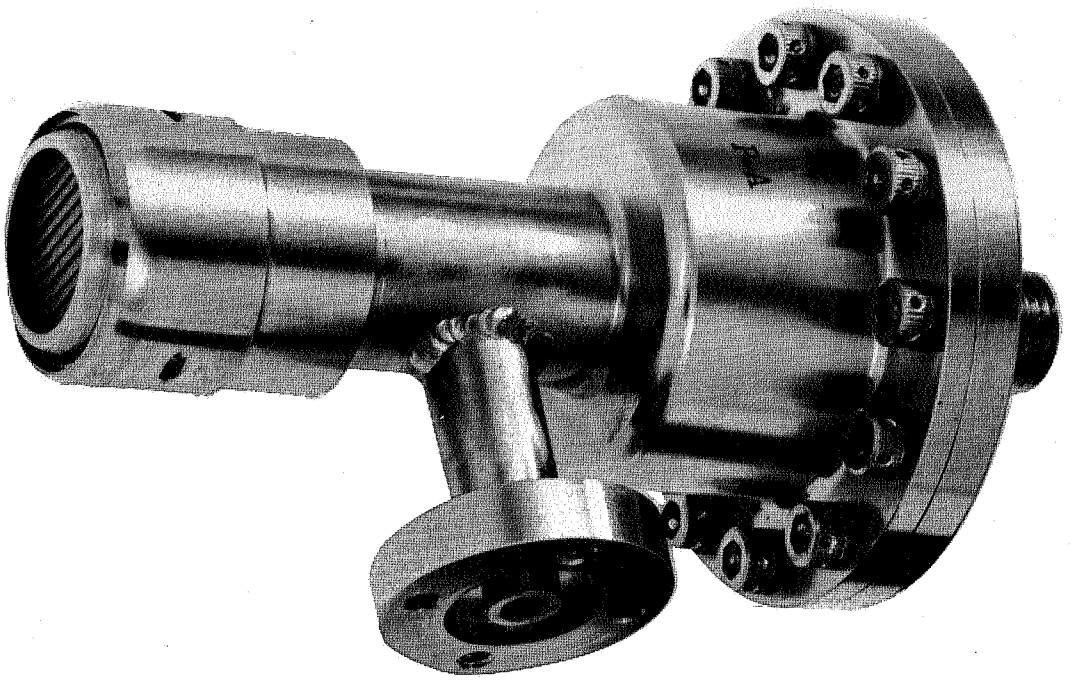

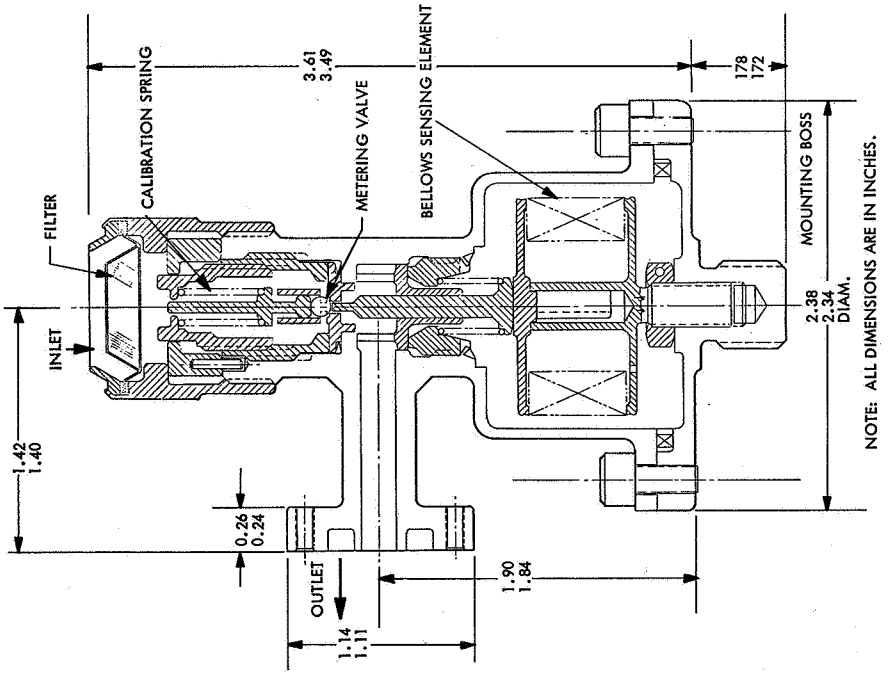

Fig. 15 Fluid Removal and Expansion Unit

The pressure regulator contains a large, integral 25-micron filter or fluid removal unit to protect the poppet and seat from particulate contamination. Figure 16 shows the expected thermodynamic performance of the expansion unit as a function of tank pressure. The regulated downstream pressure is assumed to be constant at 4 psia.

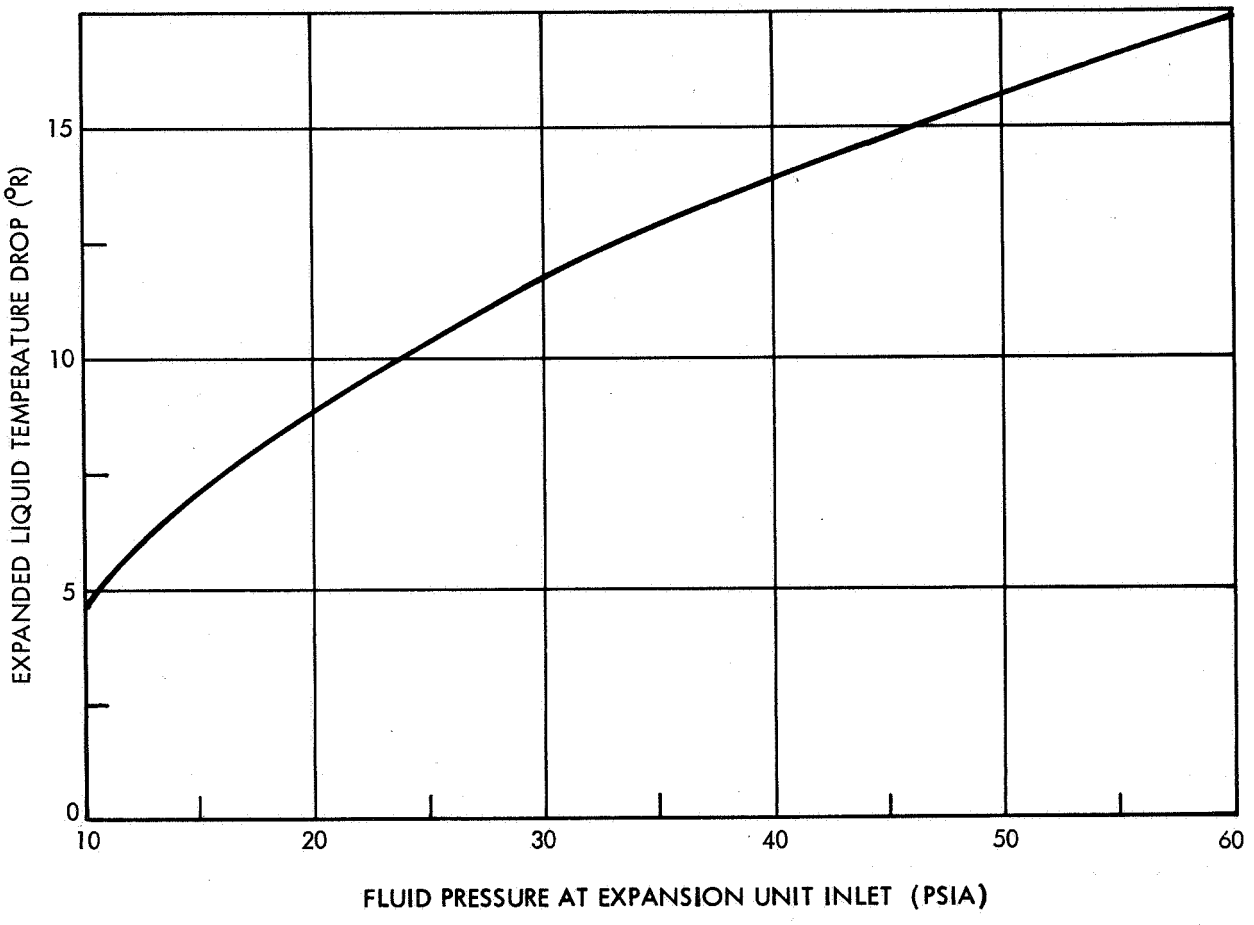

Fig. 16 Influence of Tank Pressure on Expansion Unit Temperature Drop

Figure 15 also shows a photograph of the fabricated expansion unit, which weighs 1 lb. Table 3 lists the specifications of the unit.

This valve is capable of checkout at room temperature. Flow, pressure control, and leakage tests were conducted at 70° F and - 320° F. The unit met all performance requirements except for internal leakage. At ambient temperature, the leakage rate

Table 3

EXPANSION UNIT DESIGN SPECIFICATIONS

Fluid	Liquid or gaseous hydrogen
Operating Pressure	17−28 psia (inlet); 4.0 ±0.4 psia (regulated)
Proof Pressure	50 psia
Burst Pressure	70 psia
Temperature	37.4° (inlet); 37 to 530° R (ambient)
Flow Rate	0−2 lb/hr of gaseous hydrogen with an inlet pressure of 17 psia and an inlet temperature of 37.4° R
Leakage	91 cc/hr of GH_2 with saturated gaseous hydrogen at 17 psia and downstream pressure of 6 psia
Weight	1 lb

was 8.4 cc/hr and at - 320° F, 800 cc/hr. However, leakage past the expansion unit does not result in propellant loss providing the flow control unit which is located downstream is within leakage specifications. The important consideration with respect to expansion unit leakage is that it be sufficiently small to maintain low valve seat pressures and pressure regulation within desired tolerances. The pressure-control band width, with varying inlet pressure and temperature was very tight, as shown in Table 4. Therefore, the measured leakage was considered to be acceptable, since it did not alter the important function of this unit.

Table 4

EXPANSION UNIT PRESSURE CONTROL CHARACTERISTICS

Inlet Temperature (° F)	Inlet Pressure (psia)	Controlled Pressure (psia)
70	17	3.94
70	28	3.89
- 320	17	3.88
- 320	28	4.01

Heat Exchanger Unit

The heat exchanger must be capable of transferring to the vented propellant the heat conducted into the propellant tank from the exterior through insulation, plumbing, and support structure, as well as any heat put into the tank to drive the rotating parts of the system. The refrigeration produced by the expansion unit provides the temperature difference for heat transfer. The necessary heat transfer may be accomplished with a compact heat exchanger.

The flow phenomena in boiling and condensing hydrogen within a compact heat exchanger are usually envisioned as annular flow at low fluid quality and mist flow at high fluid quality. For annular flow, a layer of liquid hydrogen is attached to the walls of the flow passages, and high heat-transfer coefficients are obtained. For mist flow, the liquid phase exists as small droplets in the central region of the flow passage. The heat-transfer coefficients in the annular flow regime were developed using Chen's correlation. Hendrick's correlation was used in the mist flow regime. Both correlations, as well as the Martinelli correlation for pressure drop, have been computerized. With the aid of these programs, an iterative design approach was used to arrive at a final design, representing an optimum tradeoff between heat exchanger weight and mixer unit pumping power. In this design the transition from annular to mist flow was assumed to occur at 50-percent quality. The location of the transition point is conservative based on experience and tests of various investigators. For example, a design and successful test of a remote-storage evaporative oil-cooling system for aircraft assuming an 80-percent transition point has been demonstrated (Ref. 3).

A counterflow plate-fin heat exchanger design was chosen. The general configuration of the heat exchanger is shown in Fig. 17. This configuration has better flow distribution than a crossflow heat exchanger. The unit is made of stainless steel using 20 rectangular fins per inch. The fins are offset and are 0.004 in. thick. The hot-side fins are 0.075 in. high with an uninterrupted length of 0.15 in. The cold-side fins are 0.050 in. high with an uninterrupted length of 0.10 in. It has a 3- by 3-in. core frontal area and a length of 7 in.

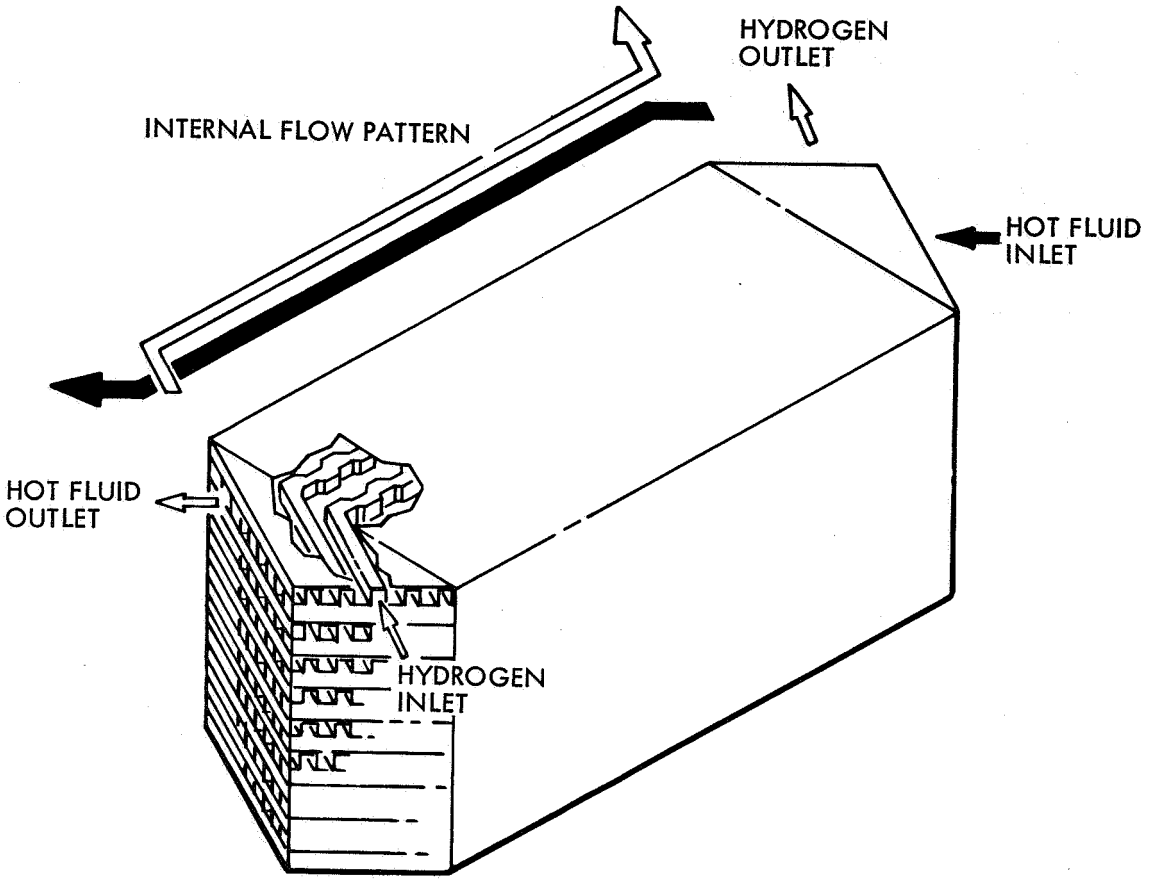

Fig. 17 General Configuration of the Selected Counterflow Heat Exhanger

The design point of the heat exchanger is that with helium gas on the hot side and with liquid hydrogen entering the expansion valve. This condition requires the largest heat-transfer rate with the lowest overall heat-transfer coefficient. The predicted performance of the system for these conditions was given in Table 2. The amount of heat removed, i.e., enthalpy change of the vented fluid, is 176 Btu/lb. The predicted temperature profile in the heat exchanger and the heat transfer coefficients are shown in Fig. 18. The sharp change in the temperature profile is due to the change in the mode of the flow from annular to mist. The area required for heat transfer is much larger in the mist regime because of the low mass flux on the cold side of the heat exchanger.

The design assumes no superheat in the exchanger on the cold side and has helium flow on the warm side. An additional 21 Btu/lb (maximum) of heat removal is possible

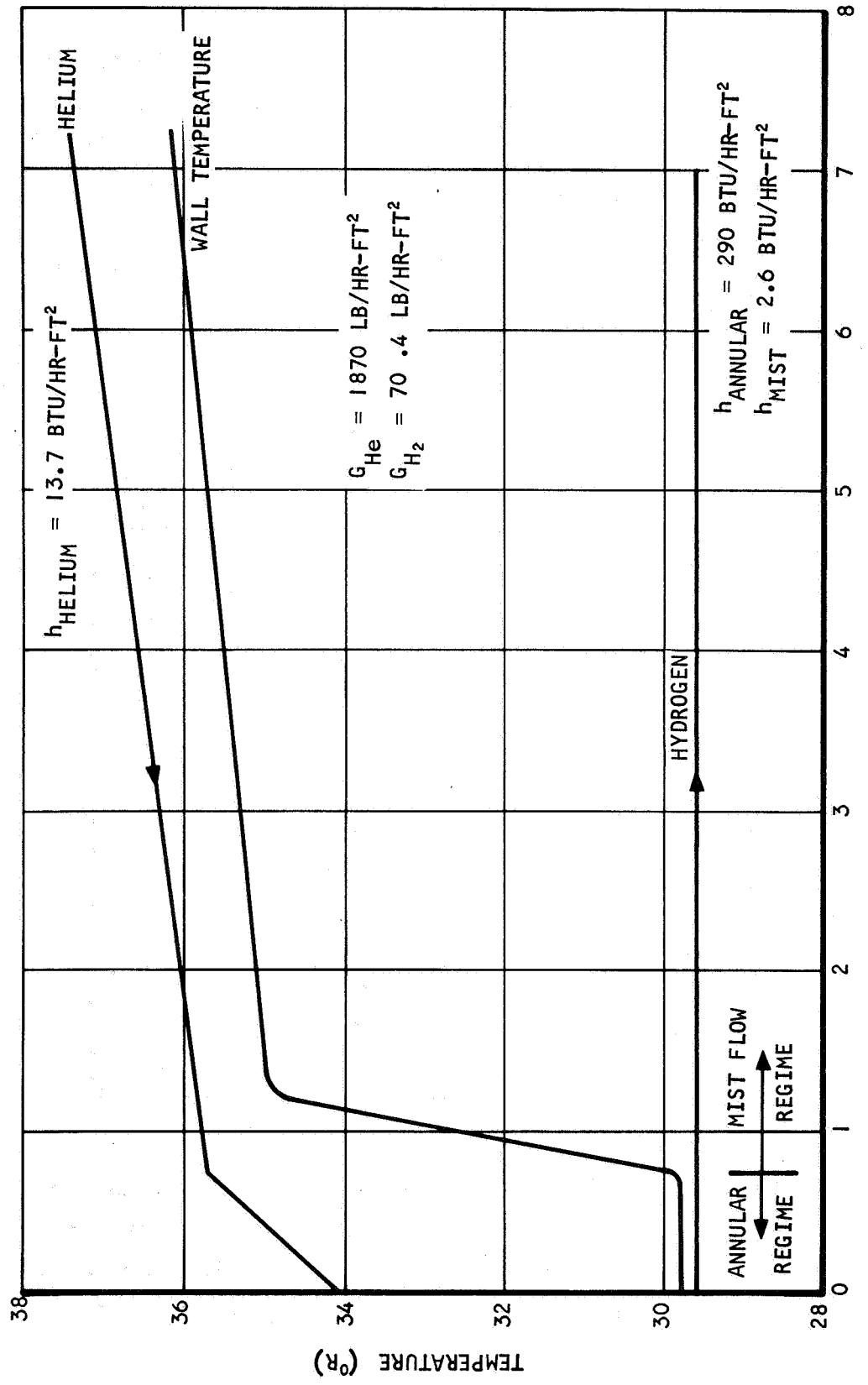

Fig. 18 Heat Exchanger Predicted Characteristics

if the cold fluid is heated to tank bulk fluid temperature. The present design should provide some superheat even with helium as the hot-side fluid, since the design is conservative. For all other conditions of hot- and cold-side flow, some superheat should be obtained.

Figure 19 shows a photograph of the fabricated heat exchanger unit, which weighs about 7.2 lb. Table 5 lists certain additional specifications.

Table 5

HEAT EXCHANGER UNIT DESIGN SPECIFICATIONS

Heat Transfer Rate – 248 Btu/hr	Cold Side	Hot Side
Fluid	GH_2 and LH_2 (8% inlet quality)	Helium
Flow Rate (lb/hr	1.4	57.4
Inlet Pressure (psia)	4	17
Inlet Temperature (°R)	29.6	37.4
Maximum ΔP, in. H_2O	6.0	0.06
Maximum Hot- or Cold-Side Pressure	28 psia	
Maximum Collapse ΔP Across Hot to Cold	24 psi	
Maximum Collapse ΔP Across Cold to Hot	11 psi	
Proof Pressure Across Hot to Cold	50 psia	
Burst Pressure Across Hot to Cold	70 psia	
Leakage – Hot Side at 28 psia	10^{-4} lb/hr of H_2	
Cold Side at 4 psia	10^{-4} lb/hr of H_2	
Weight (dry)	7.2 lb	

After the unit was fabricated and thermal shocked at -320° F, a leak was found at the outside weld of the hot-side manifold. The leak was repaired with silver braze, the unit was thermal shocked again, and the unit total leakage was found to be approximately 1×10^{-8} cc/sec of the helium (equivalent to 3×10^{-6} lb/hr of GH_2) which is well under

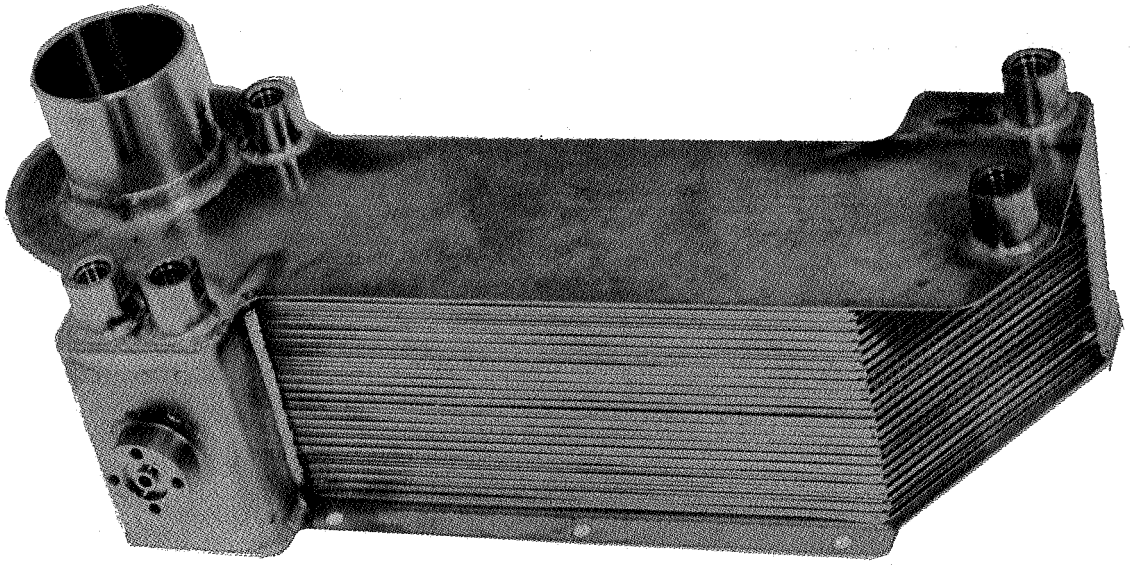

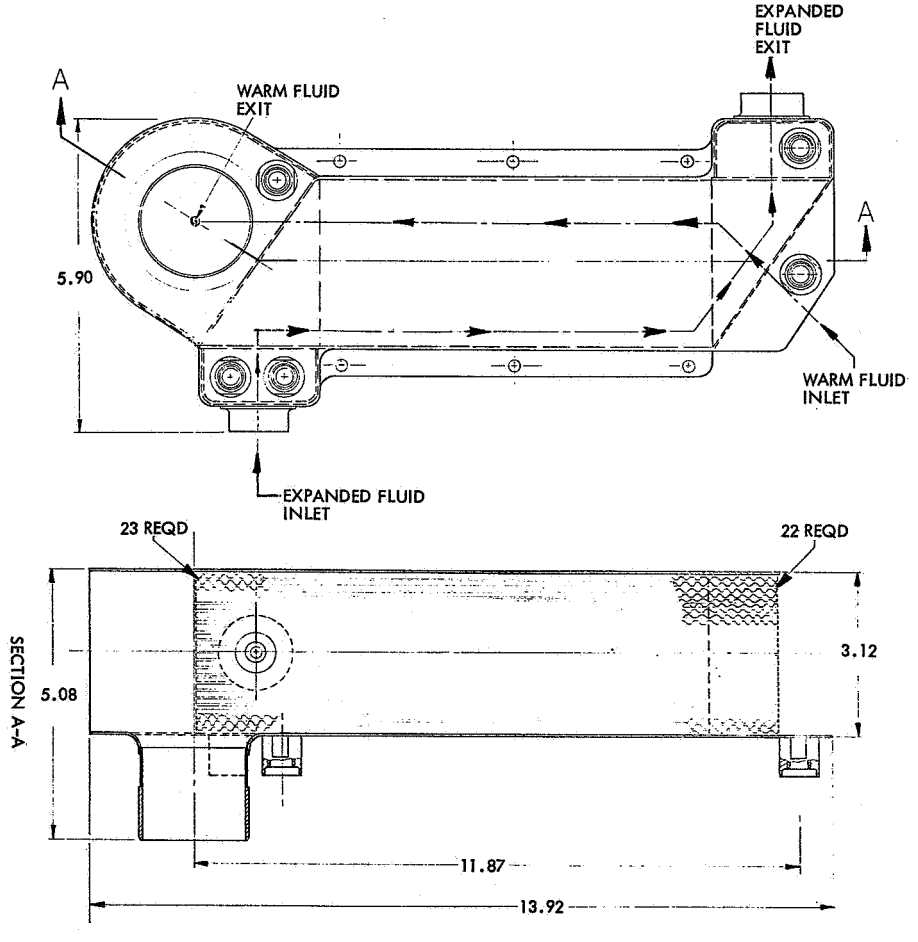

NOTE: ALL DIMENSIONS ARE IN INCHES.

Fig. 19 Heat Exchanger Unit

the performance requirement. The hot- and cold-side pressure drops were found using air. From these test data the hot- and cold-side pressure drops using helium and hydrogen gases were calculated to be slightly less than the above performance specifications. These data, as calculated from air test data, are summarized in Table 6.

Table 6

HEAT EXCHANGER PRESSURE DROPS

Hot Side: Liquid Hydrogen, 37.4°R at 17 psia	
Flow (cfm)	ΔP (in. H_2O)
3	0.44
4	0.77
5	1.13
Cold Side: 8% Quality Hydrogen, 30°R at 4 psia	
Flow (lb/hr)	ΔP (in. H_2O)
1.4	0.4

Flow Control Unit

It is necessary to place the flow control unit or shutoff valve downstream from the heat exchanger to prevent an expansion of hydrogen below its triple point. This would occur if the exhaust line from the heat exchanger was ducted directly to the vacuum environment of space. The valve can also be a flow-limiting device, which will improve system operation. The fluid state downstream from the heat exchanger will alway be gas, whether gas or liquid enters the expansion valve. The pressure at the flow limiting orifice will be maintained at a constant value of approximately 4 psia. For all conditions, the vapor will be within a few degrees of tank temperature. Thus, the orifice

will ensure that the flow through the system will be essentially constant, whether gas or liquid enters the expansion valve. This, then, allows the heat exchanger cold-side flow rate to be closely matched to system requirements.

The flow control unit consists of a solenoid valve and a current limiter. The current limiter is located outside the tank and is a semiconductor device that permits a high current to pass for 300 to 500 ms to allow the solenoid to pull in. The current then drops to a low value (about 30 ma) to hold the solenoid valve in the open position. With this approach, no coil compensation is necessary to limit current flow. The resultant holding power requirement is maintained at 0.06 w. Figure 20 shows a sectional view with dimensions of the flow control or solenoid valve and includes a photograph of the valve.

The solenoid valve is designed to limit the cold-side hydrogen flow to 1.4 lb/hr. This is a fail-closed valve. Its final specifications are given in Table 7. This valve is capable of checkout at room temperature.

Solenoid valve flow tests were conducted using helium at - 320° F with inlet pressure varying from 16.7 to 44.5 psia. No leakage was detected utilizing a helium mass spectrometer. The pull-in and holding-current requirements at - 320° F were found to be approximately 0.5 and 0.15 amp (28 vdc), respectively, which is well within the predicted performance requirements at this temperature.

The current-limiter test was conducted using a 0.25-ohm resistance across the output side to simulate the solenoid coil resistance at 37.4° R. The input power required for operation was less than 1 w for the temperature range tested (- 67 to +212° F).

Flow tests were conducted on this unit to establish the flow and pressure drop characteristics of the solenoid valve orifice. Equations (1) and (2) define an effective orifice area, CA, which can then be used to calculate the flow rate for any fluid provided the state point and fluid properties are known. The weight flow through any orifice is given by

$$\omega = CA\sqrt{2 g_c \rho \Delta P} \quad * \qquad (1)$$

*Symbols are defined on p. 112.

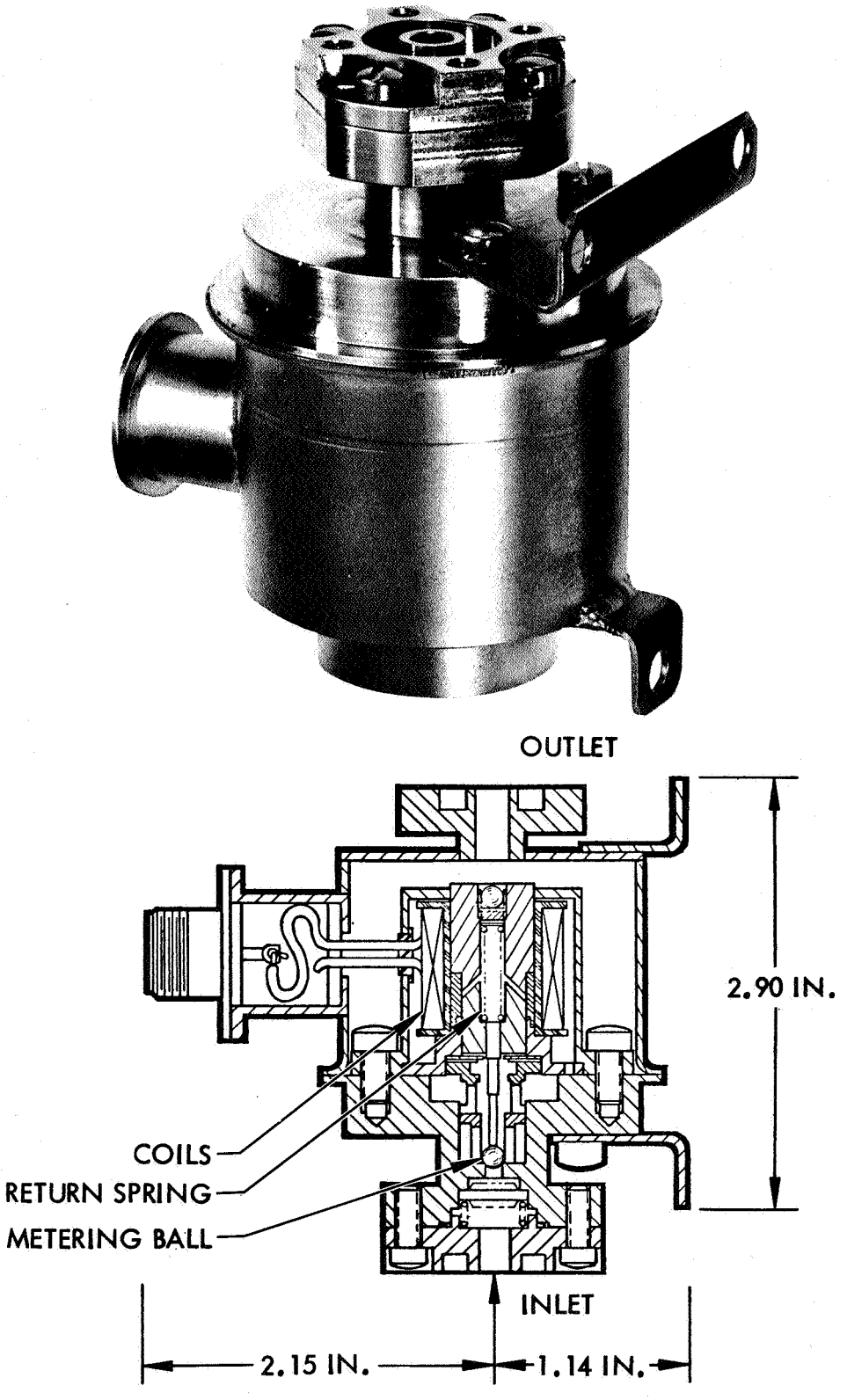

Fig. 20 Flow Control Unit

Table 7

FLOW CONTROL UNIT PERFORMANCE SPECIFICATIONS

Fluid Media	Gaseous hydrogen
Maximum Operating Pressure	28 psia (inlet); 14.7 psia (outlet)
Normal Operating Pressure	4 psia (inlet); 0 psia (outlet)
Proof Pressure	50 psia
Burst Pressure	70 psia
Temperature	32° R ±5° R (inlet to valve) 37° R to 530° R (ambient)
Flow	The valve should act as a choked orifice which limits flow of H_2 to 1.4 lb/hr at 4 psia and 30° R
Leakage (internal)	10^{-4} lb/hr of H_2 with upstream pressure of 28 psia and a temperature of 38° R and downstream pressure of 10 microns
Current Limiter and Solenoid Power Consumption	
Power Supply	28 vdc
In-Rush	10 w for 500 milisec (max)
Holding	0.06 w
Weight	1.5 lb

However, if the orifice is choked, the thermodynamics of compressible flow lead to a more useful expression, in terms of inlet conditions and fluid properties. This weight flow is

$$\omega = CA\, p_1 \sqrt{\frac{g_c \gamma}{R\, T_1} \left[\frac{2}{\gamma+1}\right]^{\frac{\gamma+1}{\gamma-1}}} \qquad (2)$$

The tests on this unit were conducted, using helium gas at liquid nitrogen temperature and air at ambient temperature. The results are shown in Fig. 21. The experimental air data are shown in Fig. 21 as equivalent lb/min of helium, and the pressure drop has been referenced to standard conditions with the normalizing factor σ, which is the ratio of actual fluid density in the valve to that at a pressure of 1 atm and a temperature of 519°R. Using these data, and the choked flow equation (2), the effective orifice area was calculated to be 0.0054 sq in. The design value, for 1.4 lb/hr of hydrogen vapor at 4 psia and 30°R is 0.0047 sq in., which indicates the valve is approximately 15 percent oversized.

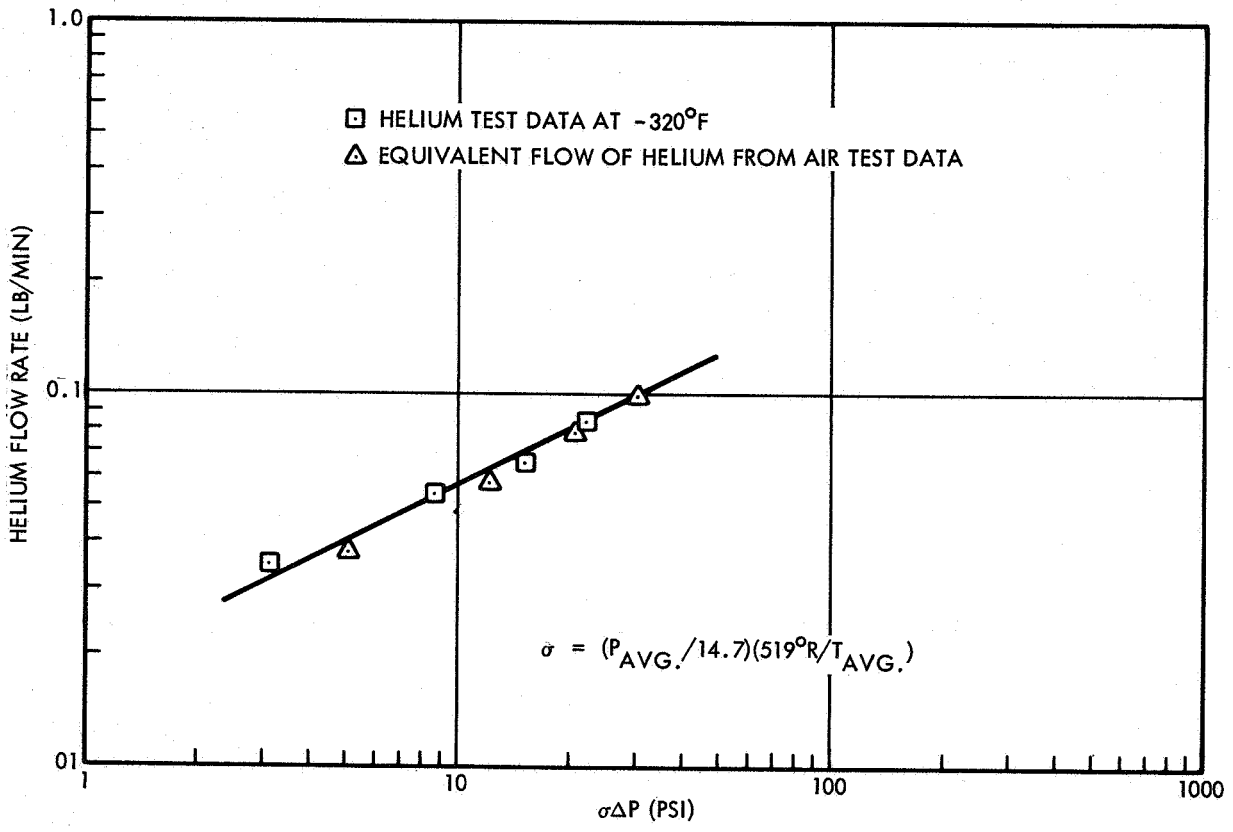

Fig. 21 Flow Control Unit Flow Data

Pressure Switch

The pressure switch, shown in a sectional view in Fig. 22, is mounted outside the tank to improve reliability and to facilitate checkout and replacement. It consists basically of an internally evacuated bellows and a hermetically sealed microswitch. The bellows assembly is exposed to tank pressure. As the tank pressure rises above the preselected closing level, the movement of the bellows actuates the switch which, in turn, closes the electrical circuit to both the solenoid valve and to the mixer motor. The switch is similarly deactuated when the pressure falls below the opening pressure level. The specifications for this unit are given in Table 8.

Table 8

PRESSURE SWITCH PERFORMANCE SPECIFICATIONS

Maximum Operating Pressure	28 psia
Proof Pressure	50 psia
Burst Pressure	70 psia
Temperature	400° R ±200° R
Actuation	
Maximum Closing Pressure	19.2 psia
Minimum Opening Pressure	16.8 psia
Electrical Data	
Operating Voltage	28 vdc
Resistive	5 amp
Inductive	3 amp
Leakage (external)	10^{-4} lb/hr of H_2 with an upstream pressure of 28 psia and temperature of 400° R and downstream pressure of 10 microns
Weight	1 lb

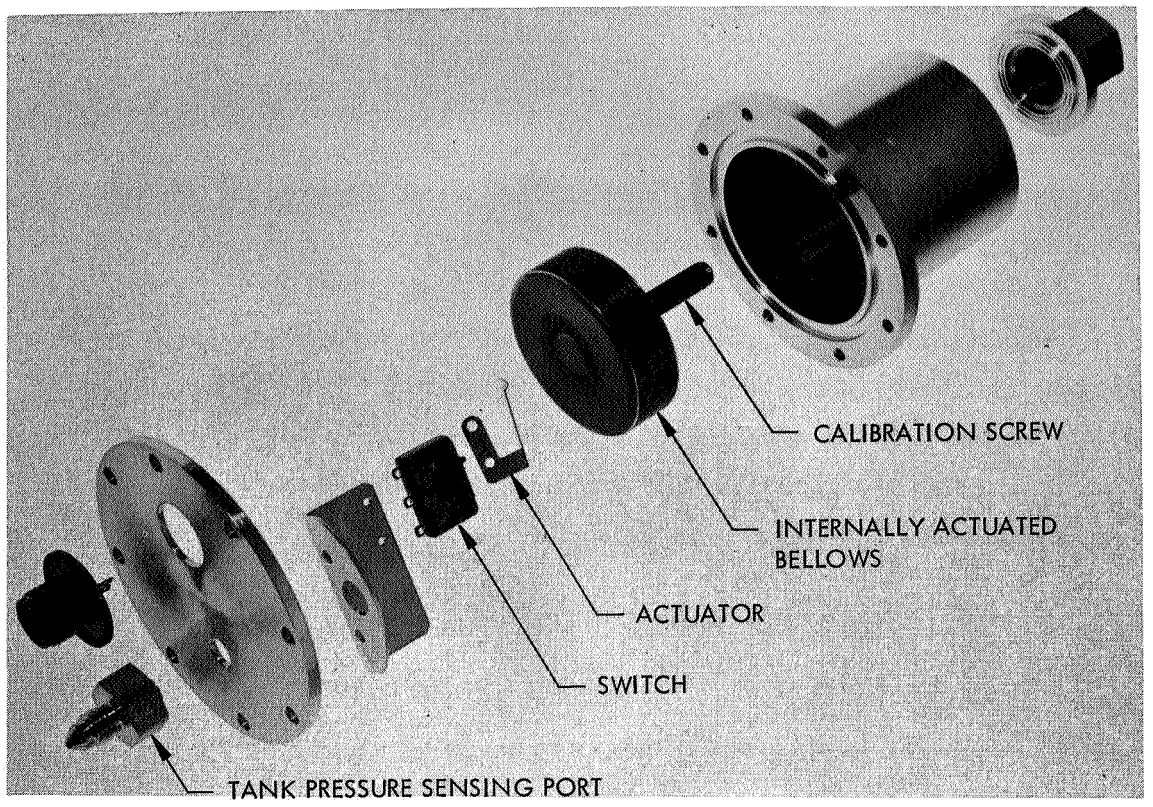

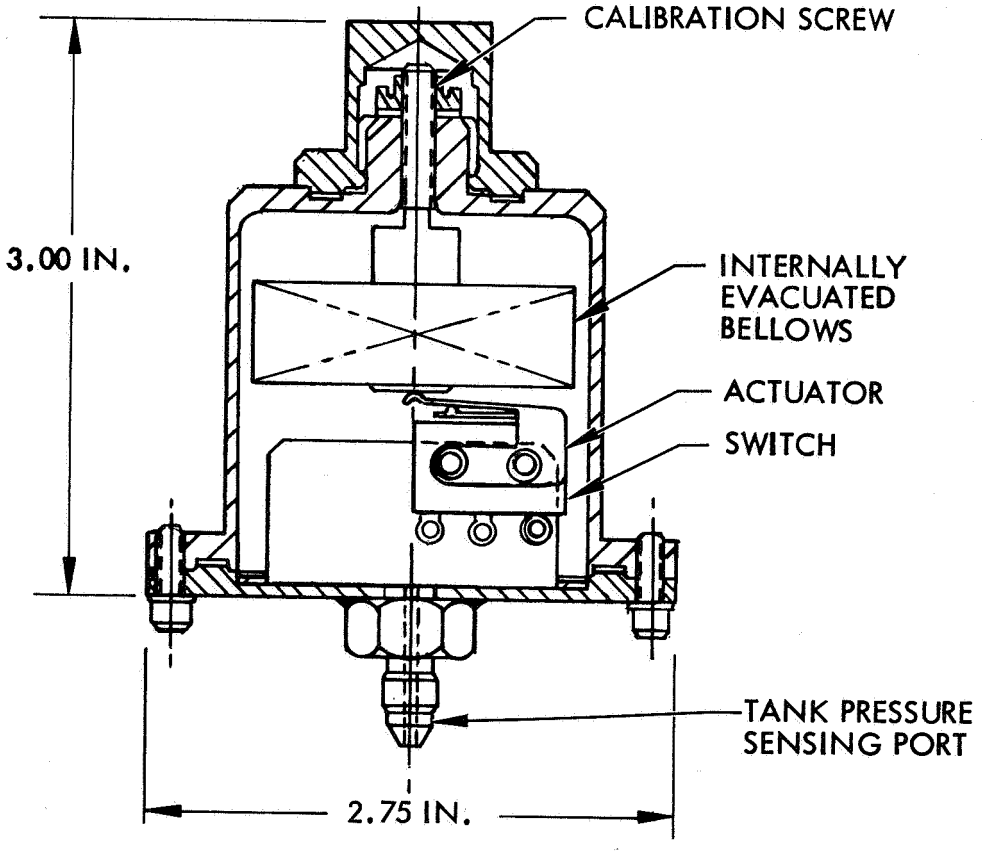

Fig. 22 Pressure Switch Components

Figure 22 shows an exploded view of the pressure switch components. After the unit was fabricated, it was calibrated and its performance was evaluated at various temperatures in an environmental chamber. First, the unit was held at -60° F and cycled 100 times. Readings were taken at every tenth cycle. The unit was then subjected to a temperature of -260° F, and again cycled 100 times. During these tests it continued to operate satisfactorily.

The chamber temperature was then increased to +140° F and cycled 100 times; readings were taken every 10 cycles. Again, the switch operated satisfactorily. The temperature was then lowered to -60° F, and the cycle tests repeated.

A summary of these tests is presented in Table 9. The closing pressure never exceeded 18.6 psia, which is within specification. At sub-zero temperatures the opening pressure reached as low as 16.5 psia, which is 0.3 psi below specification. However, it was noticed that the operating bandwidth was repeatable with 0.2 in. Hg, thus allowing a recalibration to raise the minimum opening pressure to 16.8 psia without exceeding the maximum closing pressure.

Table 9

PRESSURE SWITCH TEST RESULTS

Test Series	Temperature (° F)	Total Cycles	Pressure (in. Hg)		Max. Pressure Deviation (in. Hg)	
			Open	Close	Open	Close
1	-60	100	33.9	37.0	0	-0.1, +0
2	-260	100	34.7	37.8	-0, +0.1	-0, +0.1
3	+140	100	34.2	36.2	-1.7, +0	-0.9, +0
4	-60	100	33.5	36.8	0	0

Mixer Unit

The mixer unit in the selected system serves the following two functions:

- It provides the necessary convective velocities through the hot side of the heat exchanger.
- It provides sufficient fluid velocities within the propellant tank to mix the bulk fluid and cause hydrogen vapor condensation of bubbles that are formed at hot spots on the tank wall.

The mixer power requirements are dictated by the pressure drop in the heat exchanger and by the discharge velocity head necessary for propellant circulation. Low velocities in the heat exchanger require little power, but also result in low warm-side heat-transfer coefficients and, therefore, large heat exchangers.

The application of the thermal conditioning unit in a zero-gravity environment make it necessary to take the most conservative condition, i.e., helium on the warm side, as the heat exchanger design point, even though the unit may be operating entirely in liquid. With this ground rule, heat exchanger weights were determined as a function of volumetric helium flow rate. Since the mixer unit is essentially a constant volumetric flow device, mixer power was then determined for liquid at the same volumetric flow rate and subsequently evaluated in terms of propellant boiloff for the entire mission.

The mixing capability of that mixer unit, for which the combined heat exchanger weight and propellant boiloff were a minimum, was then assessed. A measure of that capability can be ascertained from Fig. 23, which shows the theoretical minimum jet velocities for total mixing of tank contents in a zero-gravity environment, as well as the actual jet velocity from the chosen mixer design. The analysis from which Fig. 22 is derived is given in Appendix B, and substantiating test data are described in detail in Ref. 1. It can be seen that the selected design velocity is ten times that theoretically required to provide jet continuity and mixing across the full span or diameter of the Mission (2) tank with liquid hydrogen. Also shown is the velocity requirement calculated

from the experimental data presented in Ref. 2 for ethanol, which has properties governing mixing in zero-gravity that are similar to those of liquid hydrogen. The selected design velocity is five times that predicted from these data.

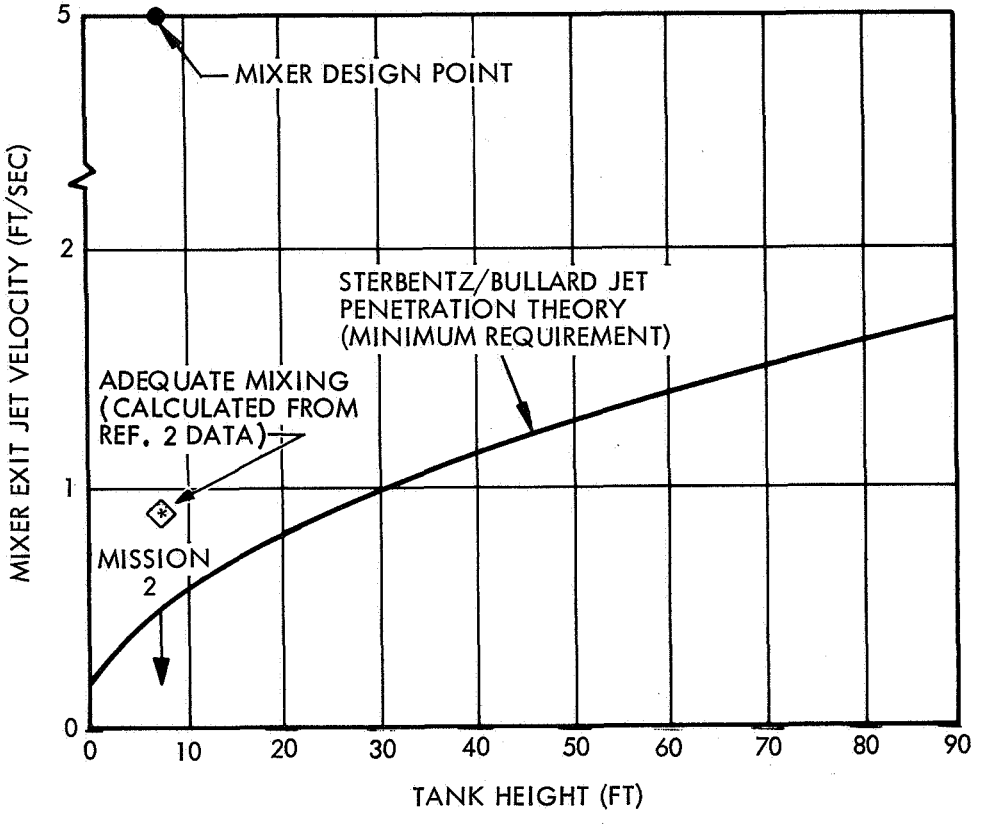

Fig. 23 Mixer Jet Velocity Requirements in Zero-Gravity for Complete Circulation (Jet Diameter = 1.75 in.)

The mixer unit design selected for an optimized Mission (2) vehicle consists of a brushless dc motor and fan (Fig. 24). The axial flow fan is connected directly to the motor, which uses an ironless stator to eliminate eddy current losses. The permanent magnet rotor provides a strong excitation in a compact size with consequent reduction in windage losses. The rotor position controls the commutation through a small permanent magnet on the rotor with inductive pickups. The actual electronic switching device is located outside the tank to avoid unnecessary dissipation of energy in the tank. The mixer duct exit diameter is 1.75 in., and provides a jet exit velocity of 5 ft/sec with either gas or liquid. The specifications for this mixer unit are listed in Table 10.

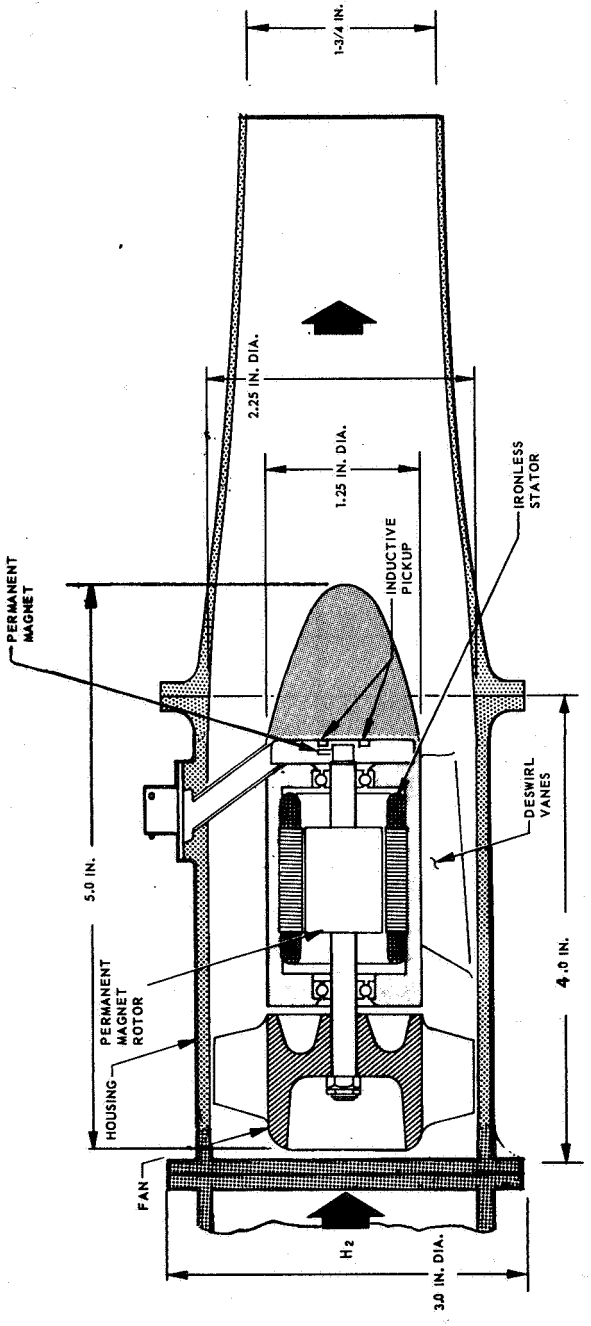

Fig. 24 Mixer Unit With Brushes DC Motor

Table 10

MIXER UNIT PERFORMANCE SPECIFICATIONS

	Gaseous Helium	Liquid Hydrogen
Density (lb/ft^3 at 17 psia)	0.18	4.4
Flow (lb/hr)	57.4	1,320
Pressure rise (in. H_2O)	0.2	2.0
Temperature	30°R to 530°R	
Maximum Operating Pressure (ambient)	28 psia	
Power Input	2.3 w	
Unit Weight	2 lb	

Brushless dc motors are not yet available for operation in liquid hydrogen, although one is now being developed under Contract NAS 3-11208. However, a mixer unit with a three-phase, six-pole, ac-induction motor and a single-stage, shrouded, axial flow fan was available for operation in liquid hydrogen. This mixer, weighing only 1.5 lb, was used in the thermal conditioning system. A sectional view and a photograph of the unit is shown in Fig. 25.

The available data on this unit (Fig. 26) showed that when operating with liquid hydrogen at 5 cfm and the design electrical input condition, the pressure rise across the unit was approximately ten times that required for the present application. If operated in the thermal conditioning system, at the design electrical input, the flow rate through the hot side of the heat exchanger would be several times the required flow and would result in an unnecessarily high power consumption. However, the flow rate and power input could be reduced by reducing the operating voltage and frequency.

A calibration test program was conducted to determine the operating characteristics of this unit at reduced frequencies and voltage.

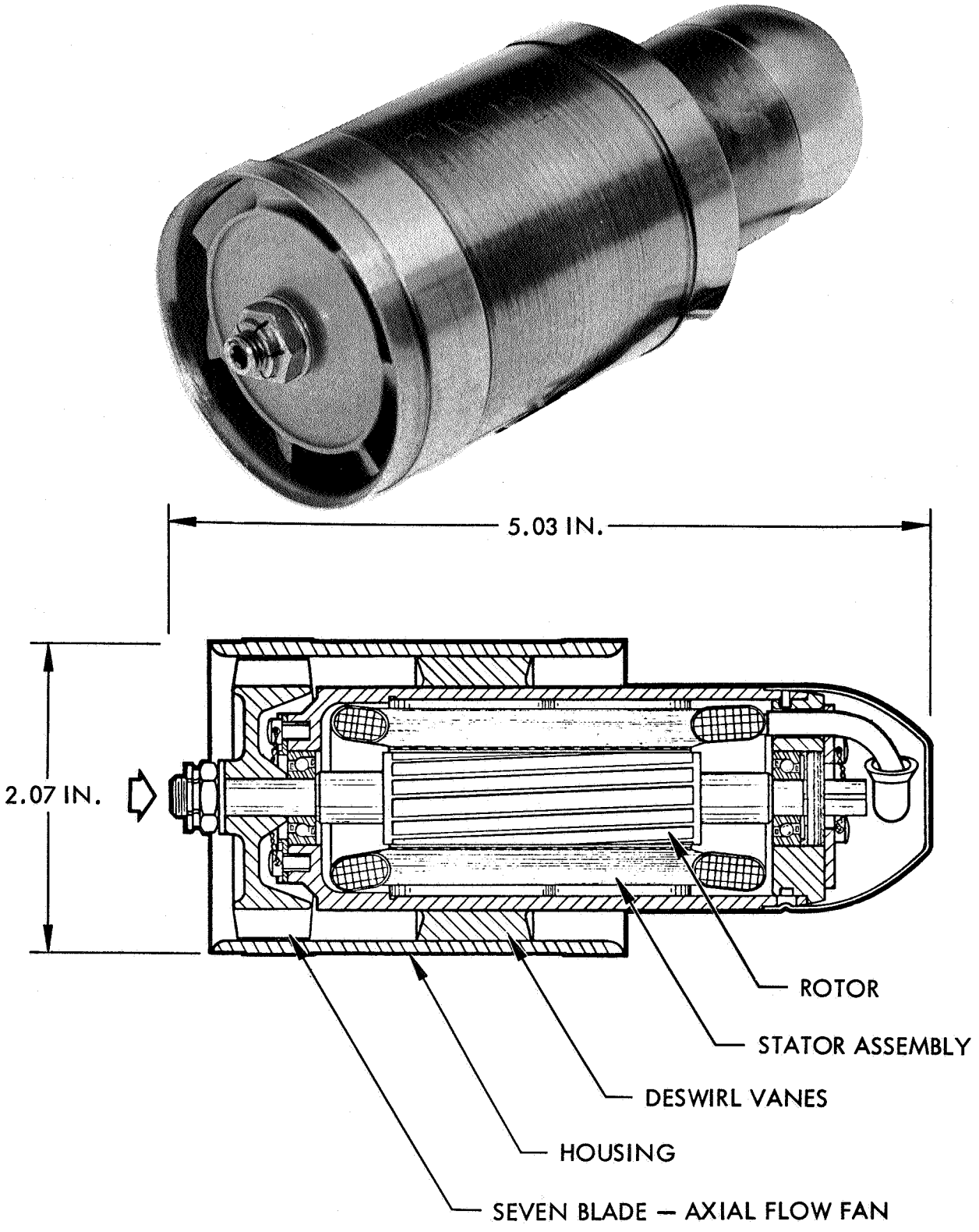

Fig. 25 Sectional View and Photograph of Mixer

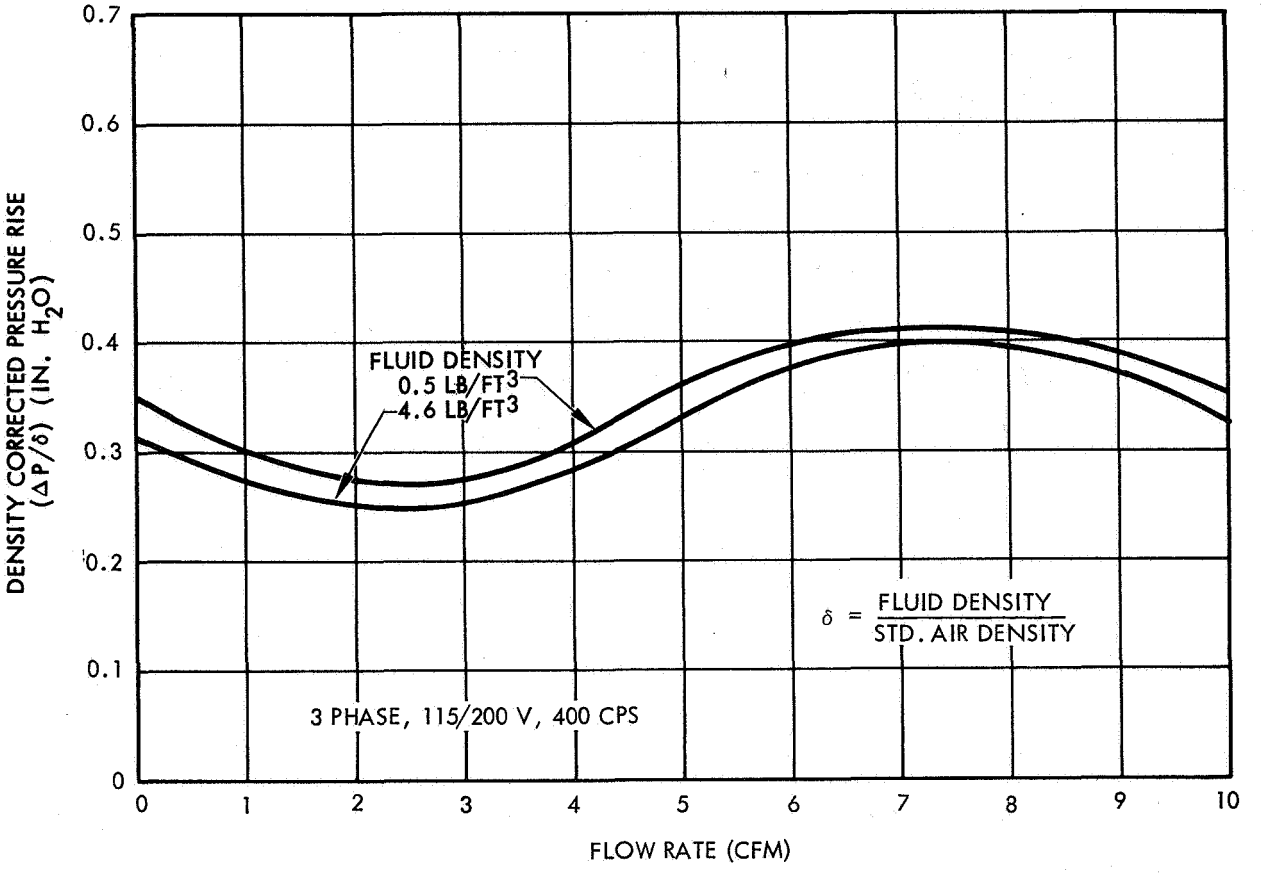

Fig. 26 Mixer Unit Characteristics

The mixer, with motor drive, was installed in the flow loop shown schematically in Fig. 27. High-pressure gaseous nitrogen was circulated through the loop using the mixer unit; the flow rate being determined by the voltage and frequency applied to the motor. The density of the circulating fluid was controlled to that of liquid hydrogen (4.4 lb/ft^3) and of gaseous hydrogen (0.09 lb/ft^3) by controlling the pressure in the loop through a throttling valve. The fluid was maintained at near liquid nitrogen temperature by circulating it through a liquid nitrogen bath.

The experimental performance data are shown in Figs. 28 through 34. Figure 28 indicates that, for a fixed set of flow conditions, there is an optimum driving frequency at which the motor will draw the minimum power. Each datum point shown in Figs. 29 through 34 was determined by maintaining a fixed flow rate and pressure drop, and varying the applied frequency as shown in Fig. 28. Thus the curves shown in Figs. 29 through 34 represent minimum (optimum) power conditions.

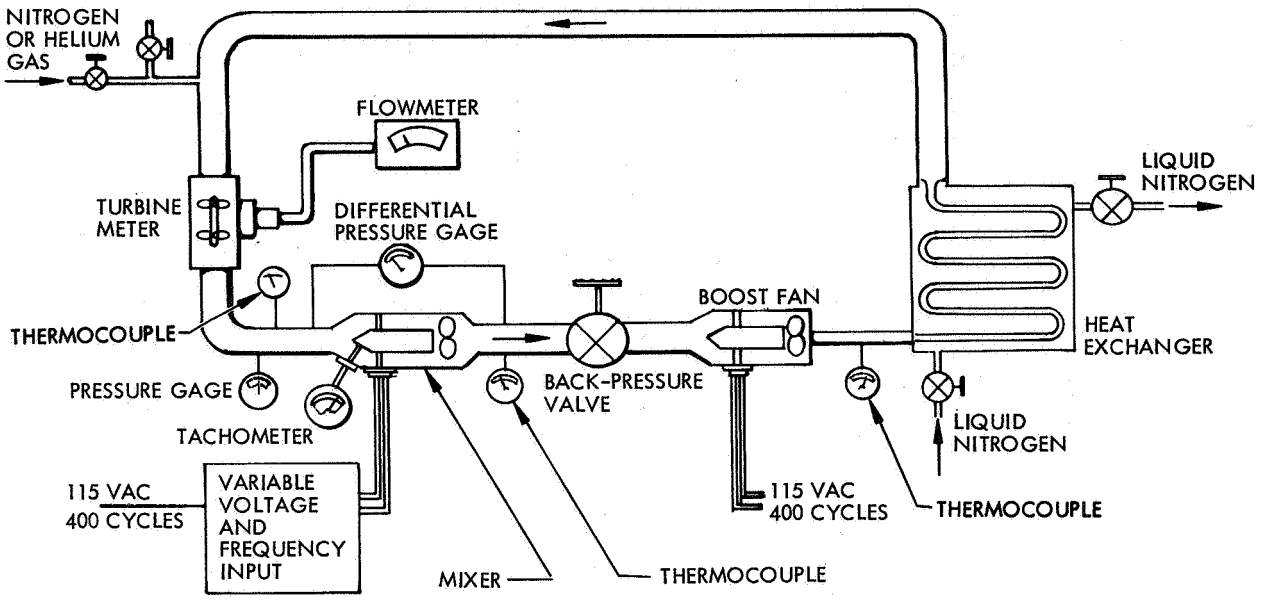

Fig. 27 Schematic of Mixer Calibration Test Loop

Figure 29 shows the relationship between the applied current frequency and applied voltage, and the fluid flow rate. When the necessary flow rate and pressure drop is known, the applied frequency and voltage that will produce this flow rate can be determined using the graph in Fig. 29.

The effect of head rise and flow rate on the motor power requirements is shown in Fig. 30 for fluid at liquid hydrogen density. When the assembled thermal conditioning system is in operation, the mixer head rise balances the pressure losses in the remainder of the system. Therefore, the pressure loss at a set flow rate can be found by entering the measured power in the curves on Fig. 30. (Most of this pressure loss will occur in the heat exchanger.) Figure 31 relates the fan speed to the power and flow rate.

Figures 32, 33, and 34 present the same data as Figs. 29, 30, and 31, respectively, for a fluid density of 0.09 lb/ft^3.

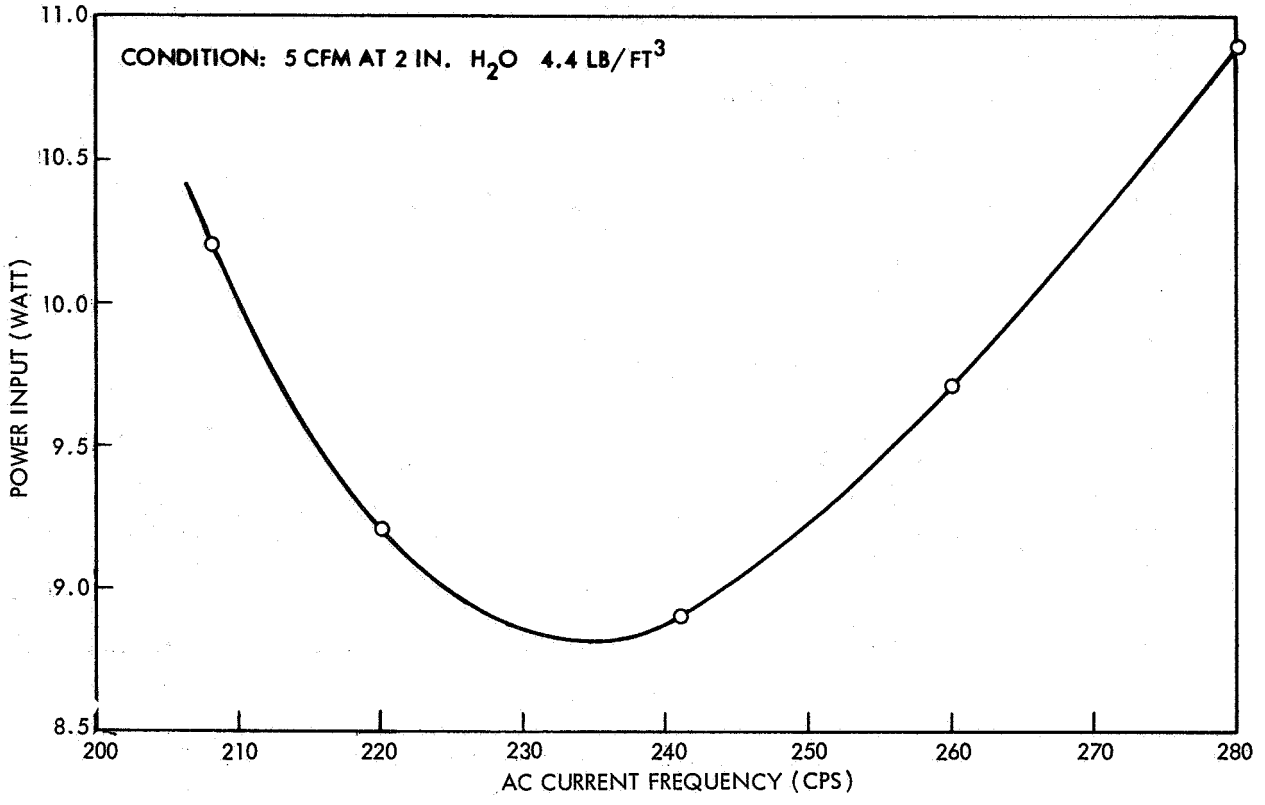

Fig. 28 Typical Frequency Optimization for the AC Induction Motor

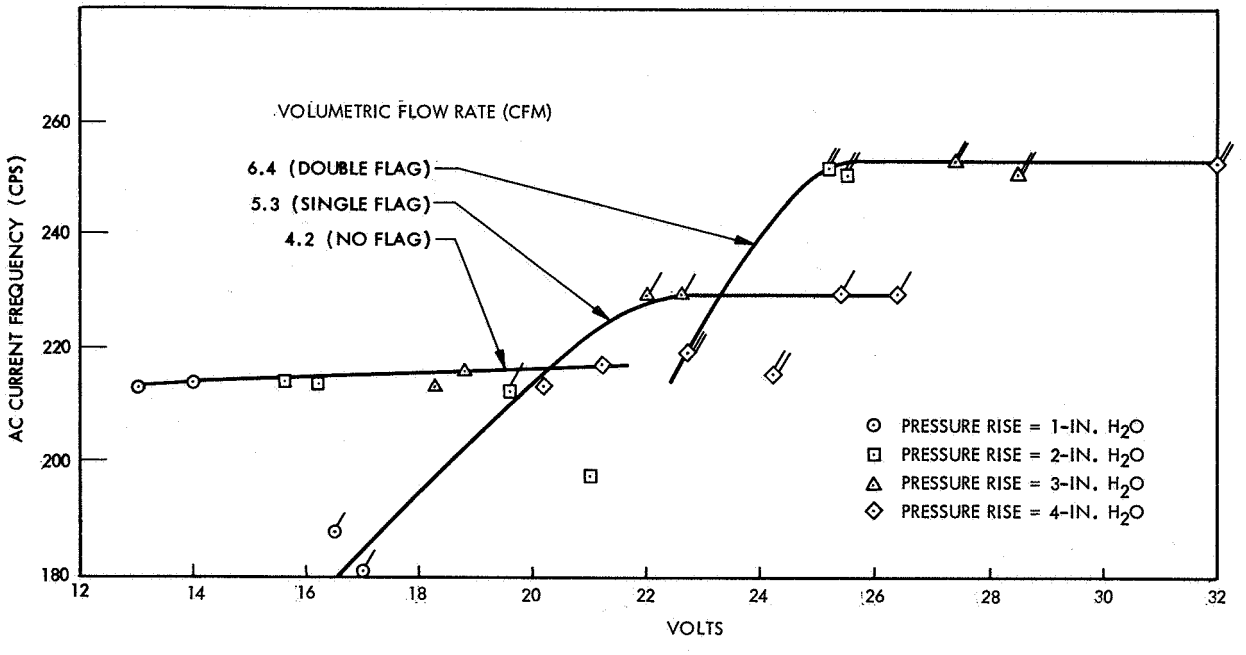

Fig. 29 AC Current Frequency and Voltage Settings for Optimum Input Power (Fluid Density – 4.4 lb/ft^3)

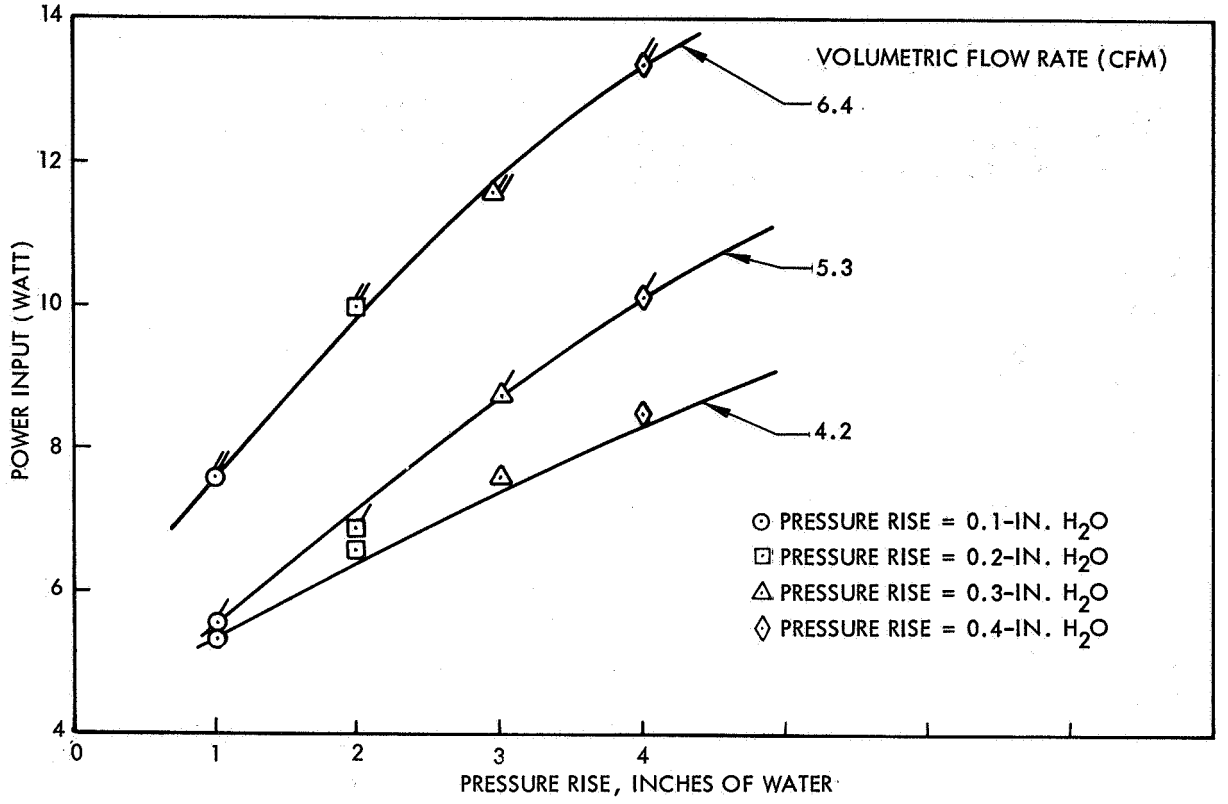

Fig. 30 Effect of Fan Head Rise on Motor Power Requirements (Fluid Density – 4.4 lb/ft^3)

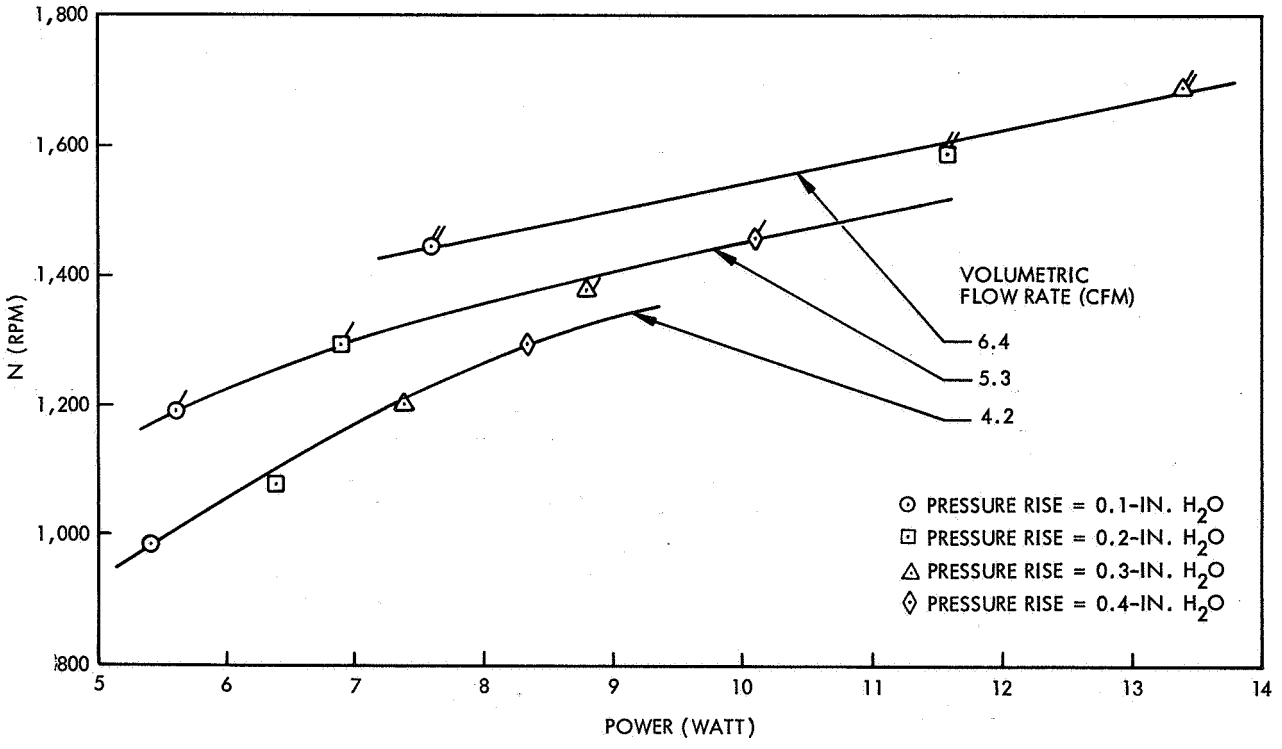

Fig. 31 Effect of Fluid Flow Rate and Power Input on Mixer Speed (Fluid Density – 4.4 lb/ft^3)

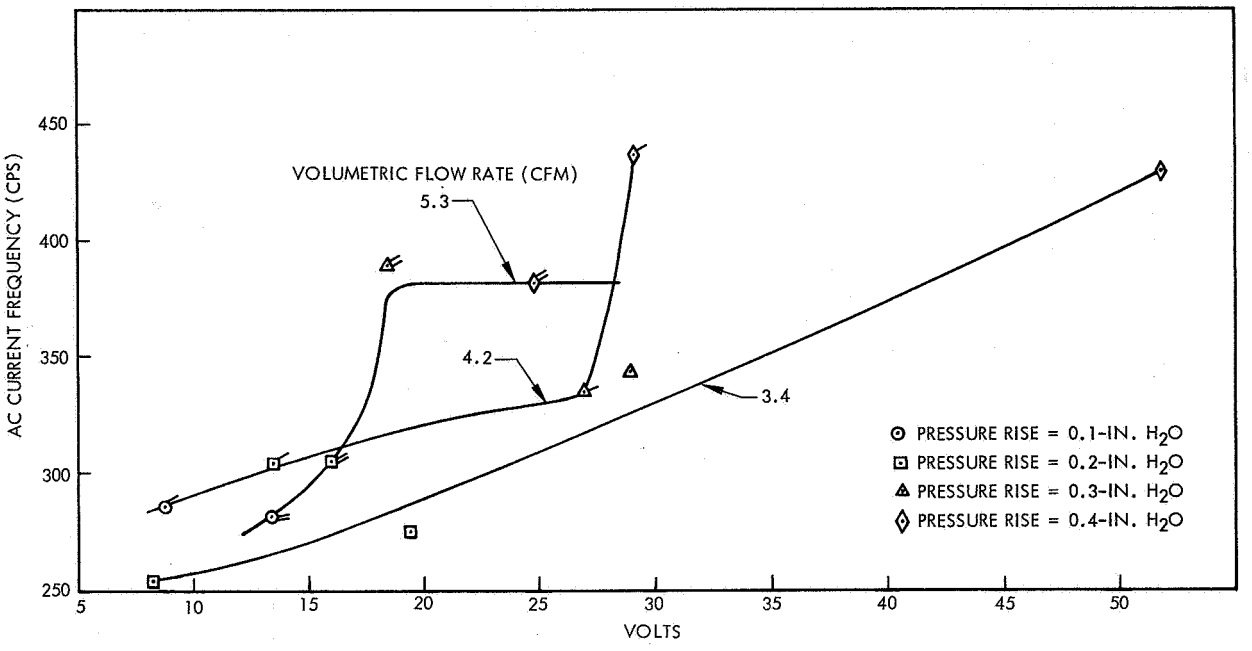

Fig. 32 AC Current Frequency and Voltage Settings for Fixed Motor Speeds (Fluid Density – 0.09 lb/ft^3)

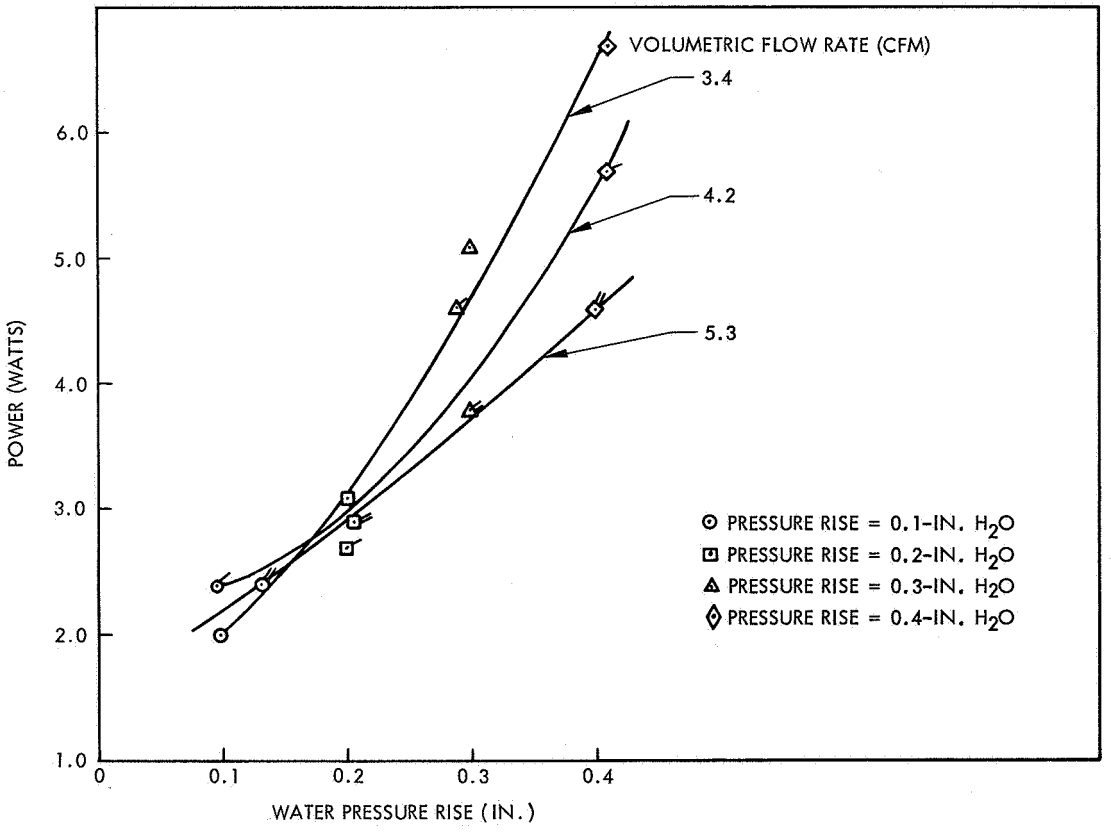

Fig. 33 Effect of Fan Head Rise on Motor Power Requirements (Fluid Density – 0.09 lb/ft^3)

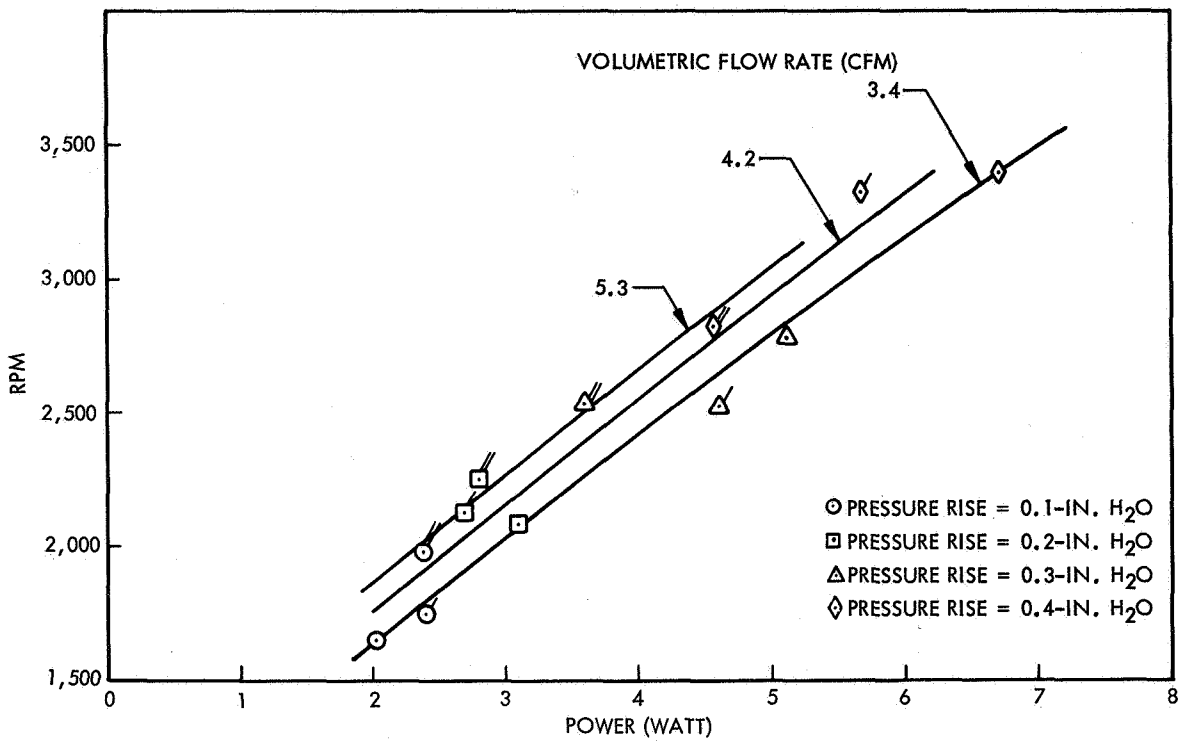

Fig. 34 Effect of Fluid Flow Rate and Power Input on Mixer Speed (Fluid Density – 0.09 lb/ft^3)

SYSTEM ASSEMBLY

After completion of the component development tests, the system was assembled and mounted on an aluminum base plate. The assembled system was then checked for leaks by pressurizing the cold side to 14 psig with freon gas and checking for leaks with a freon leak detector. The entire assembly was soaked in liquid nitrogen for 30 min and then left at room temperature for 8 hr. A helium leak check was then made at 14 psig; no leaks were detected. After the leak check, electrical power was supplied to each component to check the circuits; all components performed successfully.

The system was then cleaned, purged, sealed in a plastic bag, and stored until the subsequent liquid hydrogen tests.

THERMAL CONDITIONING SYSTEM TEST PROGRAM IN LIQUID HYDROGEN

A test program was designed to experimentally demonstrate the feasibility of the thermal conditioning system, evaluate component performance, and establish the most effective means for integrating the unit into a full-scale, flight type, liquid hydrogen tank subsystem of the Mission (2) space propulsion vehicle. This test program was divided into two series: the first consisting of functional tests in a dewar tank and the second consisting of full scale performance tests in the 110-in.-diameter Mission (2) tank. The apparatus, instrumentation, and procedures are described in this section. Data, test results, evaluations, and analyses of the test data are presented in a subsequent section entitled: Results and Analysis.

SERIES ONE: LIQUID HYDROGEN DEWAR TANK TESTS

This test program was designed to verify, in liquid hydrogen tests, the proper operation of the thermal conditioning system. The system was operated in both liquid and gaseous hydrogen and the performance recorded.

Test-Article Configuration

A 15-in. internal diameter, 36-in. deep dewar tank shown in Fig. 35 was used. The thermal conditioning system was suspended from the dewar lid on rods at an orientation angle of 40 deg as shown in Fig. 36. The dewar lid contained passthrough penetrations for the system vent, vacuum, LH_2 loading, GN_2, GH_2 purge, and pressurization lines, and an instrumentation and control wiring connector.

Proper operation of the thermal conditioning system requires that the pressure in the discharge line just downstream of the flow control unit be sufficiently low to guarantee

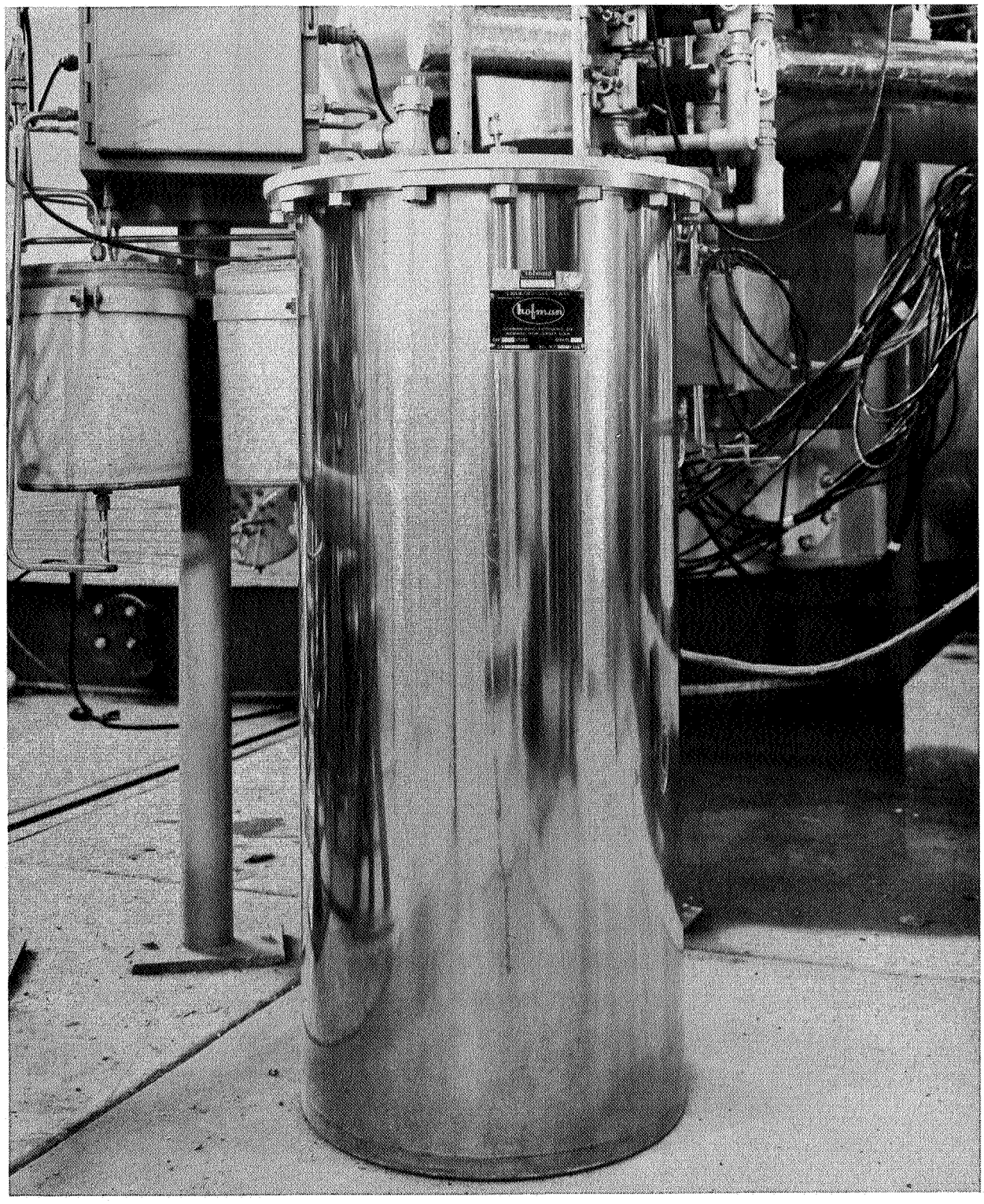

Fig. 35 15-in.-Diameter Dewar

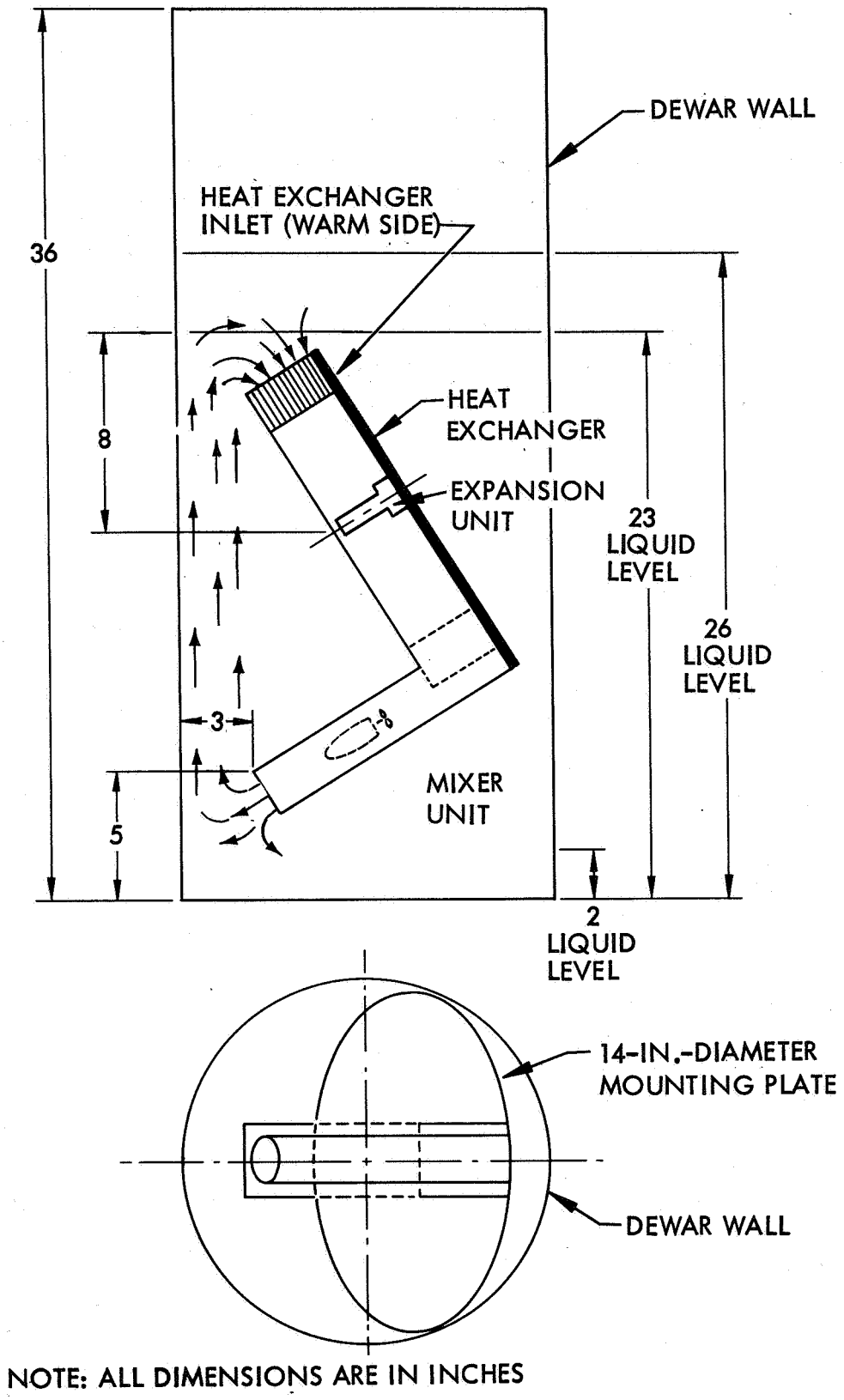

Fig. 36 Location and Orientation of Thermal Conditioning System in Subscale Dewar Test

choking of the flow control unit. Choking of the flow control unit was accomplished by connecting the thermal conditioning system vent line directly to a large vacuum chamber. This setup provided a vacuum that could be maintained in the 1×10^{-5} Torr pressure range. Figure 37 is a schematic of the test article piping connections.

The thermal conditioning system was instrumented at the locations shown in Fig. 38. The type, range, and function of the instrumentation used are given in Table 11. All data were recorded on dual pen Mosely strip-chart recorders.

Pretest Activity

The following preparations were made prior to testing the thermal conditioning system:

- The system was mounted in the 15-in.-diameter dewar with an orientation as shown in Fig. 36.
- Instrumentation cabling and fan power cables were connected, and a fan rotation check and instrumentation functional checkout performed.
- The system was pressurized with helium to 5 psi and checked for leaks with a mass spectrometer. No leakage at any connection was found.
- The lid was secured and the dewar was evacuated to 10 microns for 2 hr to minimize condensable gases within either the dewar or the thermal conditioning system.
- The entire system was then inerted, first with ambient GN_2 and then with ambient GH_2. This procedure purges air and purge GN_2 from any part of the test apparatus that will contain liquid hydrogen. A special purge of the thermal conditioning system was performed at this time to ensure that all passages within the system were clear and free of any media that could freeze and impair the operation of the unit. To effectively purge the unit, the solenoid valve was opened and the purge gases allowed to flow through the unit for at least 30 min.
- The vacuum pumping system was verified.

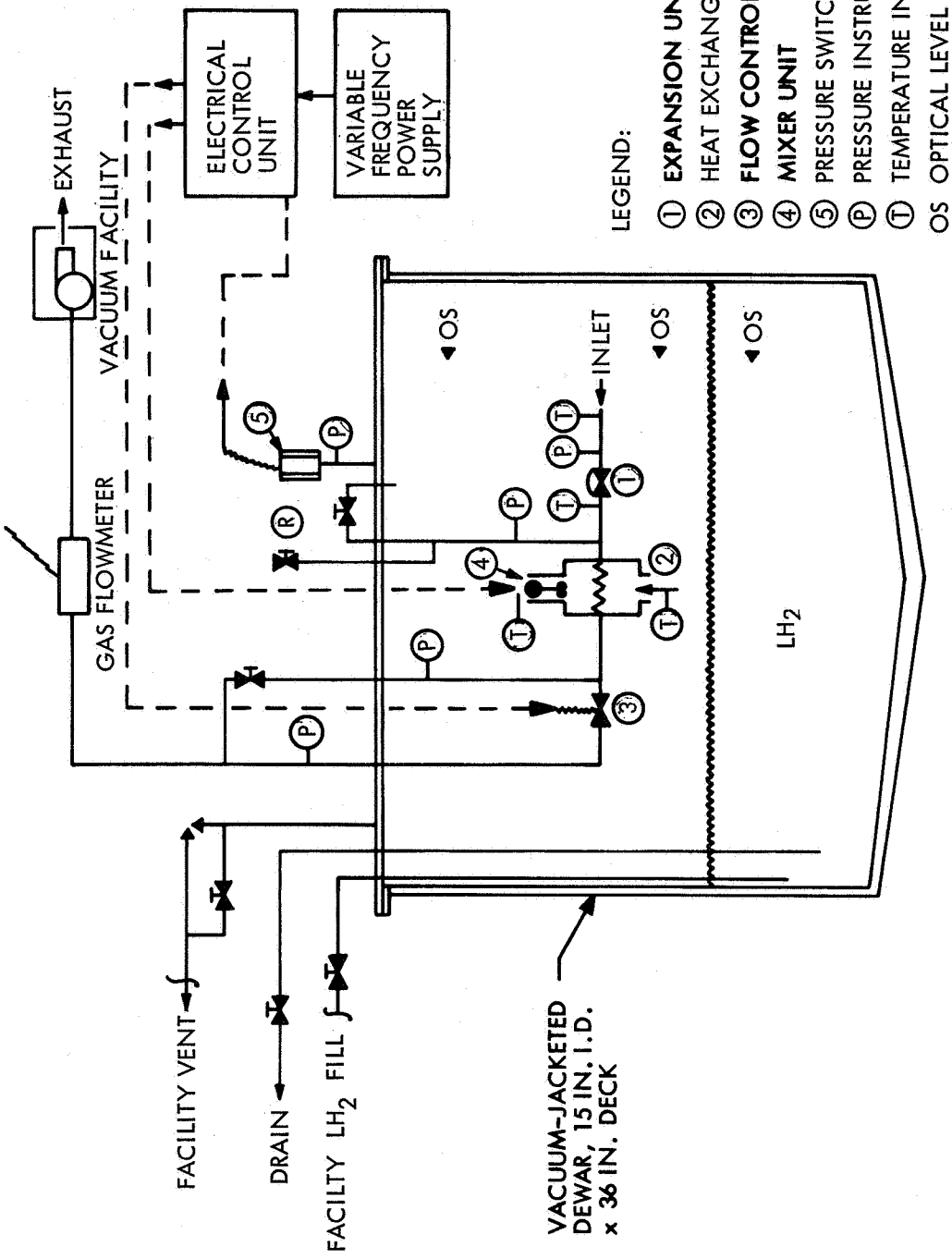

Fig. 37 Thermal Conditioning System Piping Schematic

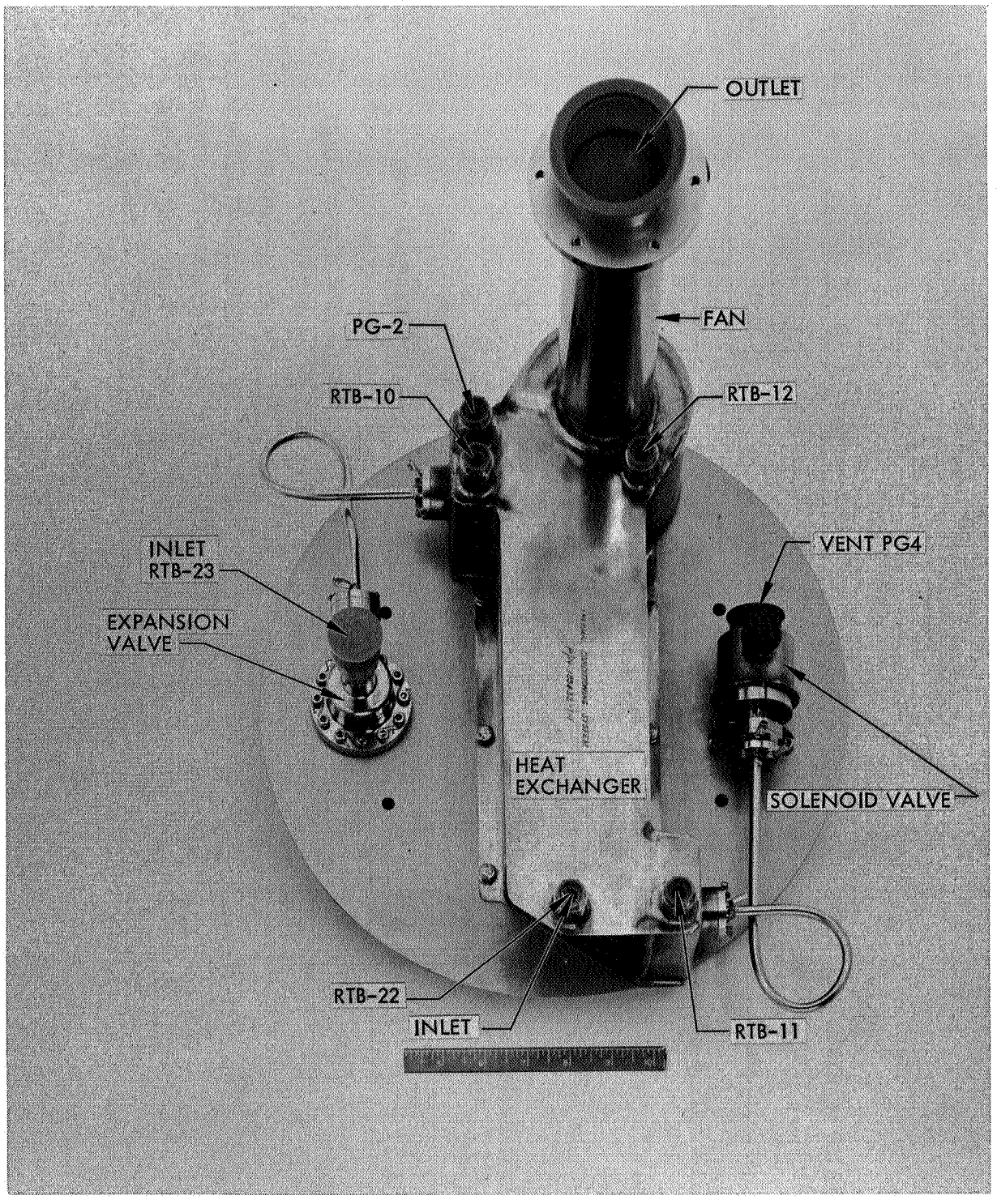

Fig. 38 Thermal Conditioning System Instrumentation Locations

Table 11

THERMAL CONDITIONING UNIT INSTRUMENTATION
(DEWAR TEST)

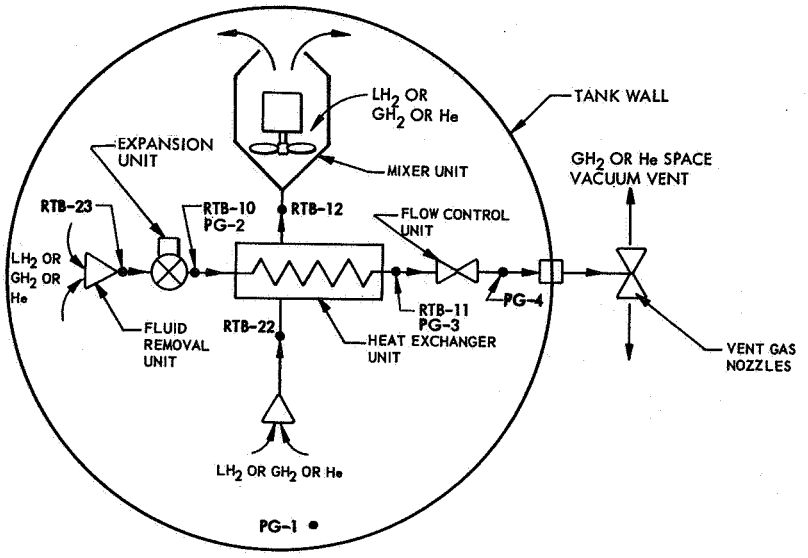

Function	Range	Type	Identification
Pressures (psia)			
P_1, Dewar ullage	0 to 25	Strain-gage transducer	PG-1
P_2, Heat exchanger inlet	0 to 10		PG-2
P_3, Flow control unit outlet	0 to 10		PG-4
Temperatures (° F)			
T_1, Expansion unit	-300 to -425	Platinum resistance thermometer bulb	RTB-23
T_2, Heat exchanger inlet, cold side	-400 to -425		RTB-10
T_3, Heat exchanger exit, cold side	-400 to -425		RTB-11
T_4, Heat exchanger inlet, hot side	-400 to -425		RTB-22
T_5, Heat exchanger exit, hot side	-400 to -425		RTB-12
T_6, Brooks flowmeter inlet	-300 to -425		–
Flow rate (lb/hr)			
W, Thermal conditioning cold side flow	0 to 10	Brooks thermal mass flowmeter	
Electrical			
F, Motor frequency supply	–	Counter	
e, Motor voltage	–	Voltmeter	
a, Motor current	–	Ammeter	

Testing Sequence

Thirty tests were conducted with the system installed in the dewar; four in gaseous hydrogen and 26 in liquid hydrogen. The operational sequence for these tests was as follows:

- Fill the dewar to a liquid level of 2 in.
- Set mixer motor voltage and frequency
- Close dewar gas vent and allow thermal conditioning system to control dewar pressure automatically (4 tests)
- At conclusion of gas tests, shut down system and open dewar gas vent valve.
- Fill dewar to 26-in. level
- Set mixer voltage and frequency to control dewar pressure automatically
- Change voltage and frequency as desired (10 tests)
- At conclusion of 26-in. liquid level tests, change liquid level to 23 in.
- Repeat procedure used for 26-in. liquid levels (16 tests)

Post-Test Activity

Post-test activity consisted of the following procedures:

- The dewar was drained of LH_2 and purged with GH_2 and then GN_2 to inert the entire system
- The test apparatus was disassembled and the thermal conditioning system was then ready for installation in the 110-in.-diameter tank.

SERIES TWO: MISSION (2) FULL-SCALE TANK TESTS

The dewar tests were necessarily limited to functional and performance feasibility demonstrations, which were successful. The 110-in.-diameter tank program was designed to thoroughly demonstrate the thermal conditioning system as a flight system.

A major objective of these tests was to experimentally establish the most effective means for integrating a liquid hydrogen thermal conditioning system into a liquid hydrogen tank subsystem of a Mission (2) propulsion vehicle and to demonstrate tank pressure control. The objective also included evaluation of liquid-level effects, system orientation effects, and mixing requirements, as well as individual component performance.

Testing was performed with the unit mounted in two orientations and at various ullage volumes and liquid levels. In one test series the unit was mounted inside at the top of the tank, and in another test series it was mounted inside at the side of the tank.

Thermal Conditioning System – Top Mounted Configuration

The thermal conditioning system was mounted on 15-in. long rods attached to the tank lid as shown in Fig. 39. These 15-in long rods were used to ensure testing at completely immersed liquid hydrogen conditions. In a flight configuration the unit would appear as shown in Figs. 3 and 8. The system vent was connected to a passthrough in the tank lid, and then attached to the vacuum pumping system as illustrated in Fig. 40. The pumping system was capable of maintaing a pressure of less than 0.5 psia while the thermal conditioning system was venting. The tank was installed within the cryo-flight simulator (Fig. 41).

The flight simulator is a 16-ft-diameter by 24-ft high vacuum chamber with the following capabilities:

- Rapid depressurization to 0.5 psia to simulate launch ascent depressurization
- An LN_2 coldwall and quartz lamp heat array to simulate ascent and space flight thermal flux
- Vacuum pumping system for sustained operation at a pressure of 1×10^{-6} Torr
- Liquid hydrogen loading and handling
- High-pressure GN_2, GH_2, and helium storage and flow control

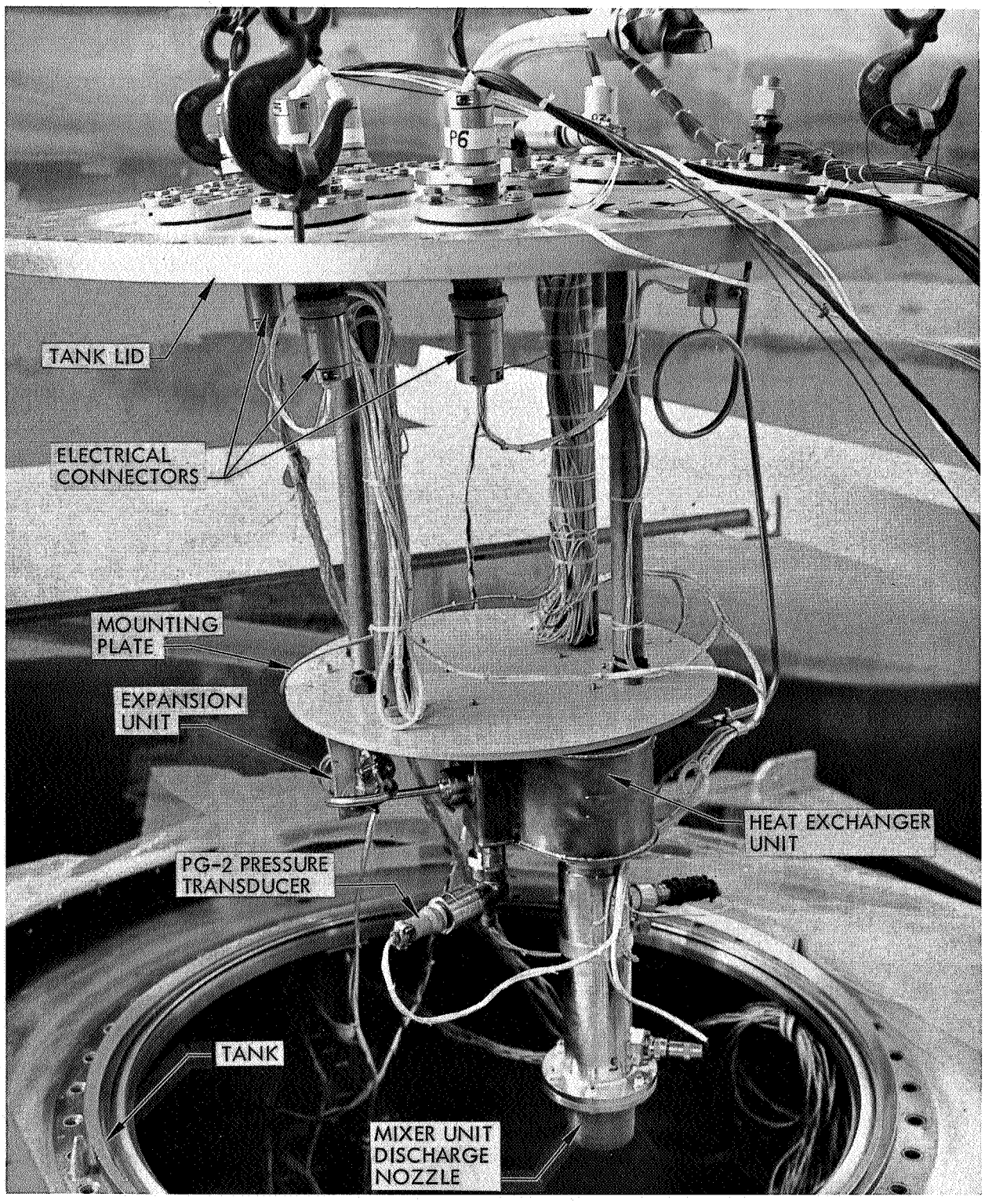

Fig. 39 Thermal Conditioning System Top-Mounted From Tank Lid

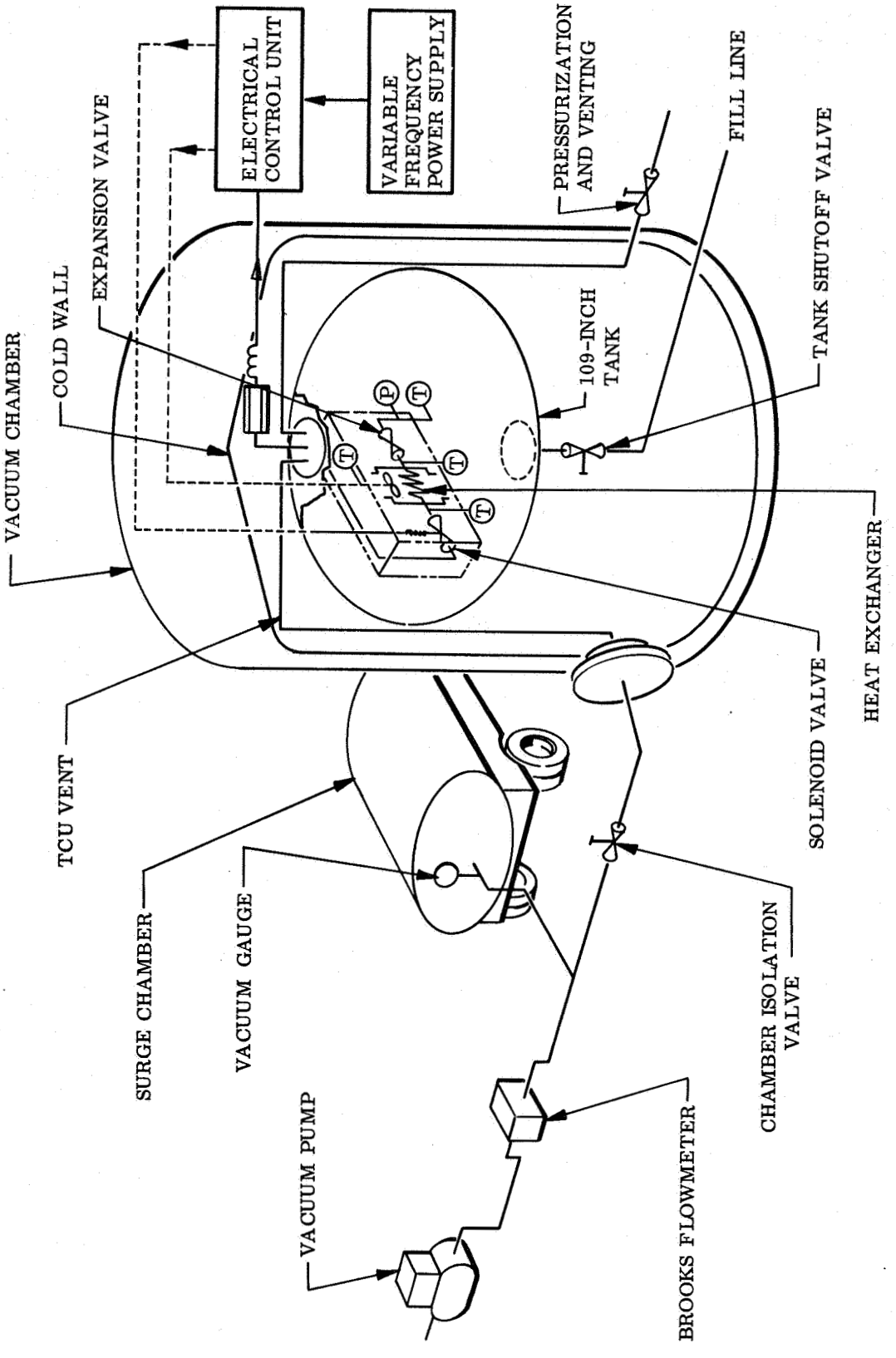

Fig. 40 Thermal Conditioning System Test Schematic

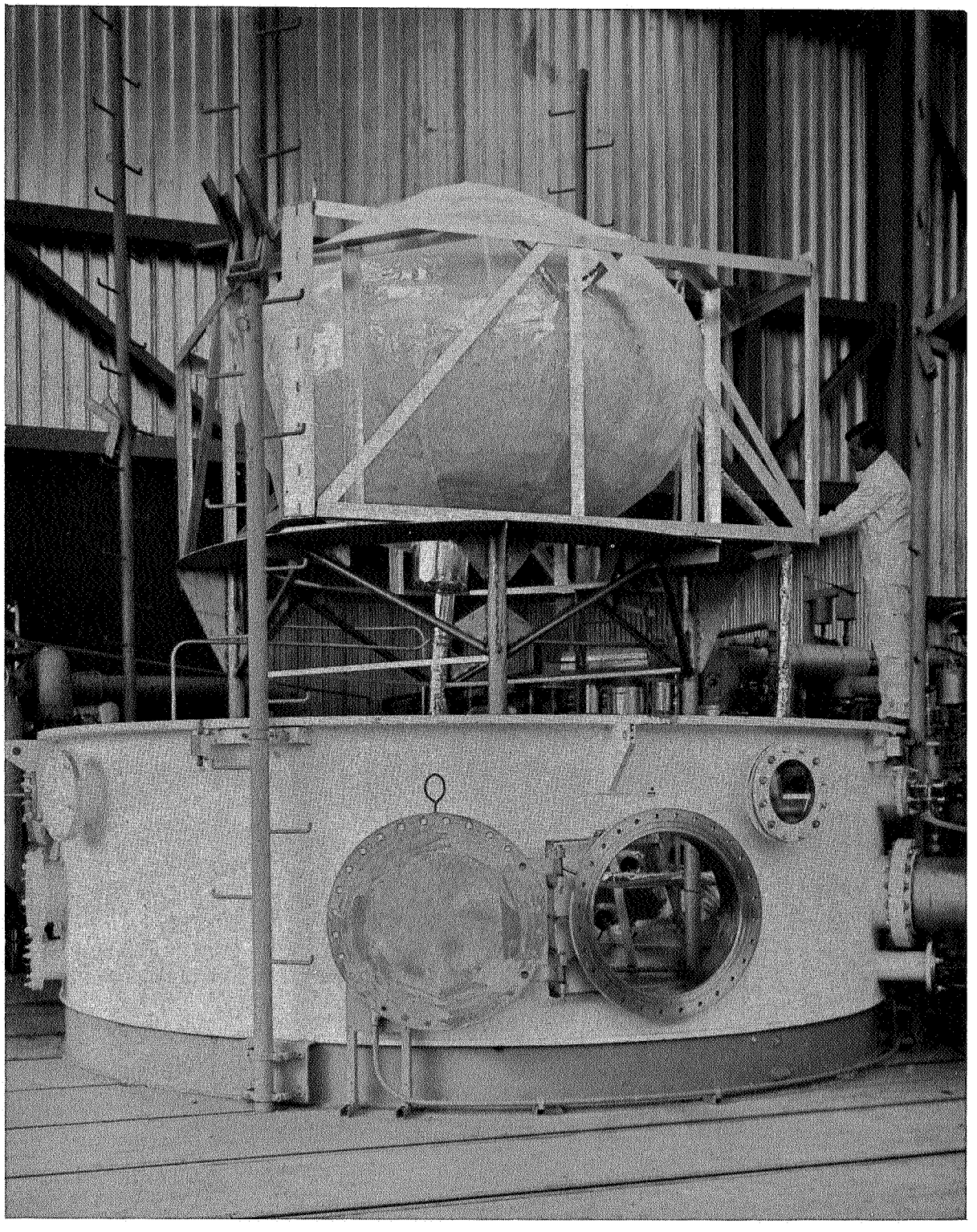

Fig. 41 LH_2 Tank as Installed Prior to Assembly of Cryogenic Flight Simulator

The 110-in-diameter tank (Fig. 9) was insulated with 100 layers of multilayer insulation composite of double-aluminized Mylar with Tissuglas spacers and supported within an aluminum holding frame. The tank is supported by eight tubular flight-type, low heat-leak, fiberglass struts.

Table 12 is an instrumentation schedule of the instruments used for the test. Locations of the instrumentation for the thermal conditioning unit are shown in Fig. 38.

A Dymec digital recorder and strip chart recorders were used to record the data. Plotting was accomplished during the test to obtain an immediate trend of the system performance from the data printed out on the Monroe printer. The data were stored on magnetic tape for future engineering analysis. Liquid level was controlled using optical sensors mounted on a probe positioned axially in the tank.

Pretest Activity. The following preparations were made prior to conducting the tests:

- The 110-in.-diameter tank was received at the flight simulator completely insulated and mounted in the aluminum holding fixture as shown in Fig. 41
- The insulation protective covering and the tank lid were removed.
- The thermal conditioning system was mounted to the tank lid as shown in Fig. 39 so that the mixer jet was directed down, parallel to the tank axis.
- A bench leak check of all connections was made with a mass spectrometer. No leaks were found.
- Instrumentation was installed and checked out, and a fan rotation check performed. The thermal conditioning system and tank lid were mounted on the tank, all piping was connected, and a helium leak check performed. No leakage was detected.
- The insulation system fiberglass dome was installed over the assembled tank lid.
- The piping leading to the tank from the chamber passthroughs was insulated with Mylar Tissuglas blankets.
- The LN_2 coldwall was installed and the chamber assembled.

Table 12

CRYOGENIC FLIGHT SIMULATOR INSTRUMENTATION

Function Name	Drawing Code	Sensor				Data Acquisition		Accuracy
		Mfgr.	Model	S/N	Range	Digital Recoder Channel No.	Strip Chart No.	
Tank Ullage Pressure	PG-1	CEC	4354-0118	T3139	0–50 psia	1	7-2	1%
Cold-Side Heat-Exchanger Inlet Temp.	RTB-10	Winsco	2448	141	0 to 560°R	2	3-2	±0.2°R
Cold-Side Heat-Exchanger Outlet Temp.	RTB-11	Winsco	2448	140	0 to 560°R	3	4-1	±0.2°R
Expansion Valve (Reg.) Inlet Temp.	RTB-23	Winsco	2448	139	0 to 560°R	4	4-2	±0.2°R
Solenoid Valve Switch Trace	–	–	–	–	On-Off	5	8-2	–
Expansion Valve Outlet Pressure	PG-2	CEC	4-354-0118	T3141	0 to 20 psia	6	5-2	1%
Warm-Side Heat-Exchanger Inlet Temp.	RTB-22	Winsco	2448	152	0 to 560°R	7	6-1	±0.2°R
Warm-Side Heat-Exchanger Outlet Temp.	RTB-12	Winsco	2448	C952	0 to 560°R	8	6-2	±0.2°R
Solenoid Valve Downstream Line Temp.	RTB-8	Rosemont	1186	S592793	0 to 560°R	9	2-1	±0.2°R
Solenoid Valve Downstream Pressure	PF-4	Statham	PG-285	150	0 to 50 psia	10	2-2	1%
Tank Internal Bulk Temp., Bottom Ref.	RTB-9	Winsco	2448	138	0 to 560°R	12	3-1	±0.2°R
Tank Internal Bulk Temp., 30% Level	T/C9-4*	CU/CN	Differential	–	0 to 460°R	13	–	±2.0°R
Tank Internal Bulk Temp., 60% Level	T/C9-5*	CU/CN	Differential	–	0 to 460°R	14	–	±2.0°R
Tank Internal Bulk Temp., Vent Inlet	RTB-13	Rosemont	1186	F503	0 to 560°R	15	1-2	±0.2°R
Tank Pressure-Line Gas Temp.	T/C-19	CU/CN	LN_2 Ref.	–	0 to 460°R	16	–	±3.0°R
Tank Vent-Line Gas Temp.	T/C-20	CU/CN	LN_2 Ref.	–	0 to 460°R	17	–	±3.0°R
Tank Liquid Level	OS-1	Bendix	GL-103	–	On-Off	18	–	–
Tank Liquid Level	OS-3	Bendix	GL-103	–	On-Off	19	–	–
Tank Liquid Level	OS-4	Bendix	GL-103	–	On-Off	20	–	–
Tank Liquid Level	OS-5	Bendix	GL-103	–	On-Off	21	–	–
Tank Liquid Shutoff-Valve Switch Trace	–	–	–	–	On-Off	22	8-1	–
Boiloff Flow Rate, Low Range	FLW-4	Rosemont	124AD	–	0–0.2 lb/hr	23	–	±2.0%
Boiloff Flow Rate, High Range	FLW-2	Rosemont	124AD	–	0–1.2 lb/hr	24	–	±2.0%
Cold-Side Flow Rate	FLW-1	Brooks	59M	–	0–10 lb/hr	25	5-1	
Vacuum Chamber Pressure	NRC	NRC	524	–	10^{-4} to 10^{-7} Torr	26	–	12%

LEGEND: RTB – Resistive Temp. Bulb; PG – Pressure Gage; T/C – Thermocouple; OS – Optical Sensor; FLW – Flow; NRC – National Research Corp.; CEC – Consolidated Electronic Corp.; CU/CN – Copper Constantan; *Reference to RTB-9

- Instrumentation precalibrations were performed and chamber pumpdown was started.
- The tank and plumbing lines were purged with GN_2 until gas samples indicated all O_2 was removed from the system.
- The flow control unit solenoid valve was then opened, and the thermal conditioning system and tank were purged with GN_2 an additional 15 min.
- The nitrogen purge sequence was repeated with GH_2 until all nitrogen was removed from the system. This purge was continued for at least 30 min.
- All systems and instrumentation were checked prior to conducting the tests.

Test Sequence. The thermal conditioning system was tested in accordance with the following procedure:

- The tank was filled with liquid hydrogen to the 5 percent ullage (or OS-5) level where a soak and boiloff stabilization test was performed for 10 hr. During this period a leak developed causing the vacuum chamber pressure to rise from 1×10^{-6} to 2×10^{-4} Torr before it stabilized.
- Seventeen test runs of the thermal conditioning system operations were performed at different liquid levels and mixer motor settings. A typical operational sequence was as follows:
  - Adjust liquid level to provide 5 percent ullage (OS-5)
  - Set mixer motor frequency and voltage and activate the system
  - Allow system to vent until pressure rate is established
  - Set new motor frequency and voltage, and repeat sequence
  - Adjust to new liquid level, and repeat sequence

Post-Test Activity. Post-test activity consisted of the following procedures:

- The tank was drained of all LH_2 and purged with GH_2, followed by GN_2.
- The entire test tank and coldwall were purged with warm GN_2 until the temperature was greater than 500° R.
- Chamber vacuum was broken and preparations for the side-mounted test were begun.

Thermal Conditioning System – Side Mounted Configuration

The thermal conditioning system was removed from the lid and mounted to the slosh baffles on the side of the tank at the approximate tank equator so that the jet axis was directed horizontally across the tank as shown in Fig. 42. The thermal conditioning system vent line was connected to the tank cover passthrough with 10 ft of 1/4-in. tubing, and then to the same pumping system as for the top-mounted tests.

Two optical sensors were removed from the probe and placed on the thermal conditioning system aluminum mounting plate between the expansion valve and the heat exchanger and above the solenoid flow control valve. Location of the optical sensors on the system is indicated in Fig. 43.

Instrumentation was essentially the same as for top-mounted test series, except for the relocation of two optical sensors.

Pretest Activity. Pretest activity consisted of the following:

- The tank was assembled and leak checked. This check indicated a leak through the pins of an instrumentation passthrough, which was replaced.
- The sequence of assembly of the fiberglass dome through assembly of the chamber has been previously described.
- The chamber was pumped down to 1×10^{-6} Torr.
- Instrumentation precalibration was performed and all systems were made ready for testing, including the purge cycle as previously described

Test Sequence. Sixteen tests were performed in this orientation in accordance with the following sequence.

- With the liquid nitrogen coldwall operating, the tank was filled to the 5 percent ullage (or OS-5) level, and a 10-hr hold started for baseline boiloff measurements.

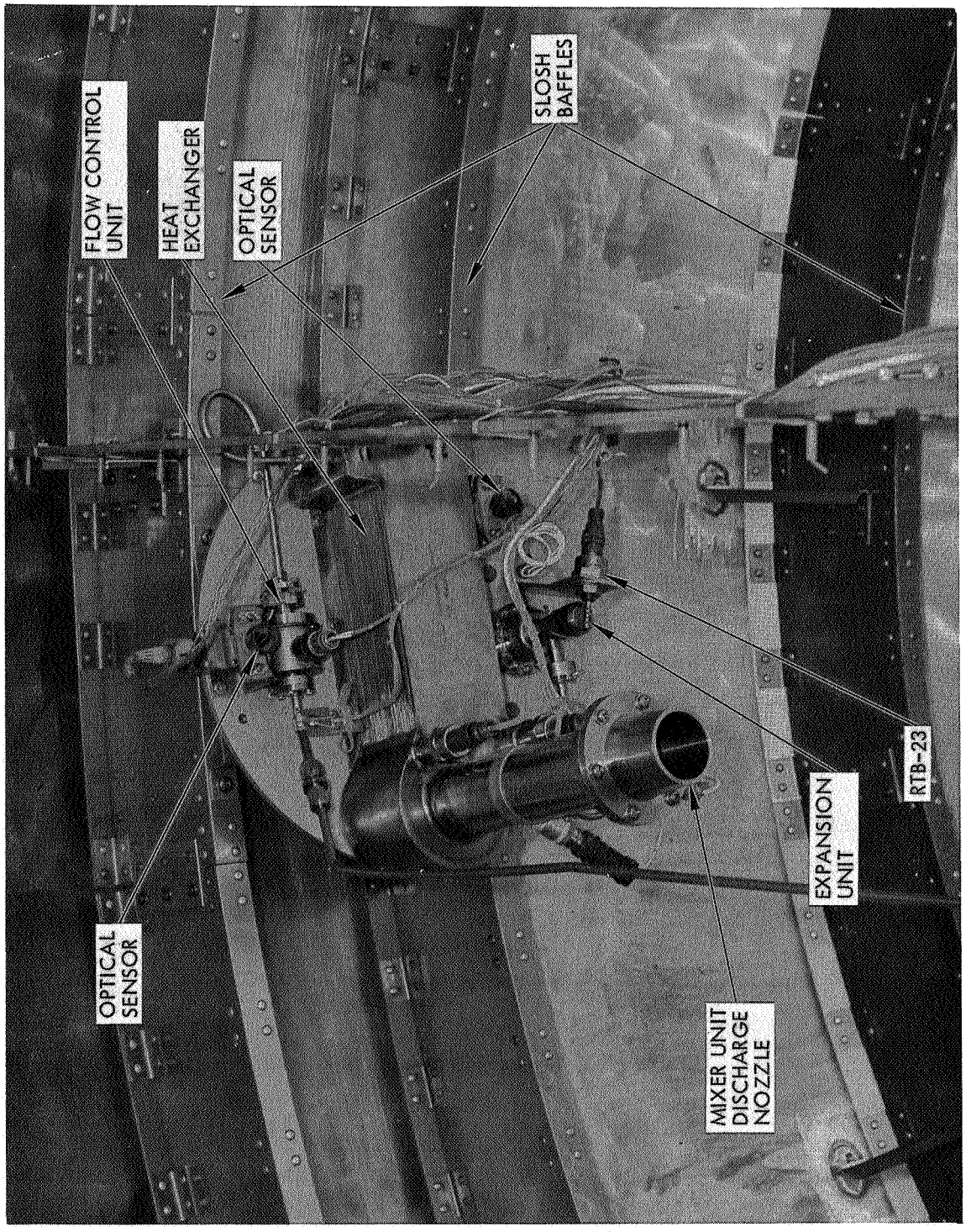

Fig. 42 Thermal Conditioning System Mounted to Baffles on Side of Tank

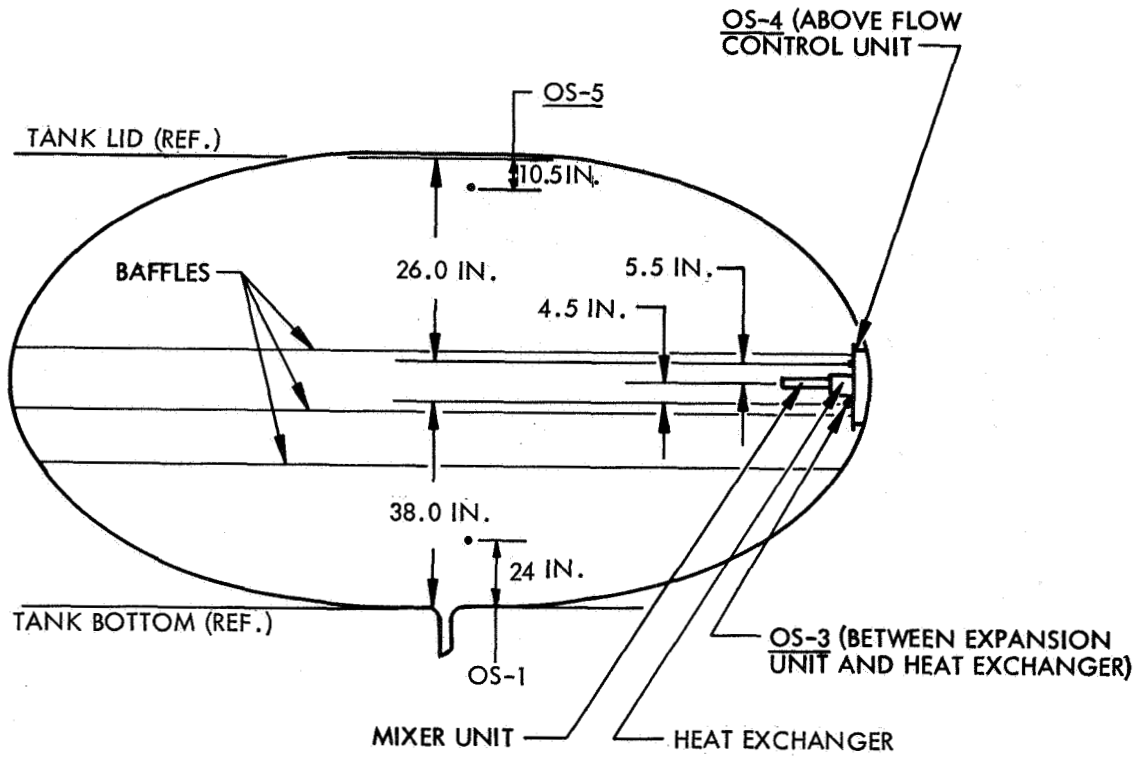

Fig. 43 Optical Sensor Locations on 110-in.-Diameter Tank

- When the boiloff reached equilibrium, tests were performed at three liquid levels and three motor settings.
- A typical test sequence is as follows:
  - Adjust liquid level to provide 5 percent ullage
  - Close tank vent valve
  - Set mixer motor frequency and voltage and activate thermal conditioning system
  - Allow system to vent for 2 to 3 hr to establish transient and steady-state performance and tank pressure decay
  - Set different motor frequency and voltage
  - Repeat 2 to 3 hr vent test to establish pressure changes
  - Set next mixer motor setting and repeat above sequences
  - Adjust to new liquid level and repeat above sequences
  - Conduct individual tests of the thermal conditioning system

Post-Test Activity. Post-test activity consisted of draining the tank and inserting all systems as previously described.

RESULTS AND ANALYSIS

The data obtained from tests of the thermal conditioning system in liquid hydrogen are presented in this section. Evaluations of the performance of the complete system as well as its individual components are presented herein. The test results are compared with theoretical predictions.

DEWAR TANK TESTS

The 30 tests included in the dewar tank test program were conducted at three different liquid levels with mixer motor input powers from 2.2 to 16.2 w. The tests showed that the thermal conditioning system is capable of automatically controlling tank pressure within a prescribed pressure band set at ± 0.5 psi. Figure 44 shows a strip chart recording of tank pressure and expansion unit discharge pressure during one complete cycle for both gas and liquid venting. All the other tests are summarized in Table 13.

The three liquid levels at which tests were conducted were 2, 23, and 26 in. At the 2-in. level, the thermal conditioning system successfully controlled dewar tank pressure while totally submerged in gaseous hydrogen (Table 13). At the 23-in. level, the dewar pressure was successfully controlled with the unit totally submerged in liquid hydrogen. Although the pressure was controlled over a range of mixer powers, as mixer powers were reduced, the duration of the cycles was increased. Therefore, the length of operating time must be considered when evaluating the efficiency of the thermal conditioning system. Over a given mission duration, the total energy put into the propellant tank, which results in propellant boiloff, is the sum of energy conducted into the tank and that due to the thermal conditioning system.

Table 13

DEWAR TESTS ON LIQUID PROPELLANT THERMAL CONDITIONING SYSTEM

Test No.	Fluid State At Inlet	Motor Frequency (cps)	Motor Voltage (v)	Motor Power (w)	Tank Pressure Opening (psia)	Tank Pressure Closing (psia)	Heat Exchanger Pressure (psia)	Bulk Fluid Temp. (°R)	Heat Exchanger Inlet Temp (°R)	Vent Flow Rate (lb/hr)	Liquid Level (in.)
1	GH_2	307	16	2.2	17.8	16.7	3.1	>140	124	0.64[a]	2
2	GH_2	307	16	2.2	↑	16.7	3.0	>140	124	0.64	2
3	GH_2	307	16	2.2	↑	16.7	3.0	>140	124	0.64	2
4	GH_2	307	16	2.2	↑	16.7	3.0	>140	124	0.64	2
5	LH_2	230	22	8.2	↑	No Control	4.5	37	28	1.7	26
6	↑	218	18	5.	↑	No Control	4.5	↑	↑	↓	26
7	↑	253	27	12	↑	No Control	4.5	↑	↑	↓	26
8	↑	280	32	14.6	↑	No Control	4.5	↑	↑	↓	26
9	↑	300	32	13.6	↑	16.8	4.5	↑	↑	↓	23
10	↑	280	32	14.5	↑	↑	4.4	↑	↑	↓	↑
11	↑	290	32	14.0	↑	↑	↓	↑	↑	↓	↑
12	↑	300	32	13.7	↑	↓	↑	↑	↑	↓	↑
13	↑	320	32	12.8	↑	16.8	↑	↑	↑	↓	↑
14	↑	253	32	16.5	↑	16.9	↑	↑	↑	↓	↑
15	↑	253	27	11.8	↑	16.8	↑	↑	↑	↓	↑
16	↑	230	22	7.5	↑	16.8	↑	↑	↑	↓	↑
17	↑	214	16	2.2	↑	16.8[b]	↑	↑	↑	↓	↑
18	↑	180	16	3.0	↑	16.8	↑	↑	↑	↓	23
19	↑	230	22	7.8	↑	No Control	↑	↑	↑	↓	26
20	↑	253	32	16.2	↑	No Control	↑	↑	↑	↓	↑
21	↑	280	32	14.5	↑	No Control	↑	↑	↑	↓	↑
22	↑	300	32	13.5	↓	No Control	↑	↑	↑	↓	↑
23	↑	320	32	12.5	17.8	No Control	↑	↑	↑	↓	↑
24	↑	320	34	14.2	17.9	No Control	↑	↑	↑	↓	26
25	↑	320	32	12.6	17.8	16.8	↑	↑	↑	↓	23
26	↑	300	32	13.4	17.8	16.8	↑	↑	↑	↓	↑
27	↑	280	32	14.3	17.9	16.9	↑	↑	↑	↓	↑
28	↑	253	32	16.1	17.9	16.9	↑	↑	↑	↓	↑
29	↓	253	27	11.8	17.8	16.9	↓	↓	↓	↓	↓
30	LH_2	214	16	3.0	17.8	No Control	4.4	37	28	1.7	23

(a) Flow rates for GH_2 are calculated.
(b) Marginal control.

FOLDOUT FRAME 1

FOLDOUT FRAME 2

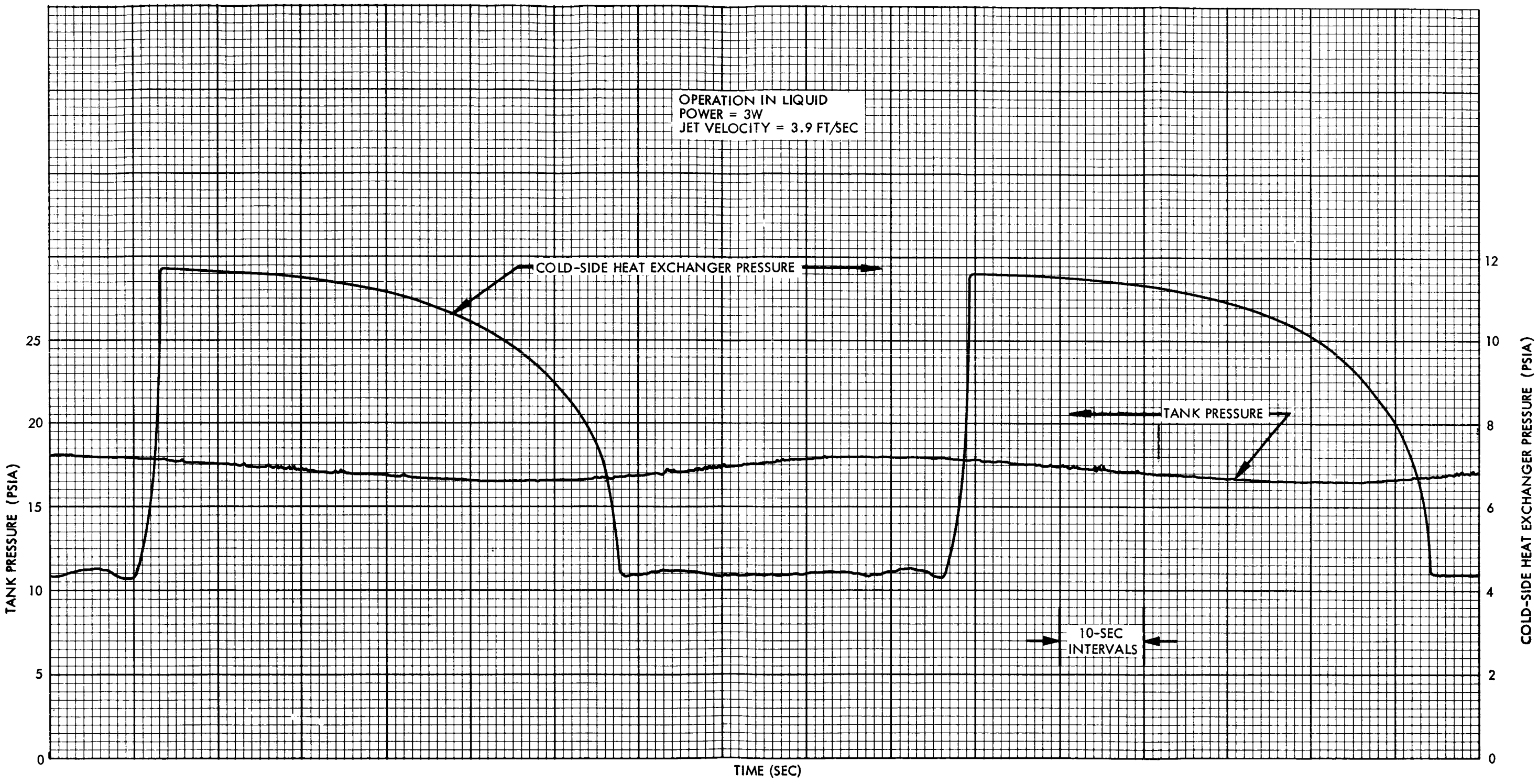

Fig. 44a Dewar Pressure Cycle with Thermal Conditioning System (Operation in Liquid)

FOLDOUT FRAME 1

FOLDOUT FRAME 2

PRECEDING PAGE BLANK NOT FILMED.

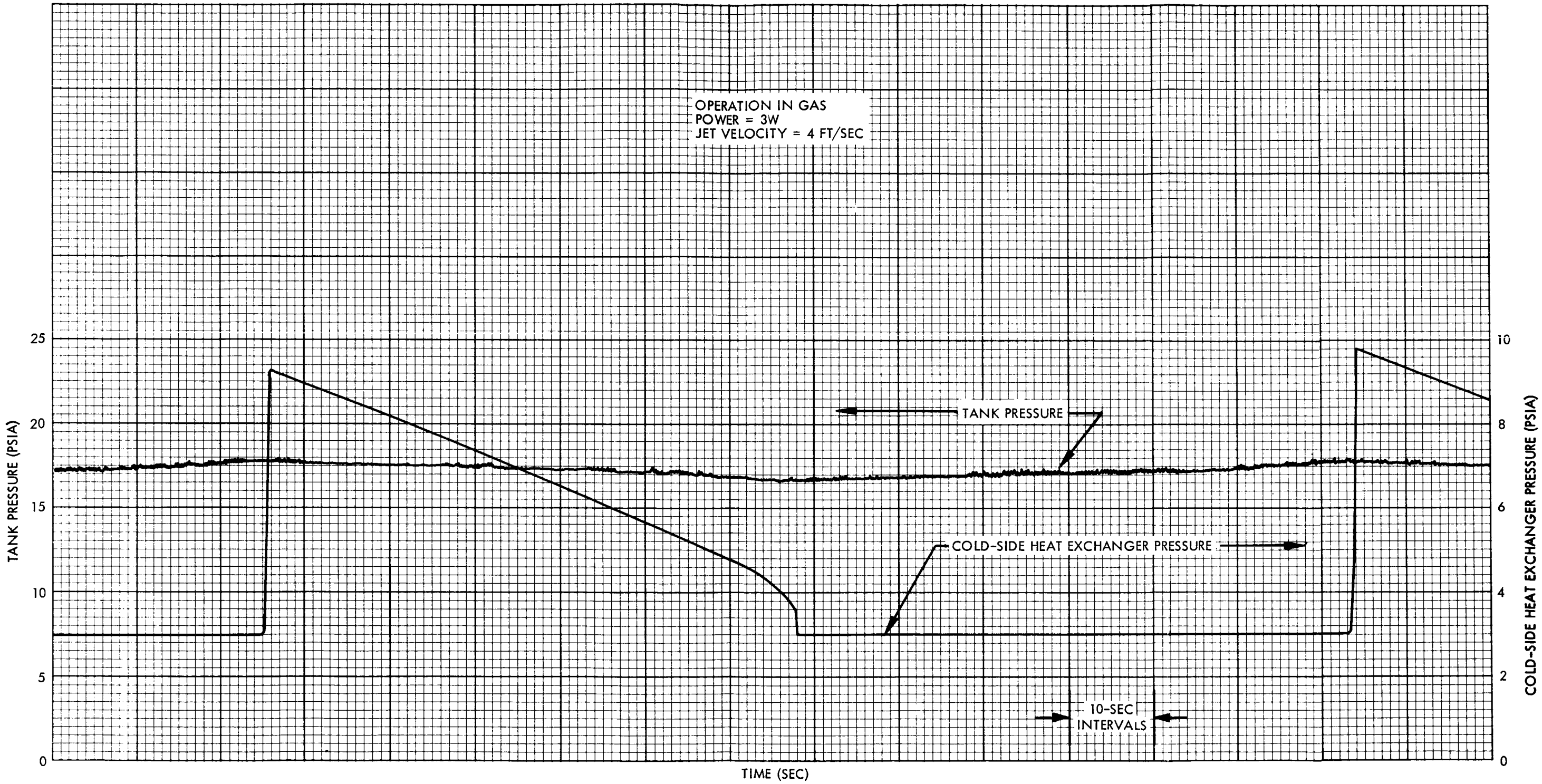

Fig. 44b Dewar Pressure Cycle with Thermal Conditioning System (Operation in Gas)

Thus

$$E_T = Q_o \eta\tau_c + 3.413\ P\eta\tau_a \qquad (4)^*$$

Since $\eta\tau_c$ is the total mission duration (τ_T) this equation can be rearranged to describe the average heating rate contributed by the mixer motor over the entire mission time. This is given by

$$\frac{E_T}{\tau_T} - Q_o = 3.413\ P\frac{\tau_a}{\tau_c} \qquad (5)$$

However, the power level affects the percentage of time the mixer and thermal conditioning system is operative, i.e., $(\tau_a/\tau_c) = f(P)$, and the desired power setting is that where the average energy rate is a minimum and tank pressure is controlled.

Figure 45 shows the average heat input from the mixer to the propellant as a function of operating power for the dewar tests at the 23-in. liquid level. These data indicate that the lowest power, 2.2 w, was also the most efficient power setting investigated.

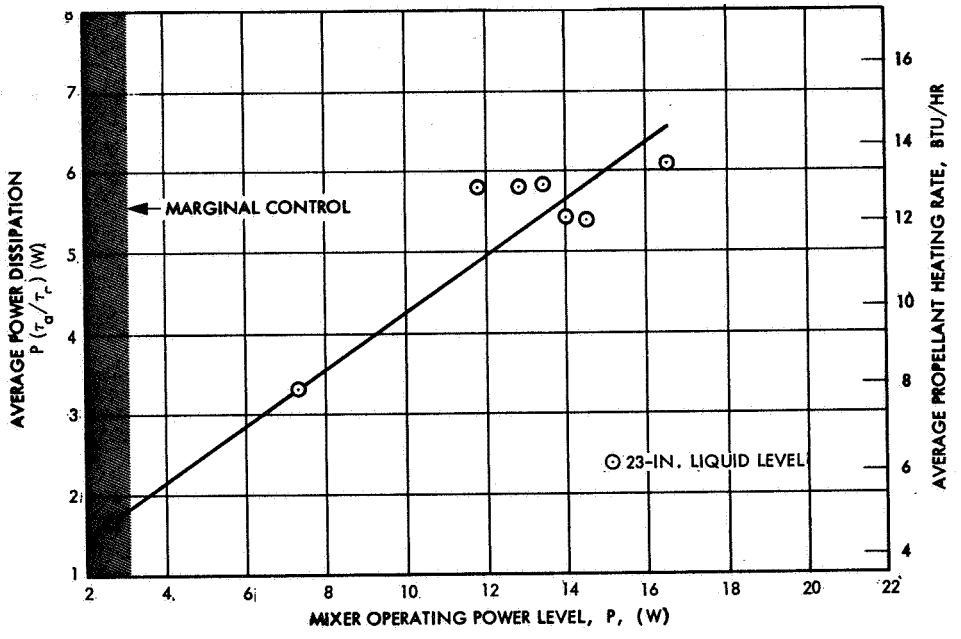

Fig. 45 Effective Mixer Heat Input as Determined from Dewar Tests

Table 13 indicates that the system did not control dewar pressure, even at power levels up to 16 w, when the liquid level was at 26 in. The performance of the individual components was not affected by liquid level, which indicates that the propellant circulation within the dewar was not sufficient to induce condensation at the liquid vapor interface. Further, the results indicate that the particular installation employed in these tests restricted the effective propellant circulation to levels below the 26-in. liquid level for the mixer flows and powers that were investigated. Referring to the installation schematic, (Fig. 37) it can be seen that the installation restricts a significant portion of the dewar. Since the inside diameter of the dewar is 15 in., the thermal conditioning system, mounted on a 14-in.-diameter plate, had to be installed on an angle, with the mixer jet discharging into the lower corner approximately 5 in. above the bottom; the plate blocked off more than 50 percent of the dewar area. These results show the necessity of good circulation within the tank and for condensation at the liquid-vapor interface for effective tank pressure control.

Table 11 and Fig. 44 indicates that the expansion unit regulates the pressure at the heat exchanger inlet to 3 psia when venting vapor and to 4.4 psia when venting liquid. The reasons for this characteristic are not understood. There is a slight reduction in vent rate during gas ingestion below that when liquid is ingested into the system, however, this presents no operational problems.

These subscale tests also verified the operation of the pressure switch, since the activation and deactivation pressures were consistently repeatable within ± 0.1 psi.

MISSION (2) FULL-SCALE TANK TESTS

Test Profiles

Tests were conducted in the 110-in.-diameter tank in both liquid and gas and with the thermal conditioning system mounted either at the top of the tank and at the side of the tank. A summary of these tests is presented in Table 14. In the top position, the

Table 14

THERMAL CONDITIONING TESTS – 110-IN.-DIAMETER TANK

Parameter	Test Number																
	1	2	3	4	5	6	7	8	9	10	11	12	13	14	15	16	17
SIDE ORIENTATION																	
Tank Liquid Level (in.)	64	64	64	64	64	48	48	48	48	38	38	38	38	24	24	64	64
Tank Ullage Volume (%)	5	5	5	5	5	27	27	27	27	50	50	50	50	75	50	5	5
Mixer Motor Frequency (cps)	253	253	230	215	215	253	232	215	215	253	253	230	215	215	215	215	215
Mixer Motor Voltage (v)	45	45	22	16	16	45	22	14	14	45	45	22	16	16	16	16	16
Mixer Motor Power (w)	27.5	27.5	9.8	4	3.8	32	15	4.2	4.2	9.6	9.6	2	2.1	1.2	1.2	–	–
Vent Flow Rate (lb/hr)	1.6	1.6	1.6	1.6	1.6	1.6	1.6	1.6	1.6	1.5	1.5	1.5	1.5	1.7	1.7	1.7	1.7
Vent Duration (hr)	15	2	3	2	1	2.5	2.3	2	2.3	2.7	2.3	1.6	2	2	2	1.5	4
Tank Pressure – Open (psi)	19.7	19.3	18.9	18.5	18.1	17.6	17.2	16.8	16.4	20.8	18.9	17.6	17.3	20.7	20.1	27.5	26.5
Tank Pressure – Close (psi)	18.3	18.9	18.5	18.1	18.0	17.2	16.8	16.4	16.2	18.5	17.6	17.3	17	20	19.5	21.4	22.0
Fluid Quality at Expansion Unit Inlet (lb vapor/lb fluid)	0	0	0	0	0	0	0	0	0	0	0	0	0	100	0	0	0
Fluid Temp. at Expansion Unit Inlet (°R)	38	37.4	37.5	37.4	37.4	37	36	36	36	38	37	37	37	46	38	38	38
Fluid Quality at Cold Side Hex Inlet (%)	9	9	9	9	9	9	9	9	9	9	9	9	9	100	9	9	9
Fluid Temp. at Cold Side Hex Inlet (°R)	29	29	29	29	29	28	28	28	–	–	–	–	–	46	28	28	28
Fluid Temp. at Cold Side Hex Outlet (°R)	38	37	37	37	37	36	36	36	36	38	37	37	37	46	38	38	38
Fluid Press. at Cold Side Hex Inlet (psi)	3.8	3.8	3.8	3.8	3.8	3.8	3.7	3.7	3.6	–	–	–	–	3	3	3.4	3.4
Fluid Quality at Warm Side Hex Inlet (lb vapor/lb fluid)	0	0	0	0	0	0	0	0	0	100	100	100	100	100	100	100	100
Fluid Temp. at Warm Side Hex Outlet (°R)	38	37	37	37	37	36	36	35	35	38	37	37	37	46	37	37	37

	Test Number																
	1	2	3	4	5	6	7	8	9	10	11	12	13	14	15	16	17
TOP ORIENTATION																	
Tank Liquid Level (in.)	43	43	43	64	64	64	64	64	64	64	64	64	64	64	64	64	64
Tank Ullage Volume (%)	50	50	50	5	5	5	5	5	5	5	5	5	5	5	5	5	5
Mixer Motor Frequency (%)	0	310	310	230	215	215	230	230	250	215	215	230	250	0	260	260	–
Mixer Motor Voltage (v)	0	58	25	22	16	20	22	25	25	25	20	20	20	0	32	45	–
Mixer Motor Power (w)	0	11	6.2	9.2	3.4	6.8	8.5	9.5	8.6	10.2	6.3	6	5.5	0	15	25	–
Vent Flow Rate (lb/hr)	1.5	1.5	1.5	1.7	1.7	1.7	1.7	1.7	1.7	1.7	1.7	1.7	1.7	1.7	1.7	1.7	–
Vent Duration (hr)	0.25	0.25	0.3	0.7	0.5	0.12	0.8	0.6	0.15	0.18	0.11	0.1	0.11	0.25	0.2	0.6	–
Tank Pressure – Open (psi)	19.7	19.6	20.3	19.2	18.4	18.1	18.0	17	16.9	16.9	16.8	16.8	16.8	16.8	16.7	16.7	–
Tank Pressure – Close (psi)	19.6	20.3	20.1	18.5	18.1	18	17.6	17	16.9	16.8	16.8	16.8	16.8	16.7	16.7	16.5	–
Fluid Quality at Expansion Unit Inlet (lb vapor/lb fluid)	100	100	100	0	0	0	0	0	0	0	0	0	0	0	0	0	–
Fluid Temp. at Expansion Unit Inlet (°R)	>107	>89	>80	37	37	37	37	37	37	37	37	37	37	37	36	36	–
Fluid Quality at Cold Side Hex Inlet (lb vapor/lb fluid)	100	100	100	9	9	9	9	9	9	9	9	9	9	9	9	9	–
Fluid Temp. at Cold Side Hex Inlet (°R)	>107	>89	>79	28	28	28	28	29	29	29	28	28	28	28	28	29	–
Fluid Temp. at Cold Side Hex Outlet (°R)	>108	>88	>78	37	29	29	29	29	29	29	29	29	29	29	29	36	–
Fluid Press. at Cold Side Hex Inlet (psi)	–	–	–	–	–	–	–	–	–	–	–	–	–	–	–	–	–
Fluid Quality at Warm Side Hex Inlet (lb vapor/lb fluid)	100	100	100	0	0	0	0	0	0	0	0	0	0	0	0	0	0
Fluid Temp. at Warm Side Hex Outlet (°F)	–	–	–	–	–	–	–	–	–	–	–	–	–	–	–	–	–

mixer jet was discharging vertically downward along the tank axis and in the side position; it was directed horizontally along the tank major diameter. Other variables were liquid level and mixer-motor power. The side-mount tests spanned approximately 90 hr of uninterrupted testing, for which a complete test profile is shown in Fig. 46.

In the first 13 hr, the tank, filled to the 5-percent ullage level, was nonvented and the pressure was allowed to rise. This was done to establish the average heat leak into the tank for subsequent evaluation of system performance. At the end of this pressure-rise test, the thermal conditioning system was activated with 27.5-w power input to the motor. A small rise and fall in pressure of approximately 0.1 psia covering 400 sec in time occurred when the thermal conditioning system was activated. This characteristic occurred repeatedly throughout the program each time the thermal conditioning system was activated with the unit submerged in liquid hydrogen. The reverse happened each time the system was turned off (i.e., a fall and rise in pressure of approximately 0.1 psi).

The tank pressure was caused to drop steadily at this mixer setting, as shown in Fig. 46. Uninterrupted venting with the thermal conditioning unit at this power setting was conducted for the next 11 hr to observe any variations in pressure decay rate and to obtain data on a complete vent cycle. At this point, the thermal conditioning system was deactivated and the pressure-rise test repeated for approximately 11 hr. The characteristic reverse pressure hump can be seen in Fig. 46 when the system was turned off.

The pressure decay test was repeated at the previous mixer setting (27.5 w), primarily to observe system repeatability. The characteristic hump was again noted, after which the tank pressure decay rate was determined to be steady and the same as during previous test. Therefore, this test was discontinued after 2 hr by changing the mixer setting to a lower power level (9.8 w). This change reduced the flow through the mixer unit and through the warm side of the heat exchanger. The test at this second power setting was conducted uninterrupted for 3 hr, during which time the pressure was still being reduced at a steady rate.

FOLDOUT FRAME 1

FOLDOUT FRAME 2

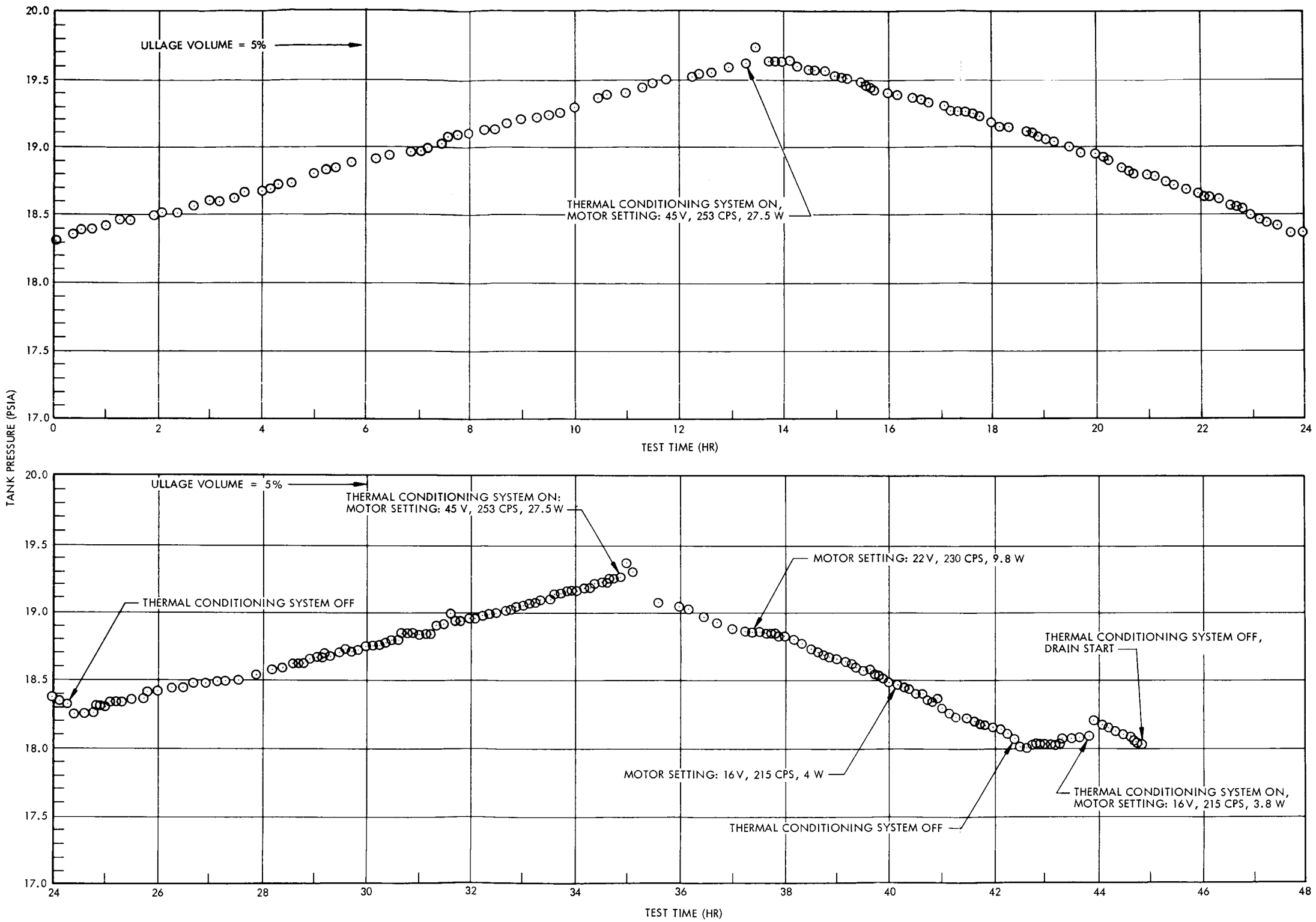

Fig. 46 Test Profile – Unit Side-Mounted in 110-in.-diameter Tank

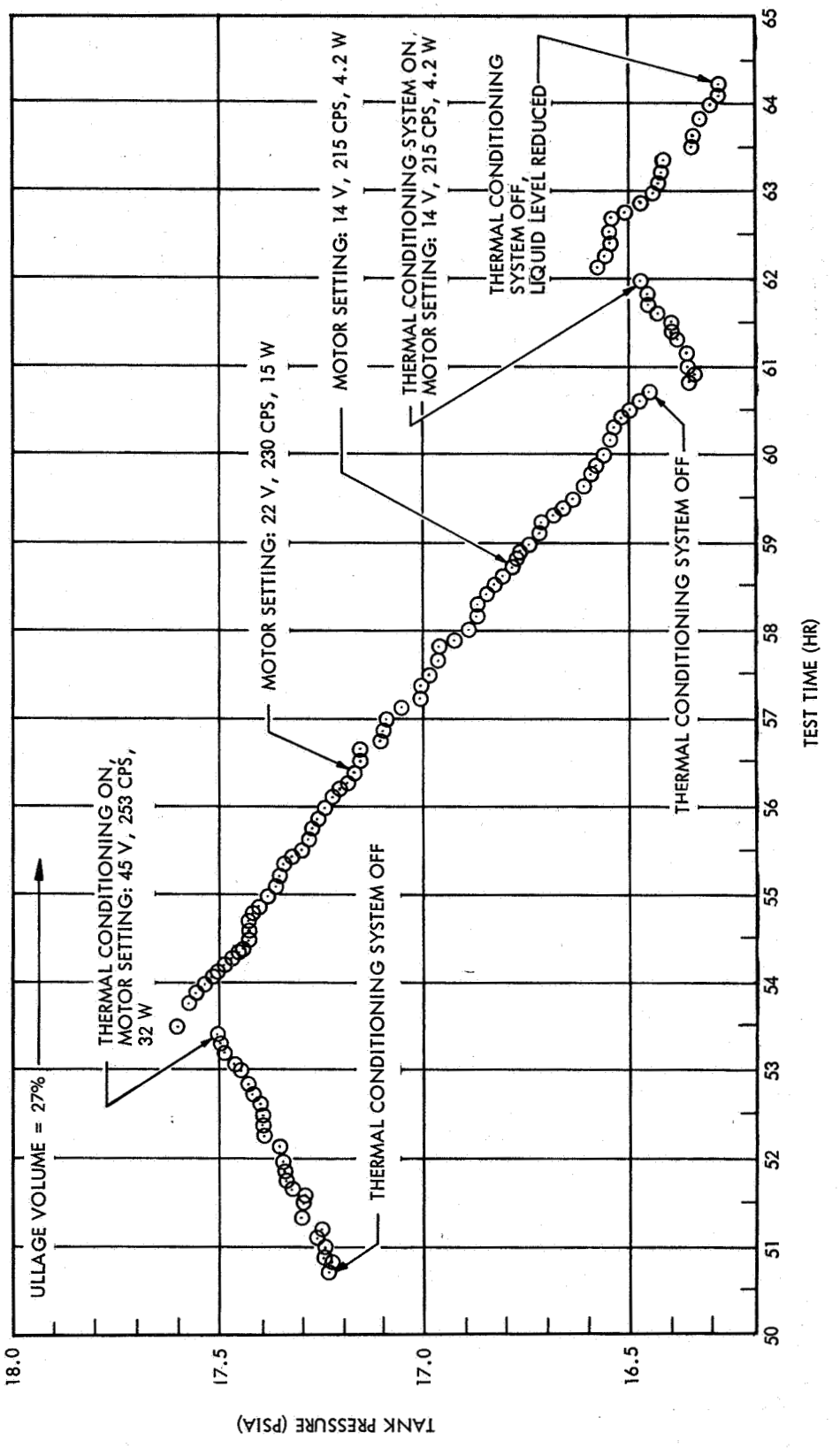

Fig. 46 (Cont.)

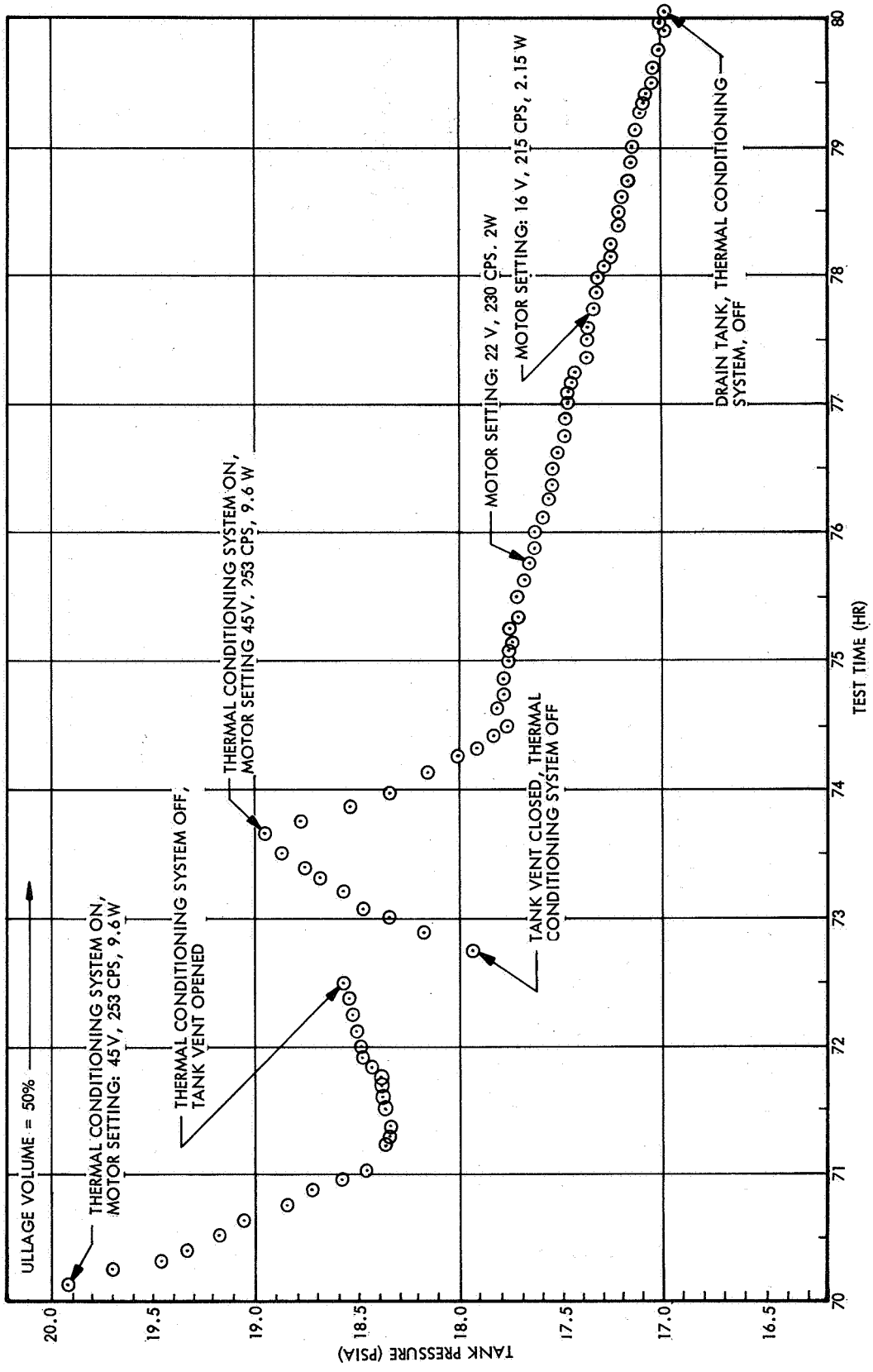
ULLAGE VOLUME = 50%
THERMAL CONDITIONING SYSTEM ON, MOTOR SETTING: 45 V, 253 CPS, 9.6 W
THERMAL CONDITIONING SYSTEM OFF, TANK VENT OPENED
THERMAL CONDITIONING SYSTEM ON, MOTOR SETTING 45 V, 253 CPS, 9.6 W
TANK VENT CLOSED, THERMAL CONDITIONING SYSTEM OFF
MOTOR SETTING: 22 V, 230 CPS, 2W
MOTOR SETTING: 16 V, 215 CPS, 2.15 W
DRAIN TANK, THERMAL CONDITIONING SYSTEM, OFF
TANK PRESSURE (PSIA)
TEST TIME (HR)
20.0
19.5
19.0
18.5
18.0
17.5
17.0
16.5
70
71
72
73
74
75
76
77
78
79
80

Fig. 46 (Cont.)

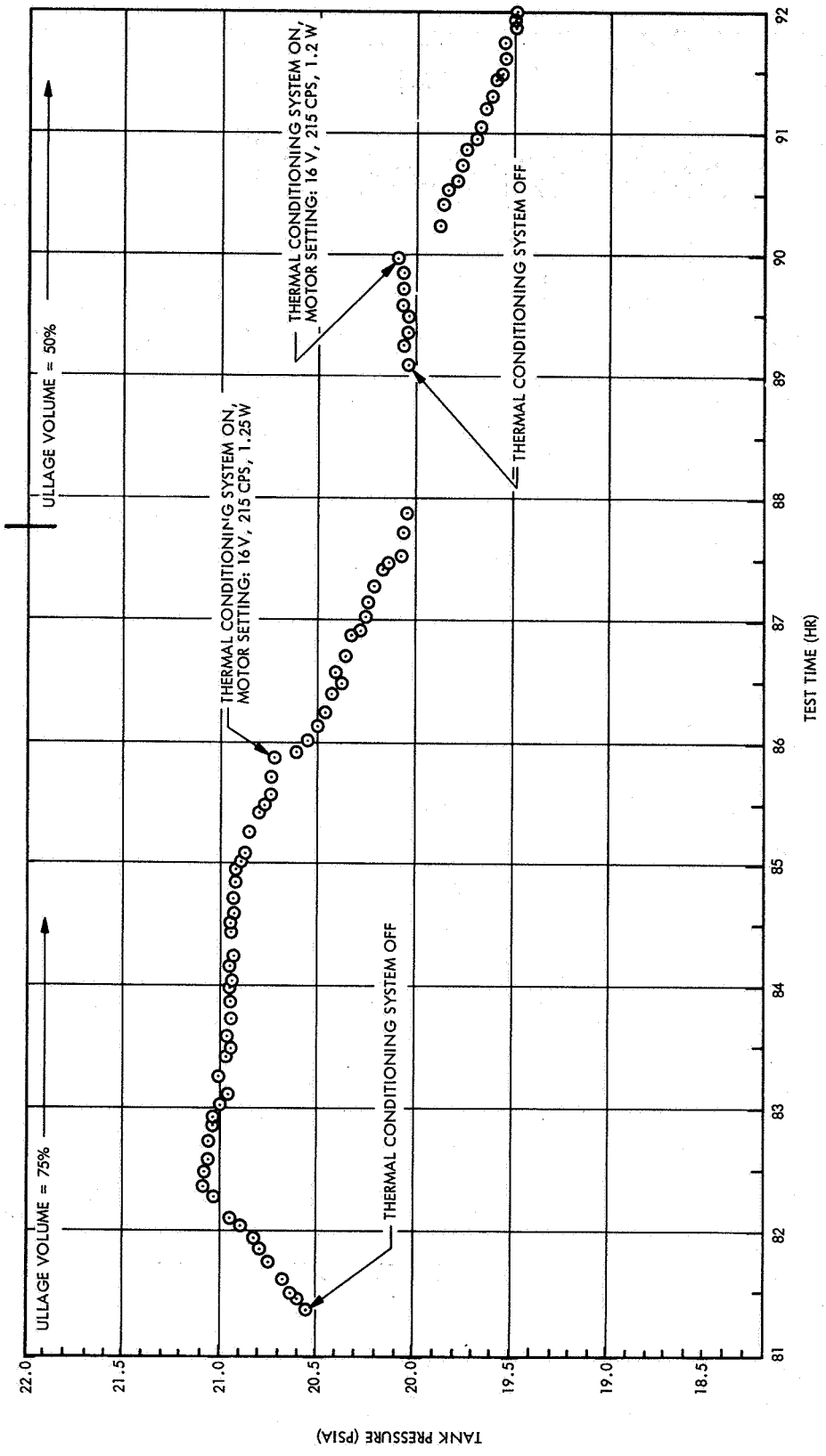
ULLAGE VOLUME = 75%
ULLAGE VOLUME = 50%
THERMAL CONDITIONING SYSTEM OFF
THERMAL CONDITIONING SYSTEM ON, MOTOR SETTING: 16 V, 215 CPS, 1.25 W
THERMAL CONDITIONING SYSTEM OFF
THERMAL CONDITIONING SYSTEM ON, MOTOR SETTING: 16 V, 215 CPS, 1.2 W
TANK PRESSURE (PSIA)
TEST TIME (HR)
22.0
21.5
21.0
20.5
20.0
19.5
19.0
18.5
81
82
83
84
85
86
87
88
89
90
91
92

Fig. 46 (Cont.)

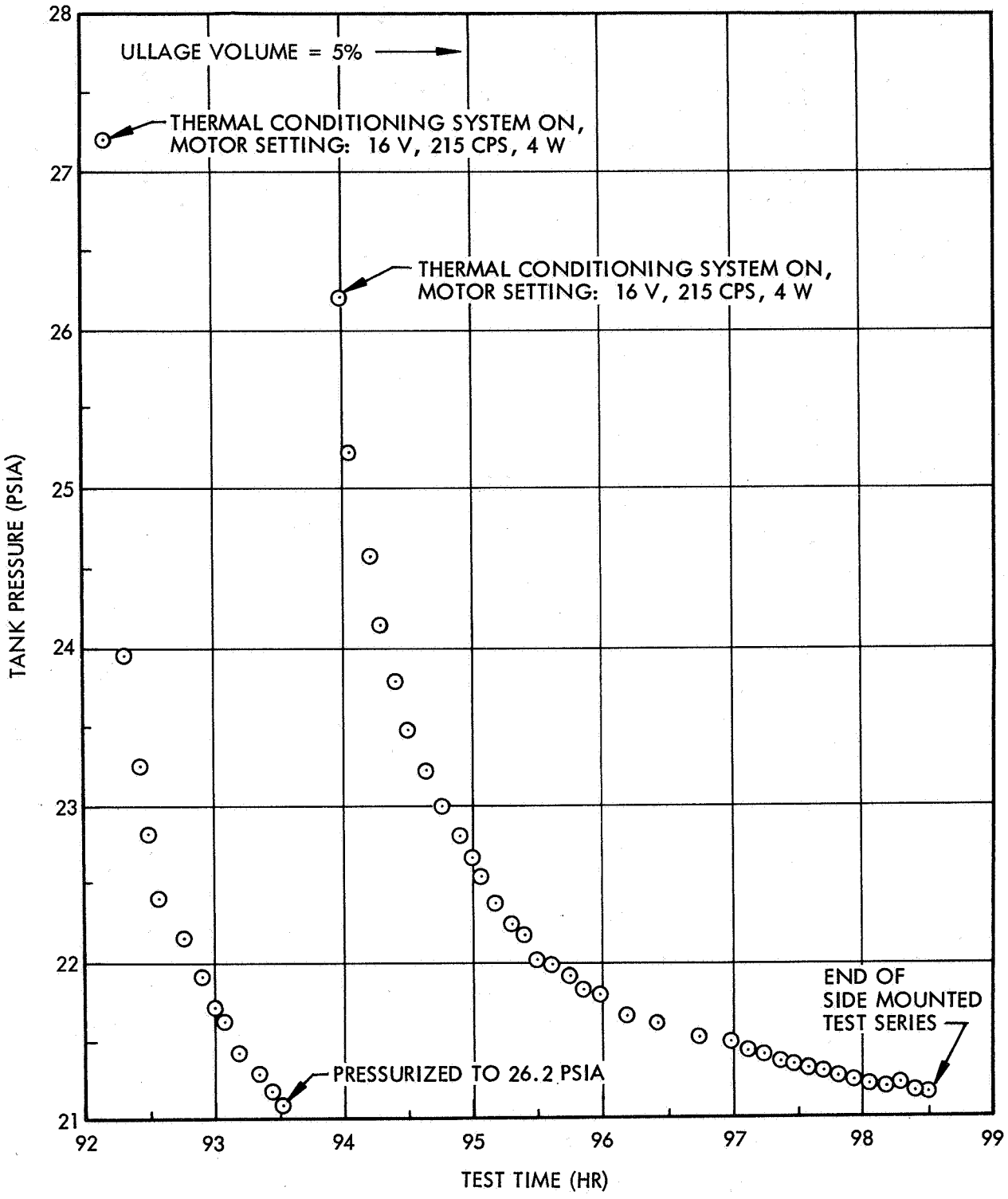
ULLAGE VOLUME = 5%
THERMAL CONDITIONING SYSTEM ON,
MOTOR SETTING: 16 V, 215 CPS, 4 W
THERMAL CONDITIONING SYSTEM ON,
MOTOR SETTING: 16 V, 215 CPS, 4 W
PRESSURIZED TO 26.2 PSIA
END OF
SIDE MOUNTED
TEST SERIES
TANK PRESSURE (PSIA)
TEST TIME (HR)
28
27
26
25
24
23
22
21
92
93
94
95
96
97
98
99

Fig. 46 (Cont.)

The mixer power setting was then further reduced to 4 w and the tank pressure decay observed for another 2 hr. As seen from Fig. 46, the tank pressure was still being reduced at approximately the same steady rate as with the previous power setting. At this point the thermal conditioning system was turned off, and again the characteristic reverse tank pressure hump was noted. A short period of nonvent pressure rise (approximately 1.5 hr) was permitted and a second thermal conditioning test at the third power level (3.8 w) was conducted in order to again determine system performance repeatability.

The tank was then drained to the next liquid level (27 percent ullage volume) and the tank allowed to thermally stabilize for approximately 5.5 hr. A pressure-rise-rate test was then conducted to determine the effect of liquid-level change. This test was run for nearly 3 hr. When the thermal conditioning system was turned on, the small pressure-rise hump was again noted.

Once the thermal conditioning system was activated, three consecutive tests were run; one at each of the motor settings used with the 5-percent ullage volume, with no intermediate nonventing tests. The duration of each of these tests was from 2 to 2.5 hr. At the conclusion of the third test, the system was turned off and, again, the tank pressure dropped approximately 0.1 psi in 10 min before it started to rise. The tank pressure was allowed to rise for approximately 1 hr, and then the thermal conditioning system was again activated for 2 hr at the lowest power setting tested (4.2 w) to confirm tank pressure control.

The liquid level was then reduced to 38 in. At this level, the thermal conditioning system expansion unit intake is in liquid, the heat exchanger warm-side intake is in gas, and the mixer unit discharge is in gas (50-percent ullage). At this point, before activating the thermal conditioning system, the tank pressure rise was observed for 2 hr with no venting. However, the rate of pressure rise was high because of the injection of warm hydrogen pressurant gas, to effect the drainage of the tank from 48 in. liquid level to 38 in. The tank pressure rose from 16 to 24 psia in approximately 2.5 hr.

At this point, the tank was vented to a pressure of 16.5 psi through the tank ullage gas vent valve, to accelerate the thermal stabilization process, by venting some of the warm hydrogen gas from the ullage. The tank ullage vent valve was then closed and the tank pressure was permitted to rise to 21 psia. The thermal conditioning system was then activated at the highest of the three mixer-motor settings. It can be seen from Fig. 46 that the pressure response was very fast, dropping the pressure from 21 to 18 psi in little more than 1 hr. This rapid response is a direct result of cooling the superheated ullage gas in the heat exchanger, and tends to demonstrate the capability of the thermal conditioning system to control tank pressure after pressurization for an engine firing. As shown in Fig. 46, the tank pressure decay bottomed out at about 18.3 psi, and then rose again to 18.5 psia before falling again even though the thermal conditioning system was still venting. This phenomenon was apparently due to the tank pressure dropping slightly below the saturation pressure at the liquid vapor interface, causing some hydrogen vaporization. The indicated temperature just below the surface was 38°R, which is the saturation temperature at a pressure of 18.3 psia.

After about 3 hr of venting at this condition, the tank was again topped off at 50 percent ullage, (OS-3) vented through the tank vent valve to 18 psi, and then nonvented to check the tank pressure rise. In approximately 1 hr, the pressure increased 1 psi. The thermal conditioning system was again activated with the high mixer-motor voltage and frequency. With vapor through the mixer, this setting resulted in 9.6 w of power to the motor. This time the pressure dropped at about the same rate as in the previous test, for 1 hr, and then settled out at a slower, and apparently equilibrium decay rate.

After 1.5 hr of steady pressure decay, the mixer power input was reduced to 2 w and the tank pressure checked for 2 hr. This operation was repeated at a third mixer power setting of 2 w, after which the tank was drained to a lower liquid level for testing the thermal conditioning system operation immersed entirely in hydrogen gas. The tank was drained to a liquid level of 24 in. which is 75-percent ullage and the rate of pressure rise established with no venting. For the first 1.5 hr, the pressure rose;

however, it was found that four optical sensors were functioning and drawing electrical power. These sensors should have been deactivated since they consume a total of 28 w, which is heat input directly into the tank. When these were turned off, the tank pressure started to drop slowly. The pressure was tracked for another 3 hr, and then the thermal conditioning system was activated at the lowest of the three power levels. This reduced the tank pressure at an accelerated rate for 2 hr before being turned off.

Following the test with all-gas operation, the tank was again filled to the 50-percent ullage level, and the thermal conditioning system test was repeated at the lowest of the three power levels. This test was conducted to establish repeatability at the low mixer input power. At the conclusion of this repeat test, the tank was pressurized with warm hydrogen gas to 28 psia, and the thermal conditioning was turned on to simulate tank pressure decay while venting with the thermal conditioning system, following engine firing. This test concluded the thermal conditioning system tests in the side-mounted configuration.

The top-mounted tests, being the first in the large tank, were conducted in a different manner, being more explorative of the basic characteristics of the thermal conditioning system operation. Since the thermal conditioning system was mounted only 15 in. below the top of the tank (10-percent ullage), only one level for operation in liquid and one in gas was investigated. However, a much wider range of mixer motor settings was covered in this test series.

The first tests were conducted with the tank only 50 percent full; thus, the thermal conditioning system was operating entirely in hydrogen vapor with the mixer discharge approximately 13 in. above the free surface. Three mixer power settings – 0, 11, and 6.2 w – were used. Figure 47 shows the resulting pressure history. It can be seen that the pressure was being reduced slowly when the thermal conditioning system was venting, but with the mixer not operating (0 w). When the motor was activated with 11 w of power, the pressure trend reversed and continued to rise until the power was reduced to 6.2 w, at which time the pressure once again started to drop. This

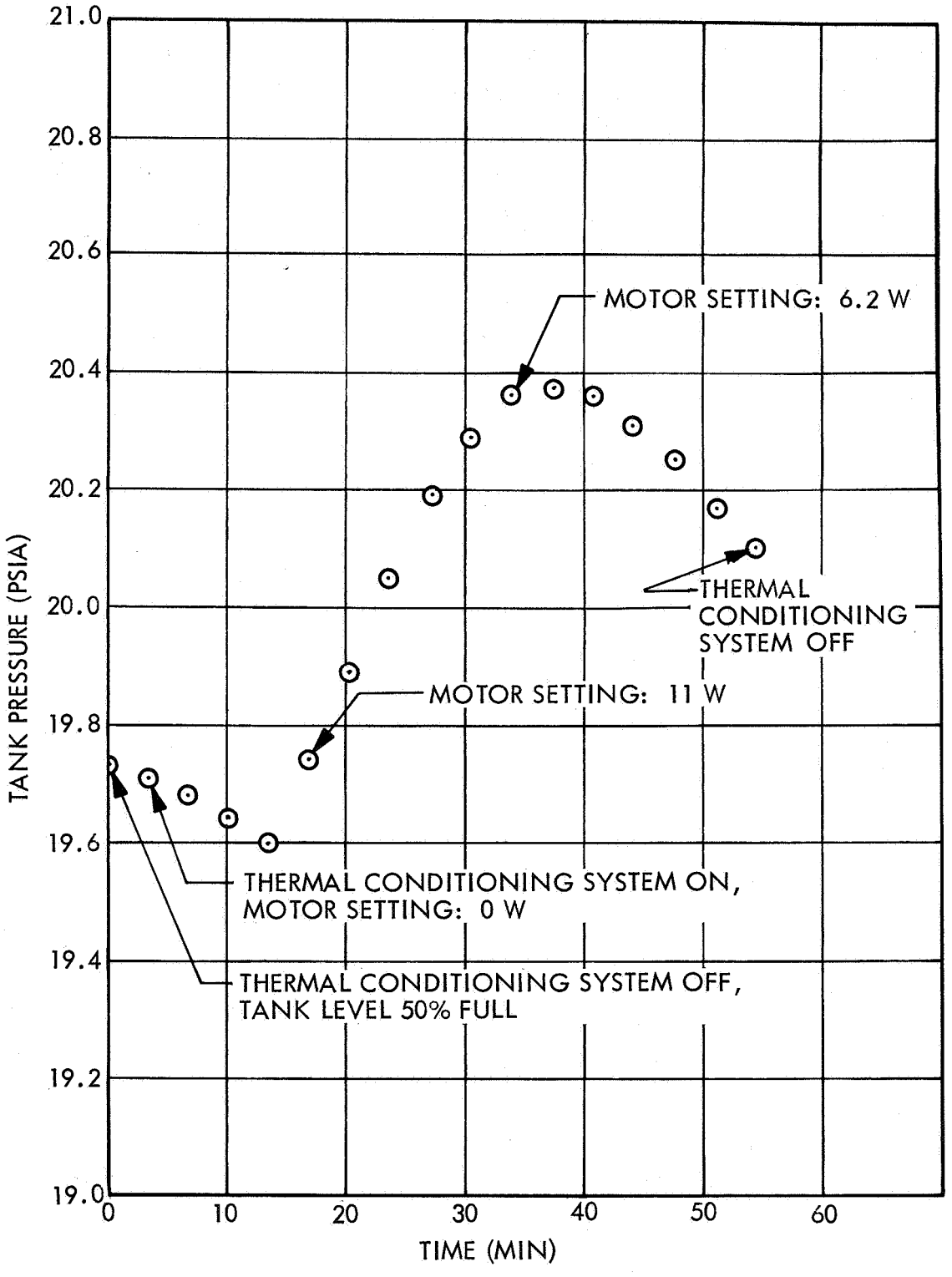

Fig. 47 Tank Pressure History With Gas Venting – Top-Mounted Orientation

double reversal is apparently due to the high degree of stratification in the ullage which occurred as a result of the warm pressurant used to pressurize and drain the tank down to the 50-percent level following a prior boiloff test. This observation is similar to the double reversal shown previously in a side-mount test at the 50 percent level. The pressure drops until it reaches saturation at the liquid vapor interface temperature. Vaporization occurs, causing a sudden increase in tank pressure. The significance of this test is that the thermal conditioning unit adequately controlled this transient situation. Note that the pressure excursion is small; from 19.6 psia to 20.4 psia.

A complete test profile for the liquid test series is described on Fig. 48. It consists of essentially one long pressure decay period, with frequent changes in motor settings to determine if the variable affected the rate of pressure decay or the performance of the heat exchanger.

During the first 3 hr, the pressure response was fairly rapid and it appeared that it might be less responsive at the lower power settings. However, this was primarily due to transients following the tank fill process. Later in the tests, when conditions in the tank were stable, there appeared to be only a moderate dependency on power level, as was the case with the side-mounted tests. Approximately 2 hr before the end of this test, the thermal conditioning system was shut off to establish a pressure rise rate. The reverse hump can be seen at this time similar to that seen earlier in the side-mount test profile.

The final tests in the top-mounted position were conducted to develop the operating characteristics line for the mixer fan. At each of four different motor frequencies discrete values of voltage between 5 and 50 v were applied to the mixer, and the resulting power was recorded. It will be seen later that these data also helped in defining the pressure drop through the warm side of the heat exchanger.

System Performance Analysis

The thermal conditioning system must be capable of controlling tank pressure efficiently. This control has been demonstrated with the system in two different orientations in the 110-in.-diameter tank with respect to the gravitational field. The efficiency with which this control is obtained may be measured in terms of boiloff propellant.

For a tank of liquid hydrogen with no temperature gradients or stratification, the rate of pressure change is given by:

$$\frac{dp}{d\theta} = \frac{1.15}{W}\left[Q_o + (3.413\ P - m_o\ \lambda)\right] \tag{6}$$

During the nonvent period, Eq. (6) reduces to:

$$\frac{dp}{d\theta} = \frac{1.15}{W}\ Q_o \tag{7}$$

See Appendix C, for the development of this equation. This equation is valid if the depressurization process is limited only by the net rate of energy removed from the tank and not by thermal diffusion or hydrogen gas condensation at the liquid-vapor interface. Thus, Eq. (6) assumes the process as being limited by the rate of heat transfer within the heat exchanger only.

Figure 49 presents a comparison of the experimental data and Eq. (6) . The theory lines are based upon a tank heating rate, Q_o , of 90 Btu/hr. This is an average value as determined from the measured pressure rise rate during the nonvent portion of the pressure cycle tests, with 5 and 27 percent ullage volumes. This pressure rise rate was 0.1 psi per hr for both ullage ratios, from which the heating rate was calculated to be 90 Btu/hr and 79 Btu/hr, for the 5 and 27 percent ullage volumes, respectively. It can be seen that there is fair agreement between Eq. (6) and the experiment at the 5 and 27 percent ullage conditions. However, as ullage volume is

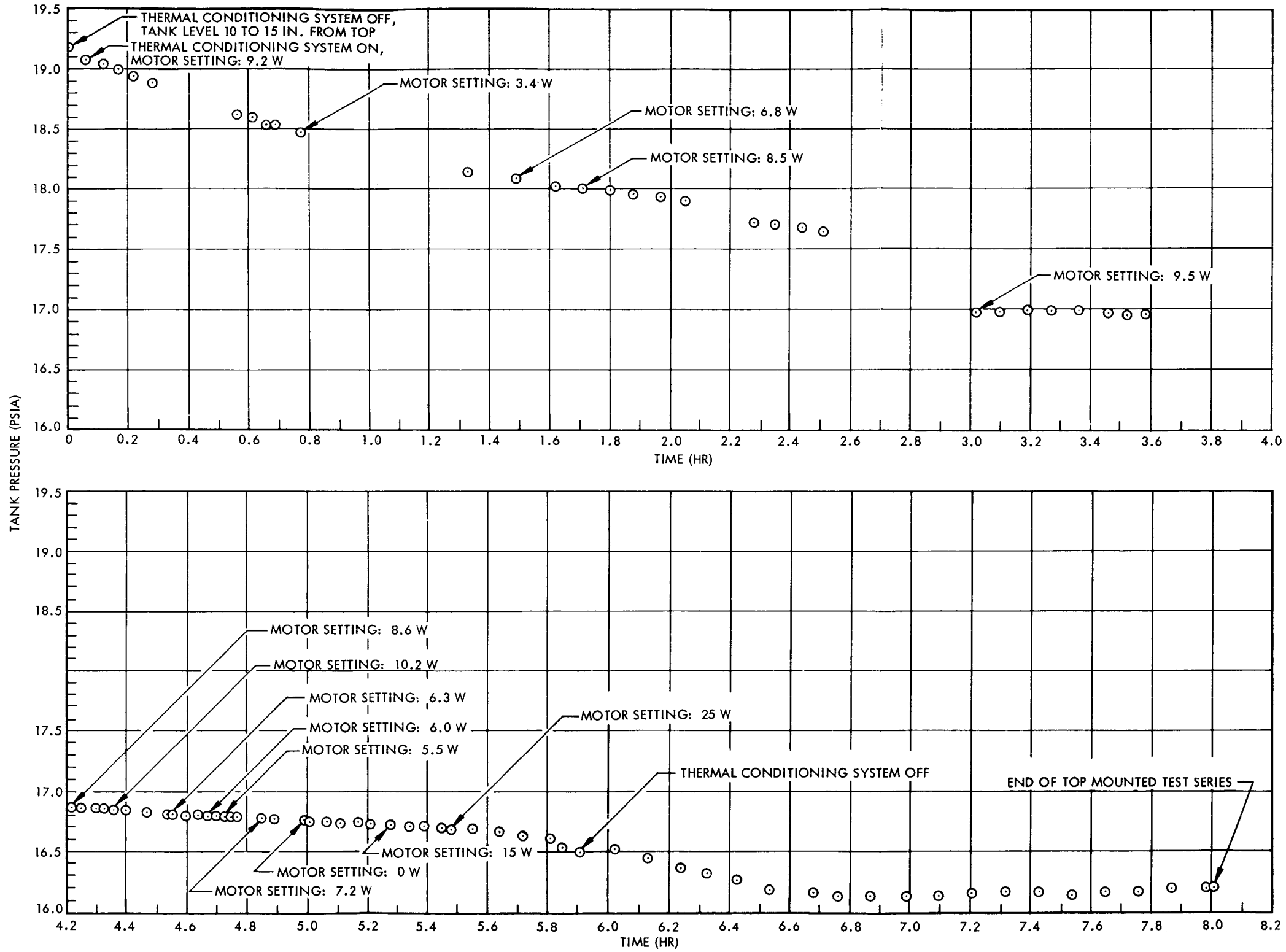

Fig. 48 Test Profile – Unit Top-Mounted in the 110-in.-diameter Tank (Ullage Volume = 5 Percent)

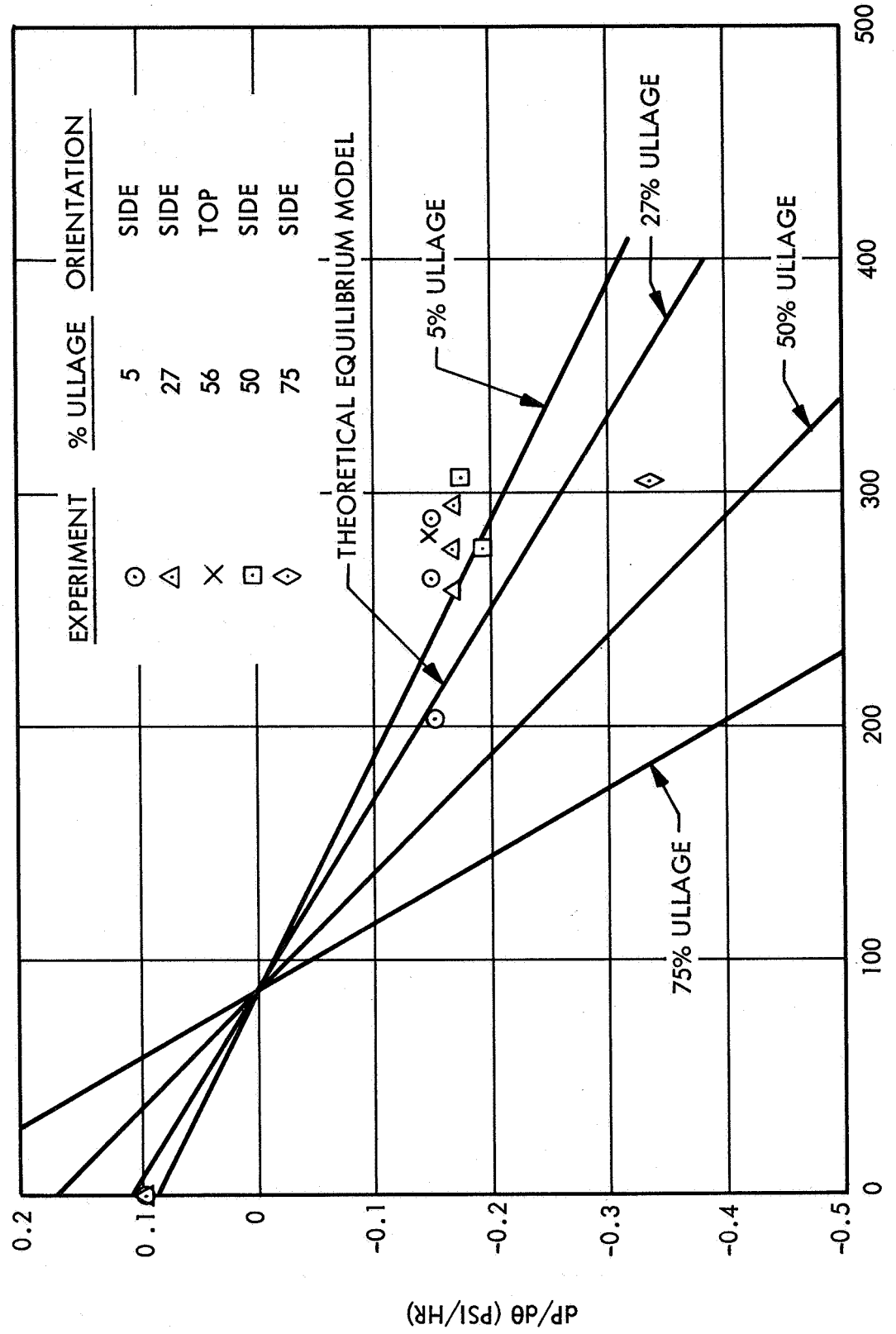

Fig. 49 Comparison of Theoretical and Experimental Tank Pressure Response

increased, there is a greater discrepancy between the theory and experimental data. Also note that the theory predicts a much greater effect of the independent variable ($m_o \lambda - 3.413\ P$) than is observed experimentally. More experimentation and greater instrumentation are needed before a satisfactory explanation of these effects are possible.

In the top-mounted orientation, the thermal conditioning system was located only 15 in. below the tank access-hole cover. Consequently, performance comparisons of the top- and side-mounted orientations while completely submerged can be made only at the 5-percent ullage volume. Figure 50 shows a comparison of normalized tank pressure response (p/p_o), at nearly identical mixer powers and flow rates. The response in both orientations was identical.

Figure 51 shows the effective average energy dissipated in the tank by the mixer, as a function of the total actual operating power. The ratio between the effective average power and the actual power is the percent of time the thermal conditioning system is venting, which is determined by the relative rates of pressure rise and decay, i.e.,

$$(\tau_a/\tau_c) = \frac{1}{1 - \dfrac{(dp/d\theta)_F}{(dp/d\theta)_R}} \tag{8}$$

Of the tank contents are well mixed, Eqs. (6), (7), and (8) combine to give:

$$P(\tau_a/\tau_c) = \left(\frac{Q_o}{m_o \lambda - 3.413\ P}\right) P \tag{9}$$

Equation (9) is also presented in Fig. 51 for comparison with experimental data. It can be seen that the experimental data for operation in either liquid or gas fall along the same general line, thus indicating that the two modes are equally efficient in controlling tank pressure. The data also indicate that the lowest power was also the most efficient, which substantiates the results of the dewar tests. Further, it tends

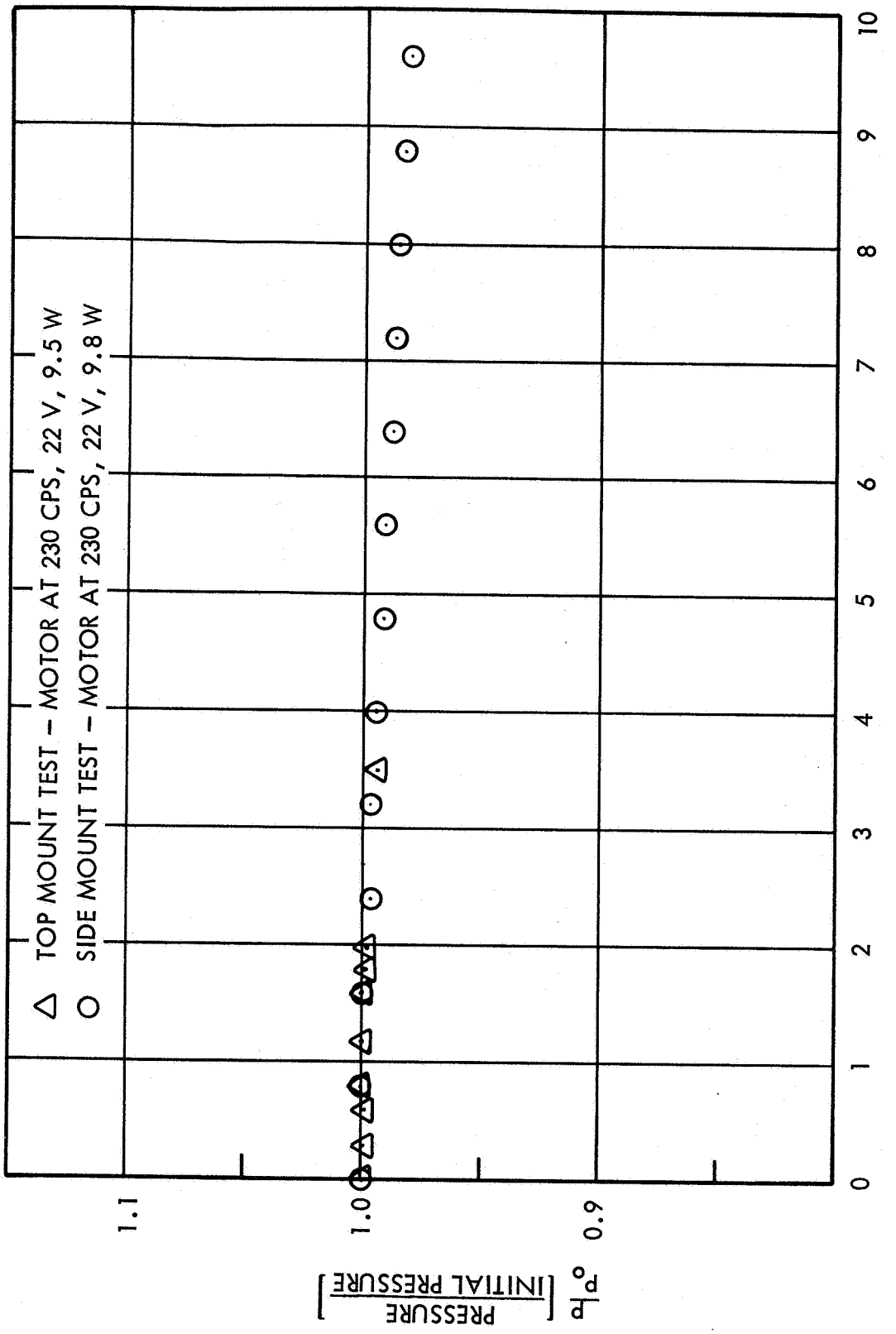

Fig. 50 Comparison of Top and Side Orientation Pressure Histories With Thermal Conditioning System Operation (Five Percent Ullage)

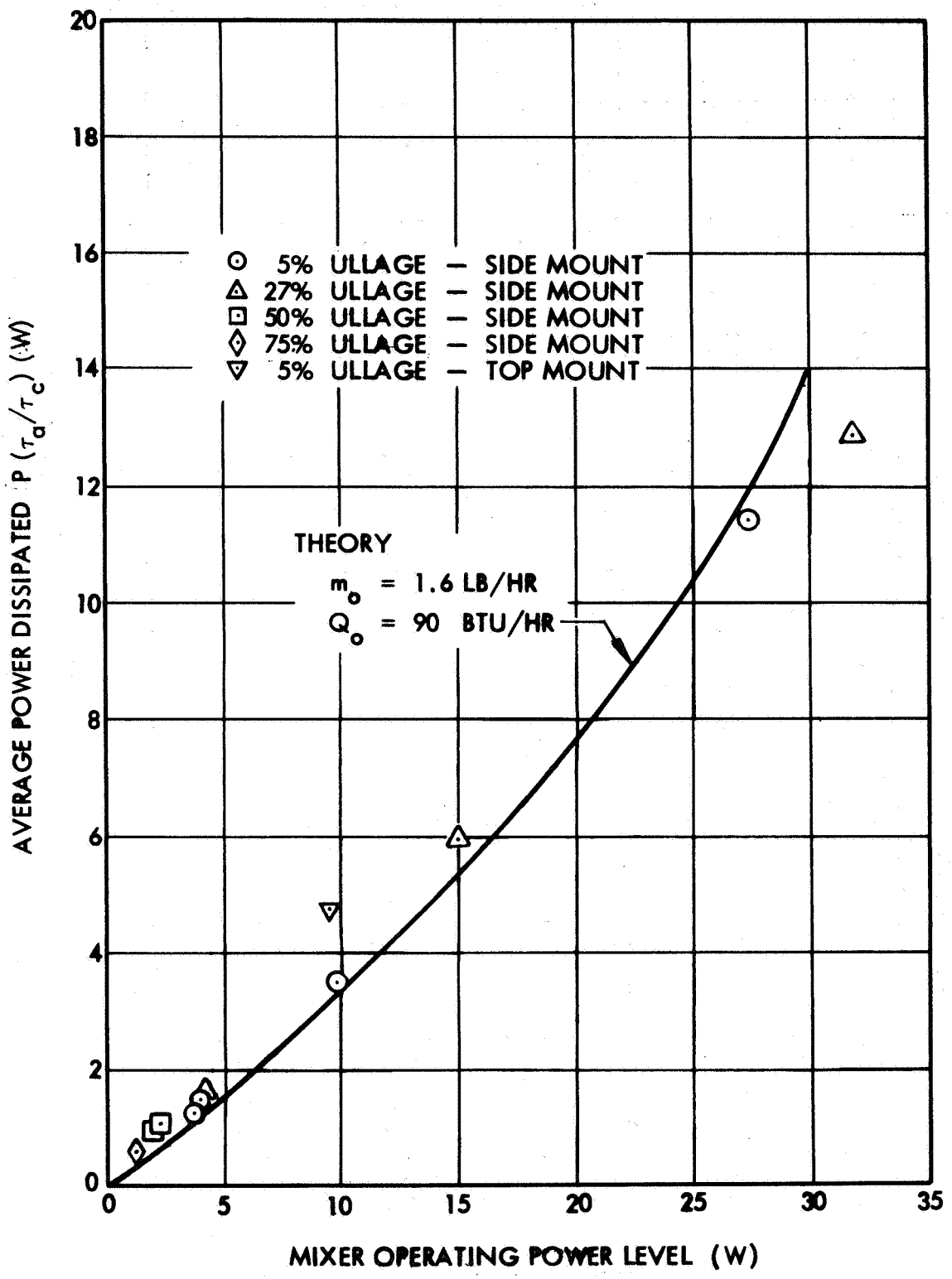

Fig. 51 Average Mixer Heat Input as Determined From 110-in.-diameter Tank Tests

to verify that the brushless dc motor currently being developed under Contract NAS 3-11208, with a design power of 2.3 watts, will further increase the system efficiency and be more than adequate for inducing mixing and tank pressure control.

These test results have demonstrated the ability of the thermal conditioning system to control tank pressure in a one-gravity environment. Further, they indicate that the control was governed by the heat transfer within the heat exchanger. Since the heat exchanger performance is forced-convection dominated, the thermal conditioning system should perform in zero-gravity as it did in one-gravity.

Component Performance

The thermal conditioning unit was instrumented to obtain some measure of the performance of each of its components. The data obtained from these measurements are presented and may be compared to the component design specifications presented in the System Design and Performance Requirements section.

Expansion Unit. The operation of this unit was very consistent throughout the entire test program: When operating with gas at the inlet, it regulated to nominally 3 psia and with liquid to nominally 3.8 psia. Figure 52 shows a typical pressure history at the inlet to the vent side of the heat exchanger when liquid hydrogen is flowing into the expansion unit. The corresponding expanded fluid temperature at the inlet to the vent side of the heat exchanger is shown in Fig. 53 to be nominally 28°R which is the saturation temperature for 2.6 psia. The predicted value of the temperature drop across the expansion unit is compared with the nominal test value in Fig. 54.

When the system was operating in gas, the variation in expansion unit discharge pressure was less than with liquid. In a typical test, this pressure varied between 2.97 and 3.01 psia. Thus, it must be concluded that this unit performed satisfactorily.

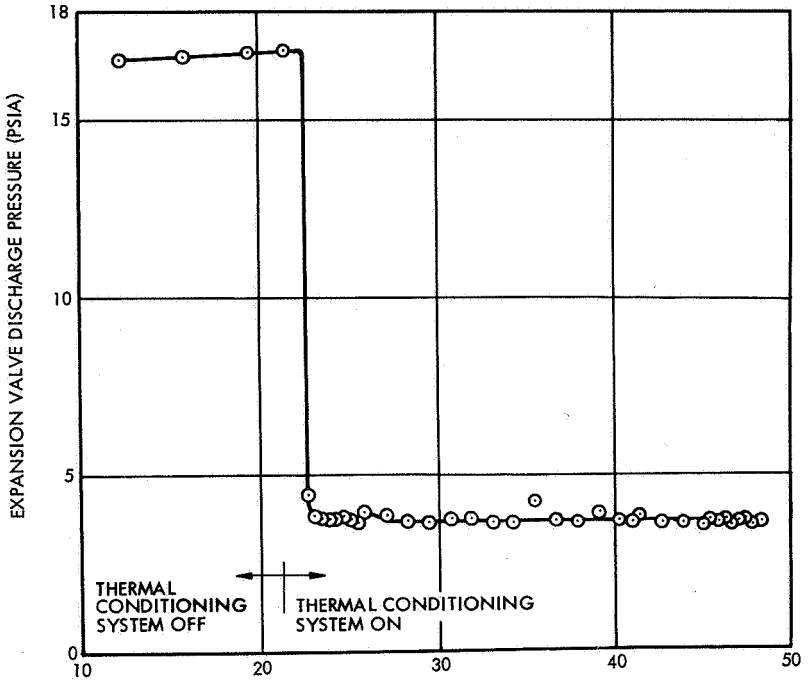

Fig. 52 Expansion Unit Discharge Pressure with Liquid – Side-Mounted Tests

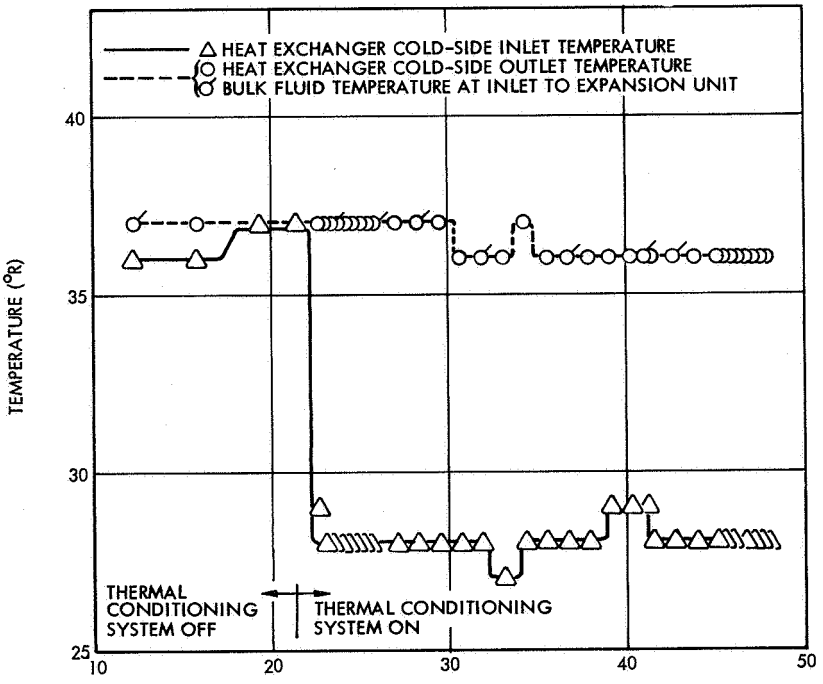

Fig. 53 System Fluid Temperatures With Liquid – Side-Mounted Tests

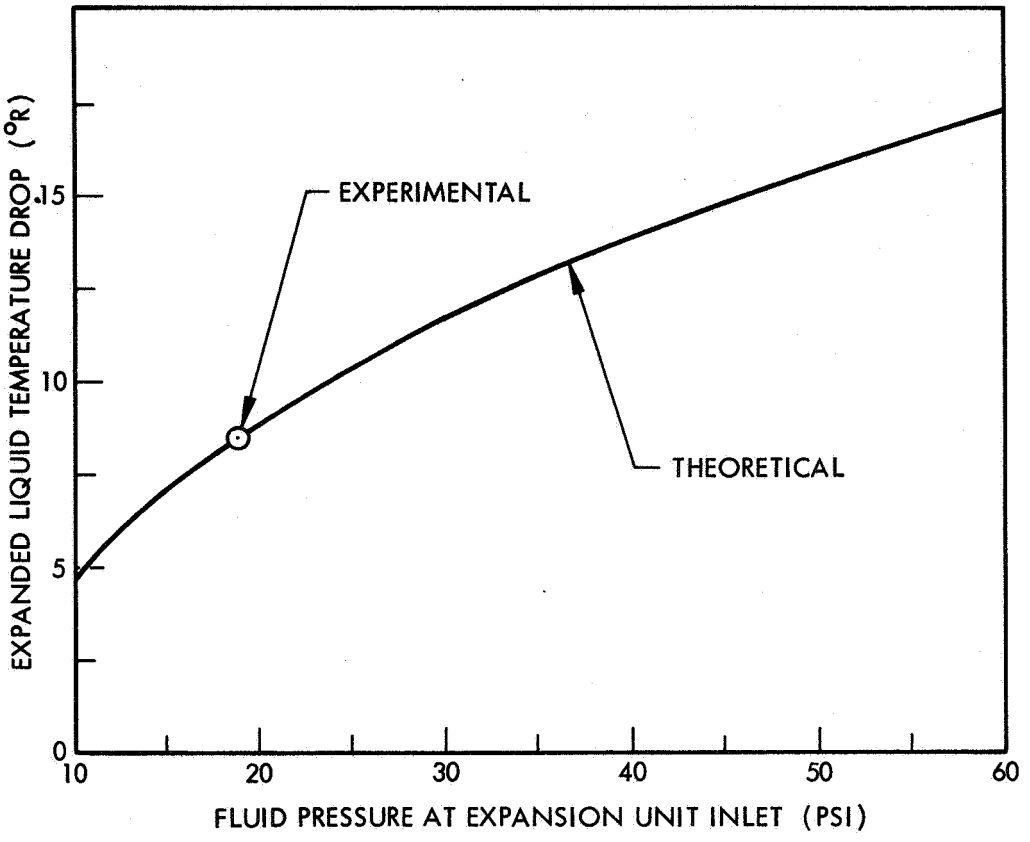

Fig. 54 Comparison Between Experimental and Predicted Temperature Drop in Expansion Unit

Heat Exchanger Unit. The full capability of this unit may not have been determined during this program because tests were limited to those with liquid or hydrogen vapor on the warm side. Both result in higher heat transfer coefficients than when helium is the warm-side fluid.

However, when the thermal conditioning system was submerged in liquid, the heat exchanger invariably superheated the vent fluid to essentially the bulk propellant temperature. Figure 53 shows the vent-side fluid-exit temperature, as well as the bulk fluid temperature at the system inlet for a typical and repeatable test condition. It is unlikely that any liquid was vented overboard in view of the superheat in the vented vapor. Thus, it seems certain that the unit will vaporize 1.7 lb/hr of liquid with hydrogen on the hot side, but its full capability is yet to be determined.

Mixer Unit. As described earlier, a series of tests were conducted with the thermal conditioning system completely submerged in liquid for the express purpose of establishing the mixer operating characteristics. Figure 55 shows the resulting power versus frequency and voltage. This can be combined with the calibration data presented earlier to evaluate the mixer flow and head rise.

It will be recalled that the calibration data represents a loci of optimum operating conditions obtained in a test loop where flow and pressure loss could be controlled independently. However, in the thermal conditioning system the pressure drop in the system is a direct and dependent function of the flow rate, but for each flow there will be an optimum frequency-voltage setting, which will correspond to one of the optimum loci determined in the calibration tests. The experimental data presented earlier in Figs. 26 through 30 are tabulated in Table 15. These were used to generate the optimum performance map shown in Fig. 56.

The data from Figs. 55 and 56 are then cross-plotted as lines of constant power on Fig. 57. When thermal conditioning system data intercepts a like power curve from the optimum calibration data, it must then represent an optimum operating condition. The frequency and voltage at this intercept is then used to determine the corresponding flow rate and head rise from the calibration data. It can be seen that the intercepts occur at flow rates slightly above 5.3 cfm for frequencies below 240 cps and for voltages below 23 v. These intercept voltage and frequencies result in a flow of 6 cfm, which is approximately 20 percent above the required warm-side flow rate through the heat exchanger when venting 1.4 lb/hr. These data also indicate that the pressure drop on the warm side is between 1 and 2 in. H_2O at 6 cfm.

Solenoid Flow Control Unit. This unit controls the vent flow rate through the thermal conditioning system.

AiResearch conducted calibration tests on this unit with air at ambient temperature and with helium at -320°F. An effective orifice area of 0.0054 sq in. was calculated from these data. Effective area for choked flow being given by

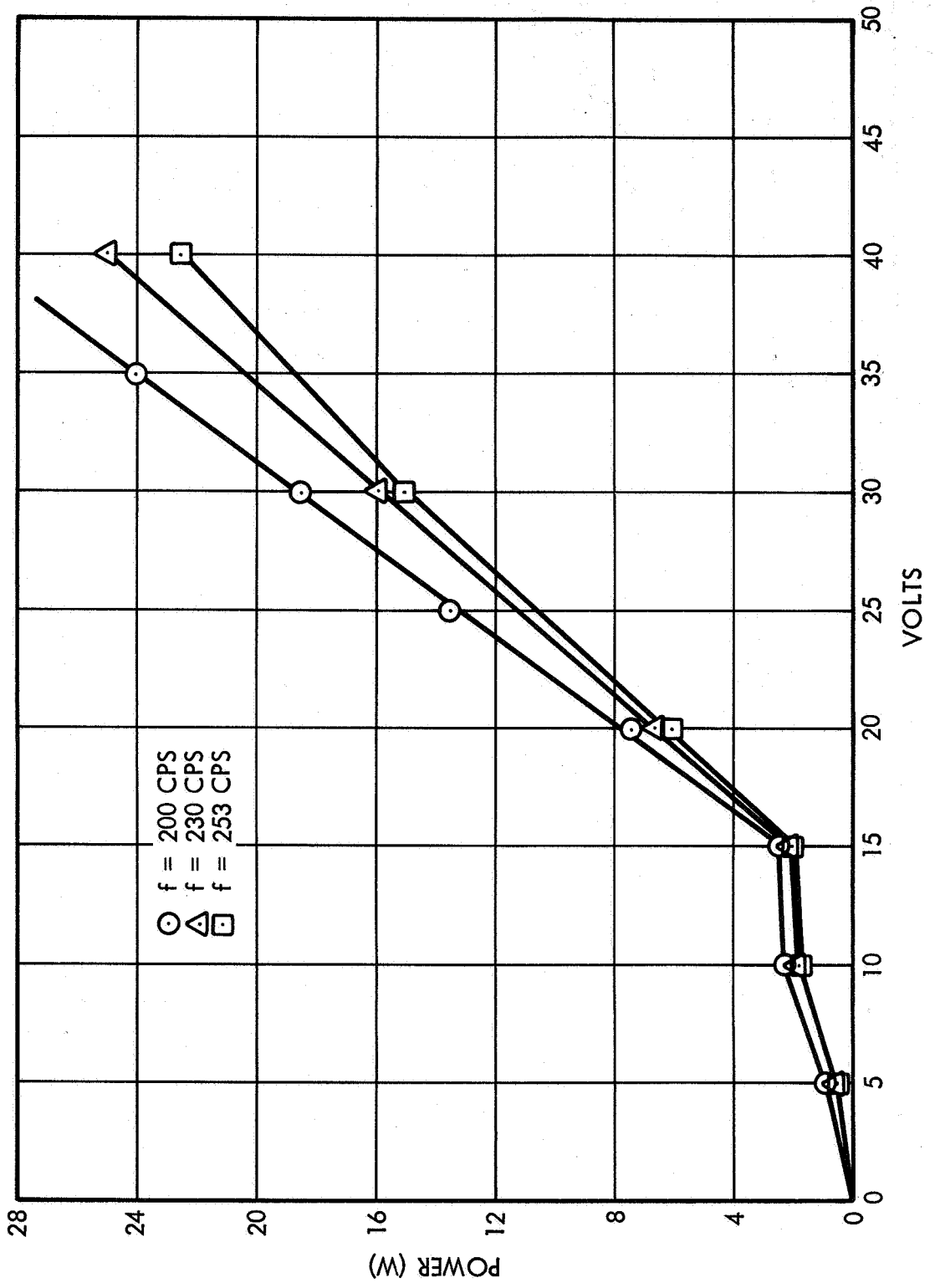

Fig. 55 Thermal Conditioning System Mixer Power Characteristics in Liquid Hydrogen

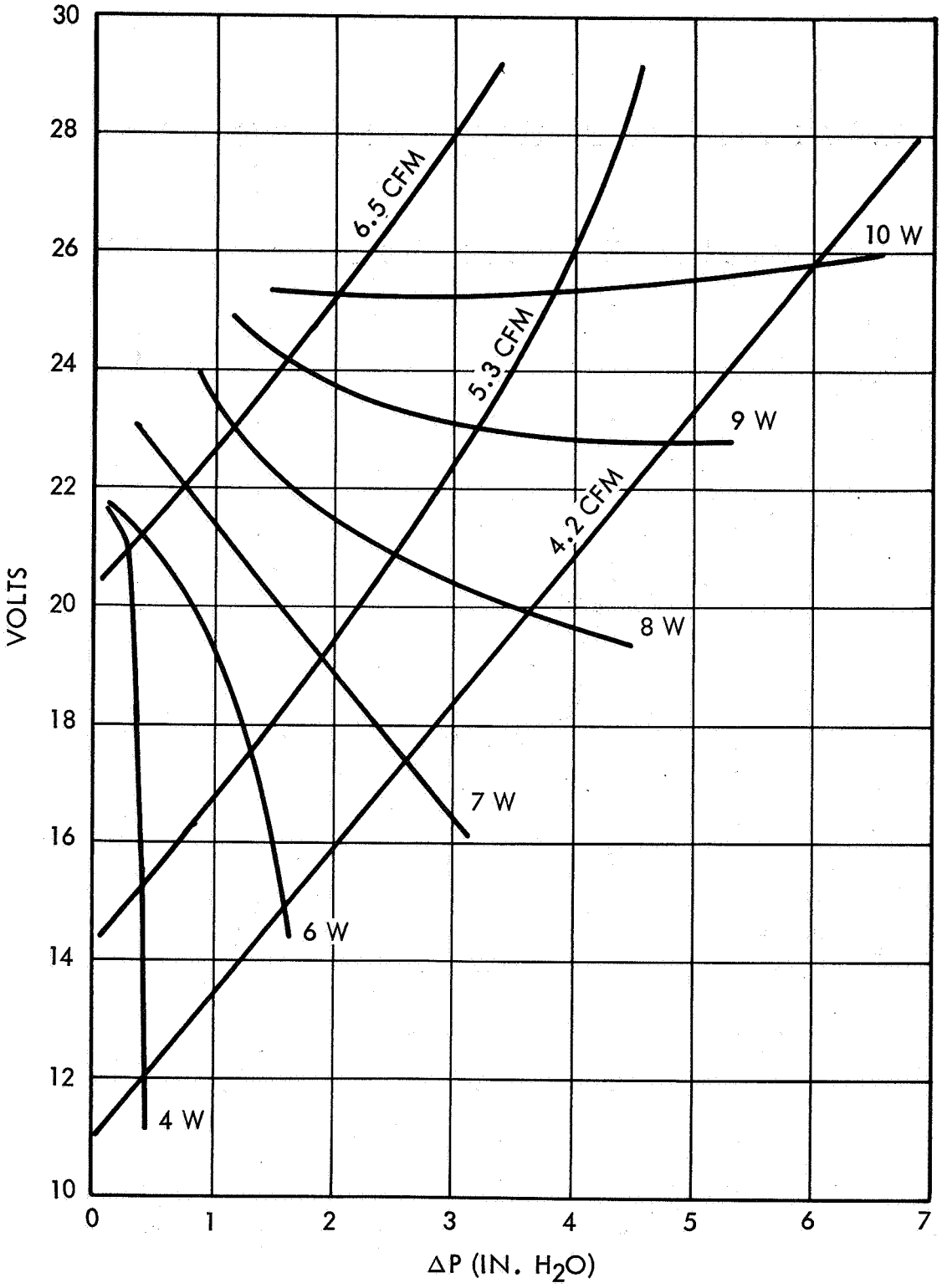

Fig. 56 Mixer Component Optimum Performance

Table 15

MINIMUM POWER OPERATING POINTS FOR FAN

Liquid Hydrogen (ρ = 4.4 lb/ft^3)												
Flow Rate, ft^3/min	4.2				5.3				6.4			
Pressure rise, in. H_2O	1	2	3	4	1	2	3	4	1	2	3	4
Input voltage	13.9	16.2	18.8	21.2	16.5	21.0	22.6	25.4	22.7	25.2	27.4	32.0
Input frequency, Hz	215	214	216	218	188	195	231	230	220	252	253	253
Power, w	5.4	6.4	7.4	8.3	5.6	6.9	8.8	10.1	7.6	10.0	11.6	13.4
Gaseous Hydrogen (ρ = 0.09 lb/ft^3)												
Flow Rate, ft^3/min	3.4				4.2				5.3			
Pressure rise, in. H_2O	0.1	0.2	0.3	0.41	0.1	0.2	0.29	0.41	0.13	0.21	0.3	0.4
Input voltage	8.4	19.4	29.0	52.4	9.6	13.5	27.0	29.2	13.5	16.0	17.4	24.8
Input frequency, Hz	255	275	344	433	290	306	332	441	273	307	390	382
Power, w	2.0	3.1	5.1	6.7	2.4	2.7	4.6	5.7	2.4	2.9	3.8	4.6

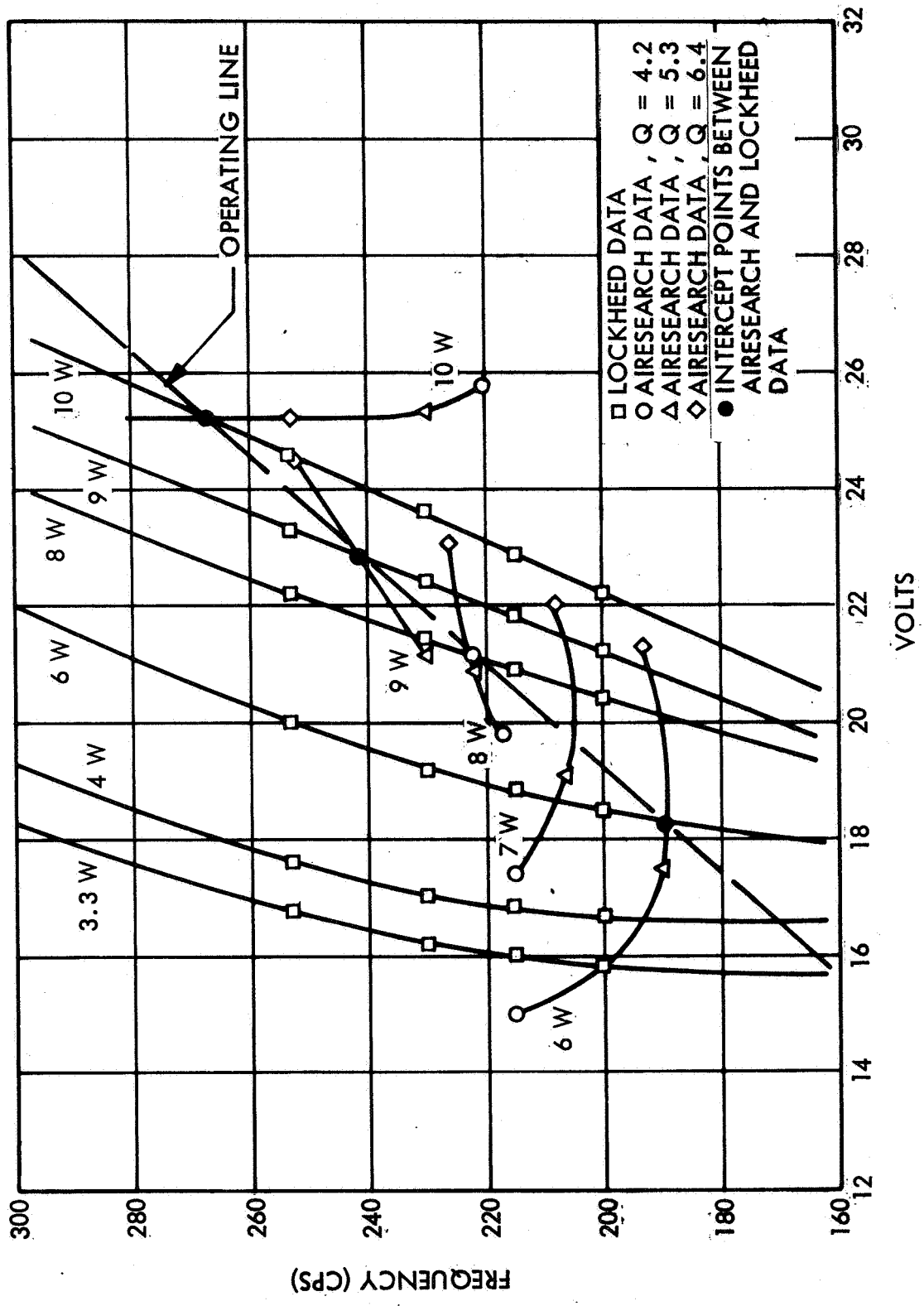

Fig. 57 Performance Map (Mixer Unit Installed in Thermal Conditioning System)

$$CA = \frac{\omega\sqrt{T_1}}{p_1}\sqrt{\frac{R}{\gamma g_c}\left(\frac{\gamma+1}{2}\right)^{\frac{\gamma+1}{\gamma-1}}}$$

With hydrogen vapor at 4 psi and 37°R, this area should provide a flow rate of 2.2 lb/hr. Lockheed conducted an independent calibration of the valve using both ambient hydrogen and helium gas. These tests gave an effective area of 0.0053 sq in. which confirms the AiResearch tests.

However, the Brooks flowmeter used to measure vent flow rates indicated flows between 1.5 and 1.7 lb/hr, which suggested the possibility that the solenoid valve was not choked during the tank tests. It should be noted here that a long run of piping is used between the solenoid valve and the vent flow vacuum pump which, when connected to the vacuum, can choke in the line and unchoke the valve.

Therefore, additional flow data were obtained with the actual test ducting attached to the solenoid valve discharge port. The top- and side-mounted ducting resistances were different with 2 ft of 1/4-in. tubing between the valve and the tank access cover for the top mount and 10 ft for the side mount. The external ducting was identical for both orientations.

All the calibration is shown in Fig. 58, which shows a shift to lower flow rates for a fixed inlet pressure, with added resistance attached to the valve. The shift to the left indicates that the choke point has moved into the duct downstream of the valve. Also shown in Fig. 58 is the flow rate as measured with the Brooks flowmeter. The performance analysis presented earlier utilized the Brooks flowmeter data.

CONCLUDING REMARKS

A number of very significant conclusions can be drawn from the work accomplished to date on this program. The most significant of these may be summarized as follows:

(1) The most general conclusion, is that the liquid propellant thermal conditioning system as formulated, designed, built, and tested in this program

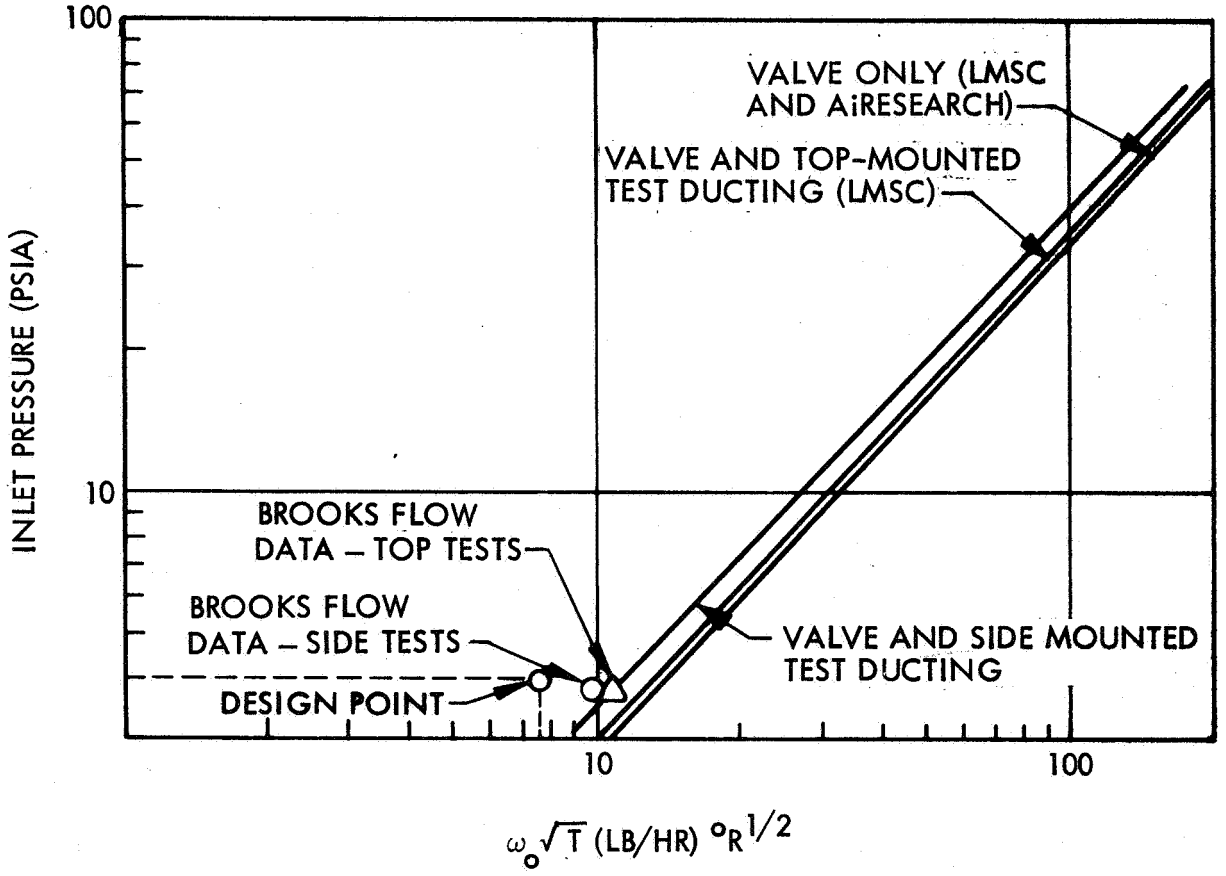

Fig. 58 Solenoid Valve Flow Calibration Data

controls the pressure level of a full-scale liquid hydrogen tank efficiently and is equally effective whether the unit is immersed in gas or submerged in liquid hydrogen.

(2) The unit controls the tank pressure effectively and with no discernible differences whether its mixer unit discharges in the direction of the one-g gravitational force or perpendicular to it.

(3) Performance of the individual components comprising the thermal conditioning unit was very close to their design performance.

(4) The overall performance of the unit in its ability to control the tank pressure in a one-g gravity environment is approximately predicted by a quasi steady-state thermodynamic theory based upon a nonstratified propellant within the tank. Explanations of the divergences of this theory from experimental observations will require additional testing and instrumentation.

(5) Lastly, the test results indicate that tank pressure control is basically governed by the rate of heat transfer within the heat exchanger. Since the heat exchanger is force convection dominated, the thermal conditioning system should be expected to perform in zero-gravity as it did in one-gravity. Inasmuch as the system controls the tank pressure effectively and with no discernible differences whether its mixer unit discharges in the direction of the 1-g gravitational force or perpendicular to it; and inasmuch as the mixer unit discharge velocity is 10 times the theoretical minimum requirement and 5 times the zero-gravity test data requirement for adequate propellant mixing in the tank, the thermal conditioning system should be expected to perform in zero-gravity as it did in 1-g. However, positive confirmation of such a conclusion can only come from space flight demonstration of the unit in a liquid hydrogen tankage system.

SYMBOLS AND ABBREVIATIONS

A	solenoid valve throat area, $in.^2$
As	liquid-vapor interface area, ft^2
CA	effective throat area, $in.^2$
E_T	total energy into the propellant tank, Btu
g_c	gravitational constant, ft/sec^2
m_o	flow rate of the vent fluid, lb/hr
P	mixer power, w
p	propellant pressure, psia
Q_o	propellant heating rate, Btu/hr
R	gas constant, ft-lb/lb-°R
T	fluid temperature, °R
V_g	ullage volume, ft^3
W	total weight of fluid in the propellant tank, lb
$(dp/d\theta)_R$	rate of tank pressure change when not venting, psi/sec
$(dp/d\theta)_F$	rate of tank pressure change when ~~not~~ venting, psi/sec
η	total number of pressure cycles
τ_a	vent time for each tank pressure cycle, hr
τ_c	total tank pressure cycle time, hr
λ	enthalpy change of vented fluid, Btu/lb
γ	ratio of specific heats
ρ_g	gas density, lb/ft^3
ρ_e	liquid density, lb/ft^3
ω	fluid flow rate, lb/hr

REFERENCES

1. Lockheed Missiles & Space Company, Liquid Propellant Thermal Conditioning System, Interim Report, NASA CR-72113, LMSC-A839783, Contract NAS 3-7942, Sunnyvale, Calif., 20 Apr 1967

2. National Aeronautics and Space Administration, Lewis Research Center, An Experimental Investigation of the Effect of Gravity on a Forced Circulation Pattern for Spherical Tanks, by S. G. Berenyi, R. C. Nussle, and K. L. Abdalla, NASA TN D 4409, 6 Feb 1968

3. W. J. O'Reilly and E. F. Busch, Study of Remote Storage Evaporative Oil Cooling Systems for High Performance Aircraft, WADD Tech. Report 60-918, Jan 1961

Appendix A
VAPOR BUBBLE CONDENSATION THEORY

The classical theories of vapor condensation such as the works of Nusselt deal with streamline flow where the condensate is removed by gravitational forces. A theory of vapor condensation developed by Sterbentz and Bullard is presented herein which is applicable in a streamline flow in zero-gravity fields.

Consider a cooler liquid flowing with velocity u_0 passing over a warmer, saturated pure vapor in the absence of gravity. Some vapor condensation occurs on the moving stream vapor/liquid interface. As a consequence, a condensate film of thickness y is deposited and flows along with the free stream. In a streamline flow, this condensate film will remain intact, having a laminar velocity profile.

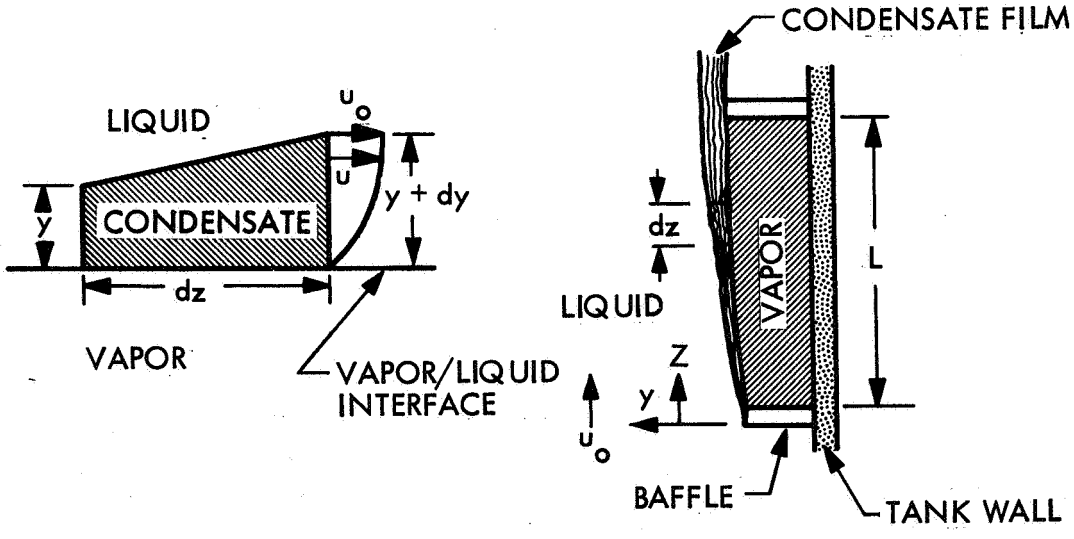

The heat transferred by conduction only across an element of the condensate film having a local thickness of y is described by the following equation:

$$dQ = \left(\frac{k_\ell}{y}\right) \Delta T \, dA = \left(\frac{k_\ell}{y}\right) \Delta T \, (b) dz = h_y \, \Delta T \, (b) dz \qquad (A.1)$$

This quantity of transferred heat is also equal to the condensation heat contained within the condensate film; therefore

$$\left(\frac{k_\ell}{y}\right) \Delta T \, (b) dz = \lambda \, dw_z \qquad (A.2)$$

For the entire length L of the vapor pocket, by definition,

$$h_m = \frac{\lambda w}{bL \Delta T} \qquad (A.3)$$

Combining equations (A.2) and (A.3) to eliminate ΔT, which is assumed constant, gives

$$\frac{k_\ell}{y} = \frac{h_m \, L \, dw_z}{w \, dz} \qquad (A.4)$$

The local mass flow in the condensate layer is given by

$$w_z = \rho_\ell \, \bar{u} \, b \, y \qquad (A.5)$$

Eliminating y from Eqs. (A.4) and (A.5) yields

$$\left(\frac{h_m L}{w}\right) w_z \, dw_z = k_\ell \, \rho_\ell \, \bar{u} b \, dz \qquad (A.6)$$

Integrating Eq. (A.6) from O to L and O to w and assuming that the u_o and therefore $\bar{u}$ is constant yields

$$k_\ell \rho_\ell \bar{u} b = h_m (w/2) \tag{A.7}$$

Eliminating w from Eqs. (A.3) and (A.7) gives

$$h_m^2 = \frac{2 k_\ell \rho_\ell \lambda \bar{u}}{L \Delta T} \tag{A.8}$$

Equation (A.8) can be rewritten in terms of constant free-stream velocity. Therefore,

$$h_m = \left[\frac{2 k_\ell \rho_\ell \lambda u_o}{L \Delta T} \left(\frac{\bar{u}}{u_o}\right)\right]^{1/2} \tag{A.9}$$

Consistent with the assumption of streamline flow, the term $\bar{u}/u_0$ will have a fixed value of 0.625. Substituting this value into Eq. (A.9) gives the desired equation for the streamline flow forced convection heat transfer coefficient

$$h_m = 1.12\left(\frac{k_\ell \rho_\ell \lambda u_o}{L \Delta T}\right)^{1/2} \tag{A.10}$$

across a vapor-liquid interface in a zero-gravity field.

In terms of the Nusselt and Reynolds number, Eq. (A.10) may be written as

$$\left(\frac{h_m L}{k_\ell}\right)^2 = 1.245 \left(\frac{\lambda}{C_p \Delta T}\right)\left(\frac{\rho_\ell u_o L}{\mu_\ell}\right)\left(\frac{\mu_\ell C_p}{k_\ell}\right) \tag{A.11}$$

or

$$(N_N)^2 = 1.245 \frac{N_R N_P}{N_\lambda} \qquad (A.12)$$

Equation (A.12) defines a dimensionless number which relates the significant physical factors controlling the condensation of vapor upon a moving cooler liquid stream in zero gravity.

SYMBOLS AND ABBREVIATIONS

A	surface area of liquid/vapor interface, ft^2
ΔT	temperature difference between liquid and vapor, °R
C_p	liquid specific heat, Btu/°R-lb
L	length of the vapor pocket, ft
N_N	Nusselt number ($h_m L/k_\ell$)
N_P	Prandtl number ($\mu_\ell C_P/k_\ell$)
N_R	Reynolds number ($\rho_\ell u_o L/\mu_\ell$)
N_λ	Zero-gravity condensation number ($C_p \Delta T/\lambda$)
Q	heat transfer by conduction across the liquid/vapor interface, Btu/sec
b	linear dimension of the vapor pocket normal to L, ft
h_m	average condensation heat transfer coefficient, Btu/sec-ft^2-°R
h_y	local heat transfer coefficient, Btu/sec-ft^2-°R
k_ℓ	thermal conductivity of the liquid, Btu/sec-ft-°R
$\bar{u}$	average velocity in condensate film, ft/sec
u_o	liquid free-stream velocity, ft/sec
w	condensation rate, lb/sec
y	condensate film thickness, ft

z	condensate film length, ft
λ	heat of vaporization, Btu/lb
μ_ℓ	liquid viscosity
ρ_ℓ	liquid density, lb/ft^3

Appendix B

JET PENETRATION THEORY

A theory of jet penetration – either a liquid jet penetrating through a vapor volume or a vapor jet penetrating through a liquid volume – developed by Sterbentz and Bullard is presented herein which is applicable in zero-gravity fields. Consider a tank containing both liquid and vapor in a zero-gravity field. Assume the emission of a steady jet of liquid or vapor from a circular jet nozzle at one end of the tank toward the other end. Assume also that the vapor condensation is negligible.

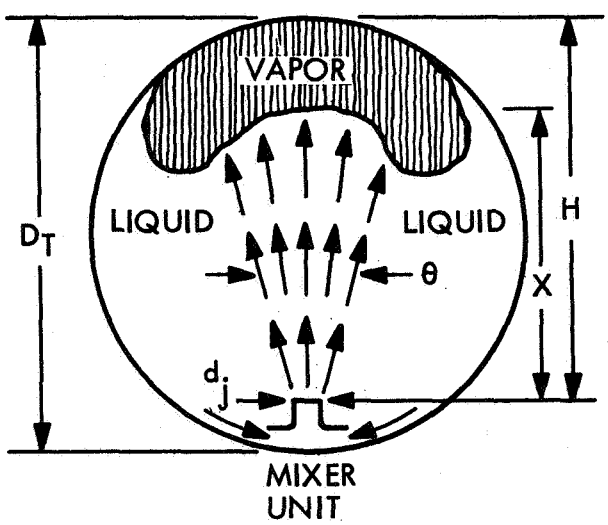

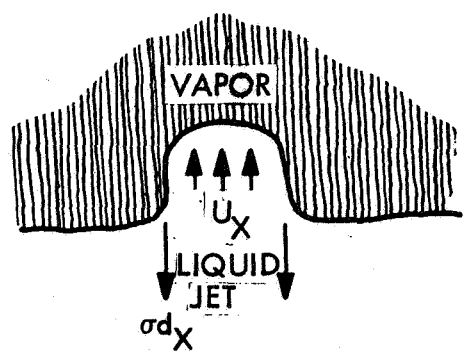

In a zero-g environment, only inertial and viscous forces act on the jet, say liquid, while flowing through the liquid in the tank. If this liquid jet, however, encounters a vapor bubble, the free surface of the bubble will be distorted by the jet dynamic forces which are opposed by the liquid/vapor surface-tension forces. If these dynamic forces are large enough, the liquid jet will break through the bubble. A free-body

diagram of the deflected portion of the liquid/vapor surface is shown in the sketch. The jet inertial force causing jet penetration of the bubble is given by

$$F_I = A_x \rho U_x^2 = \frac{\pi d_x^2}{4} \rho U_x^2 \qquad (B.1)$$

The opposing surface tension force is given by

$$F_\sigma = \pi d_x \sigma \qquad (B.2)$$

For bubble breakthrough by the jet, the following condition must be satisfied

$$\frac{F_I}{F_\sigma} > \frac{\rho U_x^2 d_x^2}{4 \sigma d_x} \qquad (B.3)$$

Therefore, a critical condition can be defined when $F_I = F_\sigma$ and Eq. (B.3) yields

$$W_{e_{cr}} = 4 = \frac{\rho U_x^2 d_x}{\sigma} \qquad (B.4)$$

This critical Weber number is based upon local conditions at the liquid/vapor interface. To relate these local conditions to the jet at its point of emission into the tank, consider the following derivation. Conservation of jet momentum gives

$$P_j A_x + \rho A_j U_j^2 = P_x A_x + \rho A_x U_x^2 \qquad (B.5)$$

In a large tank, in a zero-g environment, the pressure can be assumed to be uniform throughout, i.e., $P_j = P_x$. The momentum equation (B.5) reduces to

$$A_j U_j^2 = A_x U_x^2 \tag{B.6}$$

Substituting this into the expression for critical Weber number Eq. (B.4), we get for a critical jet Weber number at the jet nozzle

$$W_{ej_{cr}} = W_{e_{cr}} \left(\frac{d_x}{d_j} \right) \tag{B.7}$$

If we now assume that the jet spreads at a constant angle θ, then

$$\frac{d_x}{d_j} = 1 + \frac{x}{d_j} \tan \theta \tag{B.8}$$

Therefore, combining Eqs. (B.4), (B.7), and (B.8)

$$W_{ej_{cr}} = 4 \left(1 + \frac{x}{d_j} \tan \theta \right) \tag{B.9}$$

The theoretical analysis of a submerged circular jet predicts that $\theta = 9$ deg, which results in the following equation for critical jet Weber number:

$$W_{ej_{cr}} = \frac{\rho U_j^2 d_j}{\sigma} = 4 \left(1 + 0.16 \frac{x}{d_j} \right) \tag{B.10}$$

Therefore, the critical or minimum value of the jet Weber number required to cause a jet of liquid emitted into a tank at one end of the tank to penetrate all intervening vapor bubbles and to strike the opposite wall of the tank is given by Eq. (B.11) by setting x = H. Thus,

$$W_{ej_{cr}} = \frac{\rho U_j^2 d_j}{\sigma} = 4\left(1 + 0.16\,\frac{H}{d_j}\right) \qquad \text{(B.11)}$$

The critical Weber number of a vapor jet to penetrate a liquid surface is also given by Eq. (B.11) when the properties of the vapor jet are used.

SYMBOLS AND ABBREVIATIONS

A_x	flow area of jet at x , ft^2
H	distance from jet nozzle to the opposite tank wall, ft
P_j	static pressure at jet nozzle, psfa
P_x	static pressure at x , psfa
U_j	velocity at jet nozzle, ft/sec
U_x	jet velocity at x , ft/sec
$W_{e_{cr}}$	critical Weber number at liquid/vapor interface
$W_{ej_{cr}}$	critical Weber number at jet nozzle
d_j	nozzle jet diameter, ft
d_x	width of jet at x , ft
x	distance from jet nozzle to the liquid/vapor interface , ft
θ	jet spreading angle, deg
ρ	jet density, $lb\text{-}sec^2/ft^4$
σ	surface tension, lb/ft

Appendix C
PRESSURE DECAY WITH CONTINUOUS EQUILIBRIUM

Venting from a tank of LH_2 while in thermodynamic equilibrium can be described as follows in terms of the rate of tank pressure decay, $dP/d\theta$.

The total energy content Q of the liquid and gas in the tank may be expressed as

$$Q = C_{p_\ell} W_\ell T + C_{p_g} W_g T_g \approx C_{p_\ell} WT \tag{C.1}$$

The approximation is valid if $C_{p_\ell} W_\ell \gg C_{p_g} W_g$ and $T_g \approx T_\ell$. The rate of change of Q with θ is given by

$$\frac{dQ}{d\theta} = C_{p_\ell} W \frac{dT}{d\theta} + C_{p_\ell} T \frac{dW}{d\theta} \tag{C.2}$$

Also

$$\frac{dQ}{d\theta} = Q_o + E_M - m_o \lambda$$

Note that

$$\frac{dW}{d\theta} = m_o \tag{C.3}$$

Combining the mass and energy balance gives

$$C_{p_\ell} W \frac{dT}{d\theta} = Q_o + E_M - m_o \lambda \tag{C.4}$$

Also,

$$\frac{dT}{d\theta} = \frac{dT}{dp} \frac{dp}{d\theta} \tag{C.5}$$

Then,

$$C_{p_\ell} W \left(\frac{dT}{dp}\right) \frac{dp}{d\theta} = Q_o + E_M - m_o \lambda \qquad (C.6)$$

or

$$\frac{dp}{d\theta} = \frac{Q_o + E_M - m_o \lambda}{C_{p_\ell} (W_\ell + W_g)(dT/dp)_\ell} \qquad (C.7)$$

For liquid hydrogen, $(dT/dp)_\ell \approx 1/3$ when $15 < p < 30$ and $C_{p_\ell} \approx 2.6$.

Therefore

$$\frac{dp}{d\theta} \approx \frac{1.15}{W} (Q_o + E_M - m_o \lambda) \qquad (C.8)$$

SYMBOLS AND ABBREVIATIONS

C_p	specific heat, Btu/lb-° R
E_M	energy input to mixer, Btu/hr
m_o	gas vent rate, lb/hr
p	tank pressure, psia
Q_o	external heat leak into the tank, Btu/hr
T	liquid and gas temperature in tank, ° R
W	weight of liquid and gas in tank, lb
θ	time, hr
λ	heat of vaporization, Btu/lb

DISTRIBUTION LIST FOR FINAL REPORT, NASA CR-72365

"LIQUID PROPELLANT THERMAL CONDITIONING SYSTEM"

NAS3-7942

LOCKHEED AIRCRAFT CORPORATION
MISSILES & SPACE DIVISION

		Copies
National Aeronautics and Space Administration Lewis Research Center 21000 Brookpark Road Cleveland, Ohio 44135		
Attention:	Contracting Officer, MS 500-210	1
	Liquid Rocket Technology Branch, MS 500-209	8
	R. Knoll, MS 501-2	1
	Technical Report Control Office, MS 5-5	1
	W. Masica, MS 54-3	1
	Technology Utilization Office, MS 3-16	1
	R. DeWitt, MS 500-204	1
	AFSC Liaison Office, MS 4-1	2
	J. Sivo, MS 501-2	1
	Library	2
	D. Petrash, MS 54-1	1
	Office of Reliability & Quality Assurance, MS 500-111	1
	K. Abdalla, MS 54-3	1
	E. W. Conrad, MS 500-204	1
National Aeronautics and Space Administration Washington, D.C. 20546		
Attention:	Code MT	1
	RPX	2
	RPL	2
	SV	1
Scientific and Technical Information Facility P.O. Box 33 College Park, Mayrland 20740		
Attention:	NASA Representative Code CRT	6

	Copies
National Aeronautics and Space Administration Ames Research Center Moffett Field, California 94035	
Attention: Library	1
C. A. Syvertson	1
National Aeronautics and Space Administration Flight Research Center P.O. Box 273 Edwards, California 93523	
Attention: Library	1
National Aeronautics and Space Administration Goddard Space Flight Center Greenbelt, Maryland 20771	
Attention: Library	1
National Aeronautics and Space Administration John F. Kennedy Space Center Cocoa Beach, Florida 32931	
Attention: Library	1
National Aeronautics and Space Administration Langley Research Center Langley Station Hampton, Virginia 23365	
Attention: Library	1
National Aeronautics and Space Administration Manned Spacecraft Center Houston, Texas 77001	
Attention: Library	1
C. Yodis	1
C. Humphrey	1
W. Chandler	1
W. Dusenberry	1
R. Polifka	1
National Aeronautics and Space Administration George C. Marshall Space Flight Center Huntsville, Alabama 35812	
Attention: Library	1
Keith Chandler	1
Dr. W. Lucas	1
H. Paul	1
F. Vaniman	1
Clyde Nevins	1
K. Coates	1
F. Moses	1

	Copies
National Aeronautics and Space Administration Western Operations Office 150 Pico Boulevard Santa Monica, California 90406 Attention: Library	1
Jet Propulsion Laboratory 4800 Oak Grove Drive Pasadena, California 91103 Attention: Library Robert Breshears, 166-422	1
Office of the Director of Defense Research & Washington, D.C. 20301 Attention: Dr. H. W. Schulz, Office of Asst. Dir. (Chem. Technology)	1
Defense Documentation Center Cameron Station Alexandria, Virginia 22314	1
RTD (RTNP) Bolling Air Force Base Washington, D.C. 20332	1
Arnold Engineering Development Center Air Force Systems Command Tullahoma, Tennessee 37389 Attention: AEOIM	1
Advanced Research Projects Agency Washington, D.C. 20525 Attention: D. E. Mock	1
Aeronautical Systems Division Air Force Systems Command Wright-Patterson Air Force Base Dayton, Ohio 45433 Attention: D. L. Schmidt, Code ASRCNC-2	1
Air Force Systems Command (SCLT/Capt. S. W. Bowen) Andrews Air Force Base Washington, D.C. 20332	1 1
Air Force Rocket Propulsion Laboratory (RPR) Edwards, California 93523	1

	Copies
Air Force Rocket Propulsion Laboratory (RPM) Edwards, California 93523	1
Air Force Office of Scientific Research Washington, D.C. 20333 Attention: SREP Dr. J. F. Masi	1
Air Force Aero Propulsion Laboratory Research & Technology Division Air Force Systems Command United States Air Force Wright-Patterson AFB, Ohio 45433 Attention: APRP (C. M. Donaldson)	1
Aerojet-General Corporation P.O. Box 296 Azusa, California 91703 Attention: Librarian A. Weinstein	1 1
Aerojet-General Corporation 11711 South Woodruff Avenue Downey, California 90241 Attention: F. M. West, Chief Librarian	1
Aerojet-General Corporation P.O. Box 1947 Sacramento, California 95809 Attention: Technical Library 2484-2015A Dr. C. M. Beighley D. T. Bedsole	1 1 1
Aerospace Corporation P.O. Box 95085 Los Angeles, California 90045 Attention: J. G. Wilder, MS 2293 R. Krueger Library-Documents	1 1 1
Arthur D. Little, Inc. Acorn Park Cambridge, Massachusetts 02140 Attention: A. C. Tobey	1

	Copies
Astropower, Incorporated Subs. of Douglas Aircraft Company 2968 Randolph Avenue Costa Mesa, California 92626 Attention: Dr. George Moc Director, Research	1
ARO, Incorporated Arnold Engineering Development Center Arnold AF Station, Tennessee 37389 Attention: Dr. B. H. Boethert Chief Scientist	1
Battelle Memorial Institute 505 King Avenue Columbus, Ohio 43201 Attention: Report Library, Room 6A	1
Beech Aircraft Corporation Boulder Facility Box 631 Boulder, Colorado 80301 Attention: J. H. Rodgers John A. Pike	1 1
Bell Aerosystems, Inc. Box 1 Buffalo, New York 14205 Attention: T. Reinhardt W. M. Smith Kert Berman	1 1 1
The Boeing Company Aero Space Division P.O. Box 3707 Seattle, Washington 98124 Attention: Ruth E. Peeremboom (1190) J. D. Alexander C. Tiffany R. Sjack	1 1 1 1
Chemical Propulsion Information Agency Applied Physics Laboratory 8621 Georgia Avenue Silver Spring, Maryland 20910	1

	Copies
Chrysler Corporation Space Division New Orleans, Louisiana 70101 Attention: Librarian	1
Curtiss-Wright Corporation Wright Aeronautical Division Woodbridge, New Jersey 07095 Attention: G. Kelley	1
University of Denver Denver Research Institute P.O. Box 10127 Denver, Colorado 80210 Attention: Security Office	1
Douglas Aircraft Company, Inc. Santa Monica Division 3000 Ocean Park Blvd. Santa Monica, California 90405 Attention: J. L. Waisman R. W. Hallet G. W. Burge S. H. Schwartz E. Marion	 1 1 1 1 1
General Dynamics/Convair P.O. Box 1128 San Diego, California 92112 Attention: Mr. W. Fenning Centaur Resident Project Office Library & Information Services (128-00) Karl Leonhard Al Walburn R. Tatro	 1 1 1 1 1
General Electric Valley Forge Space Technology Center P.O. Box 8555 Philadelphia, Pennsylvania 19001 Attention: M. W. Mitchell A. D. Cohen	 1 1
Grumman Aircraft Engineering Corporation Bethpage, Long Island New York 11714 Attention: Joseph Gavin	 1

	Copies
ITT Research Institute Technology Center Chicago, Illinois 60616 Attention: C. K. Hersh, Chemistry Division	1
Office of Research Analyses (OAR) Holloman Air Force Base, New Mexico 88330 Attention: RRRT Maj. R. E. Brocken, Code MDGRT	1 1
U.S. Air Force Washington, D.C. 20330 Attention: Col. C. K. Stanbaugh, Code AFRST	1
U.S. Army Missile Command Redstone Scientific Information Center Redstone Arsenal, Alabama 35808 Attention: Chief, Document Section Dr. W. Wharton	1 1
Commander U.S. Naval Missile Center Point Mugu, California 93041 Attention: Technical Library	1
Space-General Corporation 777 Flower Street Glendale, California 91201 Attention: C. E. Roth	1
Stanford Research Institute 333 Ravenswood Avenue Menlo Park, California 94025 Attention: Thor Smith P. R. Gillette	1 1
Thiokol Chemical Corporation Alpha Division, Huntsville Plant Huntsville, Alabama 35800 Attention: Technical Director	1
Marquardt Corporation 16555 Saticoy Street Box 2013 – South Annex Van Nuys, California 91404 Attention: Librarian W. D. Boardman, Jr.	1 1

	Copies
McDonnell Aircraft Corporation P. O. Box 6101 Lambert Field Missouri 63145 Attention: R. A. Herzmark	1
North American-Rockewell Corp. Space & Information Systems Division 12214 Lakewood Boulevard Downey, California 90242 Attention: Technical Information Center, C/096-722 (AJ01) H. Storms	1
Rocketdyne, Division of North American Rockwell Corp. 6633 Canoga Avenue Canoga Park, California 91304 Attention: R. Morin, H. Diem	1
Northrop Space Laboratories 1001 East Broadway Hawthorne, California 90250 Attention: Dr. William Howard	1
Rocket Propulsion Laboratory DGRPP Edwards, California 93523 Attention: Capt. T. Kelly E. Stein R. Wiswell F. C. Sayles	 1 1 1 1
Wright-Patterson AFB, Ohio 45433 Attention: AFML (MAAM) AFML (MAAE)	 1 1
Air Products and Chemicals, Inc. Allentown, Pennsylvania 18101 Attention: Abraham Lopin	1
Air Products and Chemicals, Inc. West Broad Street Emmaus, Pennsylvania 180-9 Attention: Andrew Hospider	1
University of California Los Alamos Scientific Laboratory P. O. Box 1663 Los Alamos, New Mexico	1

	Copies
Cyronetics Corporation Northwest Industrial Park Burlington, Massachusetts 02103 Attention: James F. Howlett	1
The Garrett Corporation 1625 I Street, NW Washington, D.C. 20006 Attention: R. J. Wright	1
AiResearch Mfg. Division-Garrett Corp. 402 South 36th Street Phoenix, Arizona 85034 Attention: D. L. Cauble	1
AiResearch Mfg. Division-Garrett Corp. 9851 Sepulveda Boulevard Los Angeles, California 90009 Attention: Librarian T. C. Coull F. R. Ruder R. K. Fisher R. J. Gambon V. A. Vilona	1 1 1 1 1
General Electric Company Apollo Support Department P.O. Box 2500 Daytona Beach, Florida 32015 Attention: C. Day	1
Goodyear Aerospace Corporation 1210 Massillon Road Akron, Ohio 44306 Attention: Clem Shriver, Dept. 481	1
Ling-Temco-Vought Box 5907 Dallas, Texas 75206 Attention: Library	1
Linde Company Tonawanda, New York 14150 Attention: R. Lindquist L. Niendorf	1 1

	Copies
Arthur D. Little, Inc. Division 500 Acorn Park Cambridge, Massachusetts 02140 Attention: Mr. R. B. Hinckley	1
Lockheed Aircraft Corporation Marietta, Georgia 30060 Attention: Library	1
The Martin Company Blatimore, Maryland 21201 Attention: Science-Technology Library	1
National Research Corporation 70 Memorial Drive Cambridge, Massachusetts 02142	1
New York University University Heights New York, New York 10452 Attention: Paul F. Winternitz	1
Space General Corporation 9200 East Flair Drive El Monte, California 91731 Attention: John Kortenhoeven, Dept. 5131	1
Space Technology Laboratory, Inc. 1 Space Park Redondo Beach, California 90200 Attention: STL Tech. Lib. Doc. Acquisitions Pravin Bhuta	1 1
General Dynamics/Fort Worth P. O. Box 748 Fort Worth, Texas 76101 Attention: P. R. Tonnancour Dr. D. Wasterheide, MS 2660	1
The Martin Company Denver, Colorado 80201 Attention: D. W. Murphy Library	1 1
Dynatech Corporation 17 Tudor Street Cambridge, Massachusetts 02139 Attention: J. M. Bonneville	1